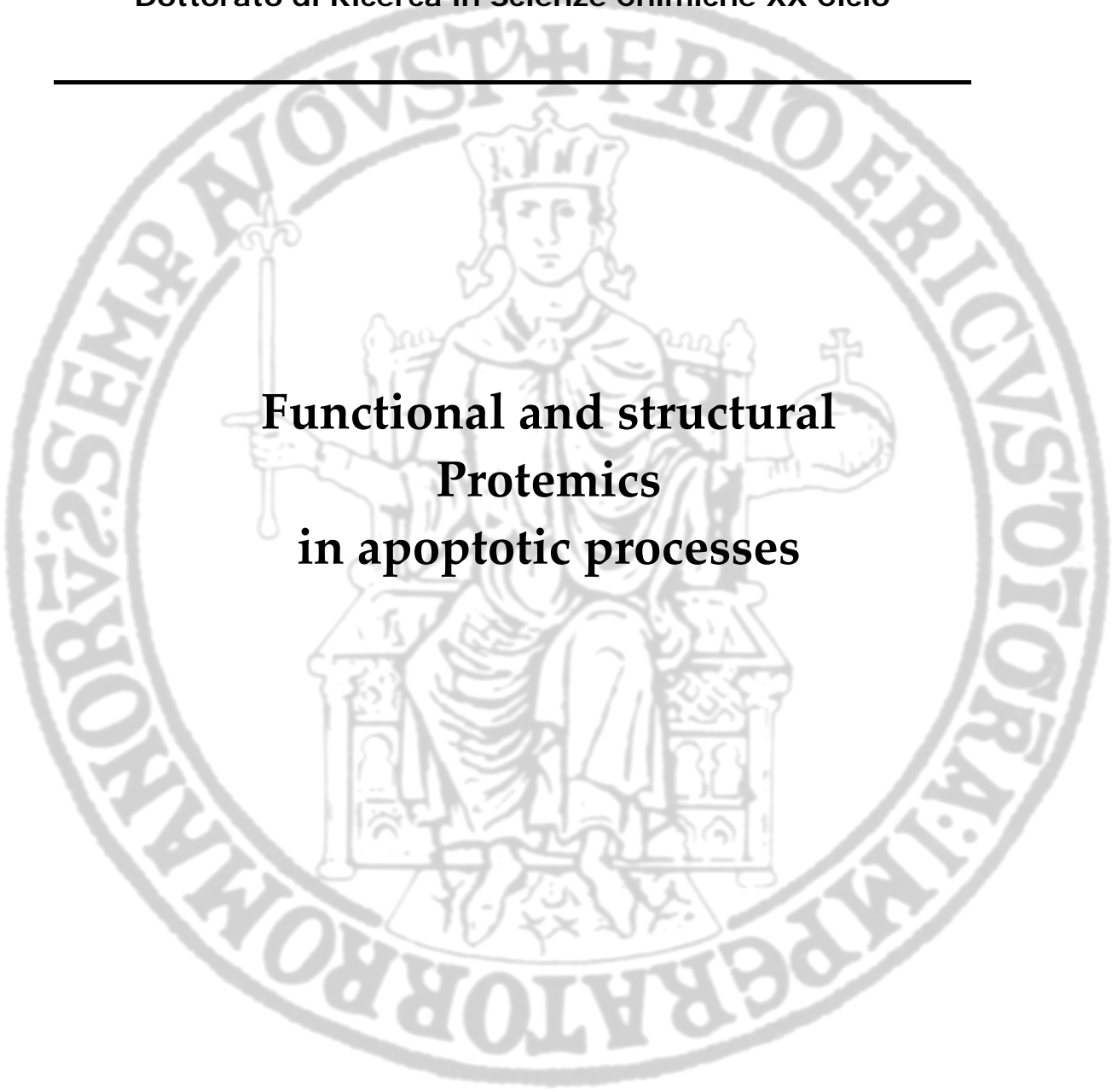


UNIVERSITÀ DEGLI STUDI DI NAPOLI

"FEDERICO II"

Dottorato di Ricerca in Scienze Chimiche XX Ciclo

The seal of the University of Naples Federico II is a large, circular emblem in the background. It features a central figure of a seated monarch, likely King Frederick II, wearing a crown and holding a scepter in his right hand and a globe in his left. The figure is surrounded by a Latin inscription: "IMPERATOR ROMANORVM SEMPER AVGVSTVS FERIVS".

**Functional and structural
Protemics
in apoptotic processes**

Relatore

Tutore

Candidato

Prof. M.Corsaro

Prof.P.Pucci

Andrea Carpentieri

INDEX

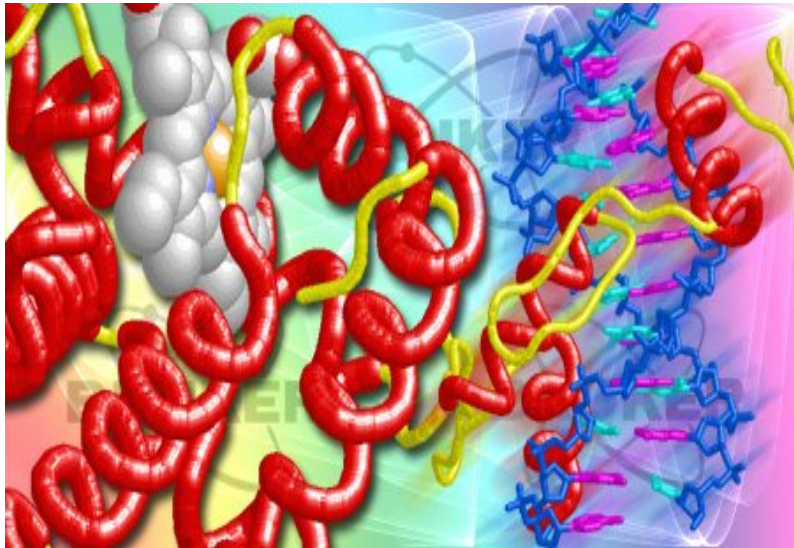
<u>1.INTRODUCTION</u>	pag.2
1.1. <i>The age of Proteomics</i>	pag.2
1.2. <i>Proteomics methods</i>	pag.4
1.2.1. <i>Two dimensional electrophoresis</i>	pag.4
1.2.2 <i>Image analysis</i>	pag.7
1.2.3 <i>Protein Identification by mass spectrometry</i>	pag.11
1.2.4 <i>Software and bioinformatics</i>	pag.22
1.3 <i>Ageing and Apoptosis</i>	pag.29
1.3.1 <i>Homeostasis</i>	pag.31
1.3.2 <i>Mitochondrial regulation</i>	pag.33
1.3.3 <i>Execution</i>	pag.37
1.3.4 <i>Removal of dead cells</i>	pag.38
1.3.5 <i>Yeast and metazoan ageing</i>	pag.40
<u>2. AIM OF THE PROJECT</u>	pag.44
<u>3. MATHERIAL AND METHODS</u>	pag.46
<u>4. RESULTS</u>	pag.53
4.1 <i>Calorie restriction and glycerol increase chronological life span</i>	pag.53
4.2 <i>ROS production, and mitochondria phenotypes during chronological aging in different carbon source.</i>	pag.54
4.3 <i>O2 consumption and cytochrome content during chronological life span in different carbon source</i>	pag.58
4.4 <i>Detection of oxidation-sensitive cysteine during chronological aging in different carbon sources</i>	pag.60
4.5 <i>Image analysis and Identification of major proteins oxidized on cysteine residues</i>	pag.67
<u>5.DISCUSSION</u>	pag.75
<u>6.REFERENCES</u>	pag.82

1. INTRODUCTION

1.1 The age of Proteomics

Once complete genome sequencing has been achieved for a wide variety of prokaryotic and eukaryotic organisms, one of the most intellectually challenging, scientifically productive, and socially applicable endeavours of modern biological science is the current effort to understand the function of living cells at the molecular level. Therefore interest has inevitably turned to proteins.

The term “proteome” (1) indicates **PROTEINS** expressed by a **genome** and is the systematic analysis of protein profiles, it refers to all protein produced by a species.

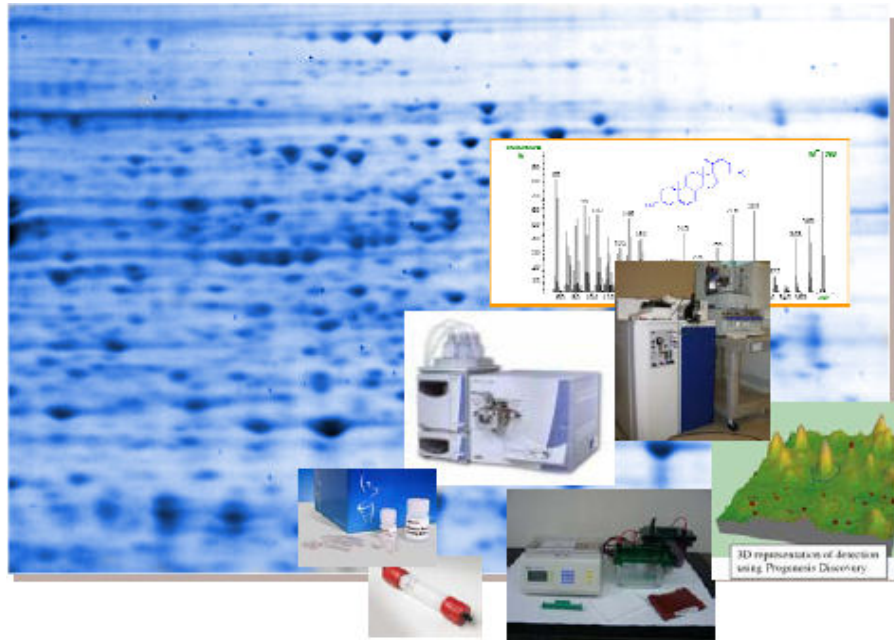


Whereas the genome is a constant feature of an organism, the proteome varies with nature of tissue, state of development, health or disease, effect of drug treatment and in response of environmental changes (such as lack of nourishments, oxidative stress, UV exposition and ageing) (2,3).

This capacity might be pointed to the ability of a proteome to regulate dynamically protein expression (4) and post translational modification; it's now known that products of a single gene represent a protein population that can contain large amounts of micro heterogeneity (5). More than 100 modification types are recorded and additional ones are yet to be discovered (6).

Proteomics can be divided into **expression** proteomics (7,8,9), the study of global protein expression, and **functional** proteomics (10, 11, 12), the

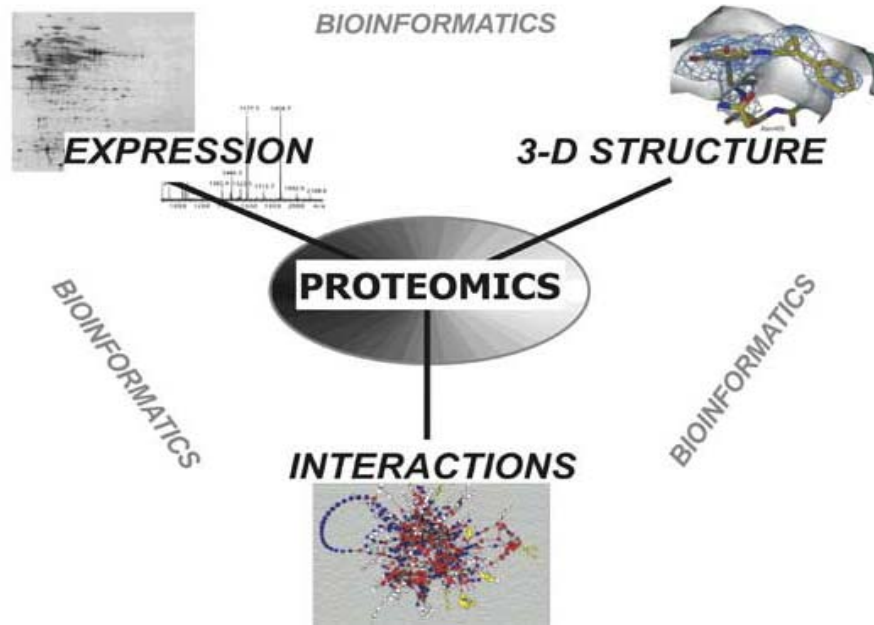
study of proteins function and their interaction through the isolation of protein complexes. However, there is a distinction to be made between the molecular function of an isolated protein and the function of that protein in the complex cellular environment as studied by proteomics technologies. Proteomics attempts to catalog and characterize these proteins, compare variations in their expression level in health and disease, study their interactions, and identify their functional roles. Proteomics is not the study of individual proteins as has been done traditionally, but rather a study of protein complexes time and environmental condition depending.



The described scenario requires advanced methodologies based on the combination of the classical biochemical approach coupled with all the modern available technologies. On the one hand, in fact, a huge and sensitive analytical capacity is required, but on the other hand a deep knowledge of protein chemistry is fundamental. The only analytical skills may lead to enormous mistakes.

A proteomic investigation mix together separative methods (such as two dimensional electrophoresis, liquid chromatography), mass spectrometry and bioinformatics (Fig 1); the enormous quantity of data produced must be analyzed by a biochemist in order to find all the relations giving a sense to his research.

Fig1



1.2 Proteomics methods

1.2.1 Two dimensional electrophoresis

Two-dimensional gel electrophoresis (2-DE) is a powerful and widely used method for the analysis of complex protein mixtures extracted from cells (13), tissues (14), or other biological samples. This technique separates proteins in two steps, according to two independent properties: the first-dimension is an isoelectric focusing (IEF), which separates proteins according to their isoelectric points (pI); the second-dimension is an SDS-polyacrylamide gel electrophoresis (SDS-PAGE), which separates proteins according to their molecular weights (MW). In this way, complex mixtures composed by different proteins can be resolved.

During the first dimension the procedure involves placing the sample in gel with a pH gradient, and applying a potential



difference across it. In the electrical field, the protein migrates along the pH

gradient, until it carries no overall charge. This location of the protein in the gel constitutes the apparent pI of the protein.

There are two alternative methods to create the pH gradient - carrier ampholytes and immobilized pH gradient (IPG) gels (15).

Development of IPG coupled with pre-cast gradient polyacrylamide gels and introduction of new sensitive fluorescent stains have considerably



simplified and greatly improved the capacity, sensitivity and reproducibility of 2D gels. The IEF is the most critical step of the 2-DE process. The proteins must be solubilized without charged detergents, usually in high concentrated urea solution, reducing agents and chaotropes. To obtain high quality data it is essential to achieve

low ionic strength conditions before the IEF itself. Since different types of samples differ in their ion content, it is necessary to adjust the IEF buffer and the electrical profile to each type of sample.



The separation in the second dimension by molecular size is performed in slab SDS-PAGE gels. Up to twelve parallel gels can be simultaneously separated in a fixed temperature to minimize the separation variations between individual gels.

These recent technological advances do not however eliminate a number of difficulties associated with the separation of proteins by 2DE.

The complexity of a proteome can far exceed the capacity of analytical systems. The whole proteome of any organism, in fact is too complicated

to be analyzed in a simple one-step process and direct attempts for the entire proteome analysis normally lead to limited amount of information (16, 17).

Historically, 2DE has been the tool of choice to resolve complex protein mixtures and to detect differences in protein expression patterns between normal and diseased tissue.

High-resolution gel electrophoresis, of which 2DE is currently the most powerful protein separation method, was already used as an analytical tool in the late 70s (18, 19). Despite these outstanding properties and widespread application, almost 20 years went by before systematic use of 2D PAGE gels became an integral part of the proteomics. The protein spots were electroblotted on the membrane and analyzed by Edman degradation to release N-terminal sequence (20); this approach was generally slow because every protein spot or peptide peak had to be sequenced individually. In addition this identification method has low sensibility and there was not complete database of genome. Furthermore, proteins are often blocked at their N-terminal in the course of the biosynthesis (acetylation, formylation or pyroglutamic formation).

2-DE remained the highest resolution protein separation method available, but the ability to identify the observed proteins was always an extremely difficult problem. In the past decade, three crucial developments have changed this situation. The first: whole genome sequencing for an increasing number of organisms has defined at the gene level all proteins that exist in that organism. The second: the development of mass spectrometers able to ionize and mass-analyze biological molecules. The third: the development of computer algorithms able to match MS and MS/MS spectra. Recently, the significant accomplishments of genomics, proteomics and bioinformatics are making the systematic analysis of all expressed cellular components a reality. Together with the completion of several genome projects and the development of bioinformatics tools for protein research, the groundwork was laid for rapid, sensitive, and accurate studies of protein in many biological organisms. Today MS is overwhelmingly used as the technology base for protein identification from 2D gels (21, 22, 23)

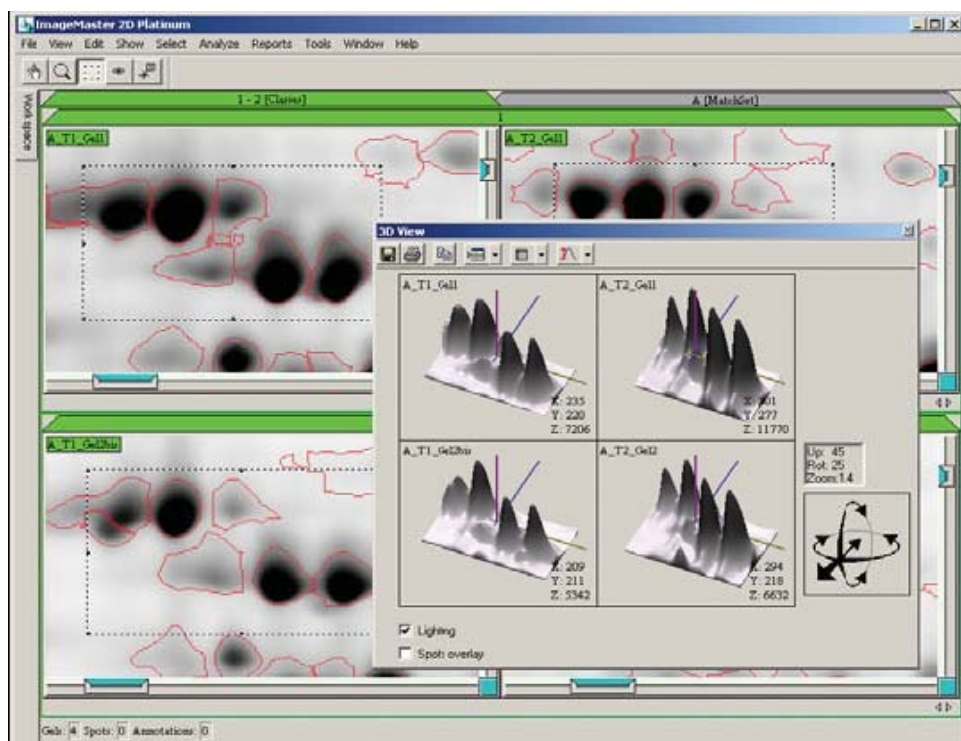
The comparative 2D gel approach is typically employed to study differences in proteins that are up- or down-regulated in a disease state. In such studies, a reliable analysis of quantitative changes of protein spots is important (24, 25). Furthermore, recently new programs for comparison of 2D-maps like algorithms based on characteristics of spot image on gel are rising. Well-known drawbacks of the technique are limitations in the pI and molecular weight of proteins. In fact, specific classes of proteins have long been known to be excluded or under-represented in 2D gel patterns. These include very acidic or basic proteins, excessively large or small proteins and membrane proteins. Furthermore, difficult automation and reproducibility problems and low abundant proteins are either not detected at all, due to the limited sensitivity achievable with commonly used dyes, or they are masked by higher abundant comigrating proteins. Incremental improvements in 2DE technology, including more sensitive staining methods (26), large-format higher resolving gels (27, 28) and sample fractionation (29) prior to 2DE have alleviated, but not eliminated, these and other shortcomings of the 2DE/MS approach.

1.2.2 Image analysis

The crucial algorithms in 2-D gel analysis software have been significantly improved over the years (30, 31) in order to account for such difficulties. In addition, program interfaces have gained a lot of ground in user friendliness. In spite of these advances, no image analysis software can solve all experimental problems. The desire to draw valuable information from low quality gels remains an illusive goal. Before starting a 2-D gel image analysis, it is therefore essential to optimize all steps in the gel production process in order to assure the best possible quality and reproducibility. Careful experimentation remains the only way to guarantee significant end results; image acquisition parameters also play a very important role.

During an image analysis a gel can be considered as a “2-DE image” that has been digitized and stored on a hard disk. It contains the raw input data from which proteins can be detected and quantified. The proteins represent the gray (or dark blue) values for all the pixels in the image. Every pixel is characterized by its X and Y coordinates, which represent the horizontal and vertical positions of the pixel on the image. The pixel's raw value, or gray value, is the signal intensity of the pixel (Z axis in a three-dimensional view) Fig 2.

Fig 2. 3-D view for several gel regions.



The software recognizes gels from several image formats. Gels can be duplicated, deleted, cropped, filtered, flipped or scaled. Gels can also be aligned, meaning that they are distorted in order to superimpose their image with another gel. Various items can be defined on a gel for detailed examination.

Spot and gel relationships

Matches

A match represents the relationship between corresponding spots in different gels. It connects the same protein in the different gels. It is composed of a spot n-tuple (S1, S2, ..., Sn) where S1 is a spot in the first gel, and Sn a spot in the last gel. Matches can be manually defined by the user or automatically determined by software's powerful gel matching algorithm. The match is the basic element for searching and investigating protein expression changes across gels through the use of reports, histograms, and statistical methods.

To be able to initiate the matching process, gels must be part of a Match set. A match set includes gels or populations of gels (in sub match sets) that should be compared and therefore matched together. Every match set is represented by a Master image. This master image is created by based on the Reference for the match set, chosen by the user.

A class is a set of gels or gel populations that you can compare with other such entities. For example, a class of gels obtained from the infected tissue samples of different patients can be compared to a class of gels representing healthy tissue from other patients.

A class allows to search and investigate protein expression changes across gels through the use of intra-class reports, histograms, and scatter plots. It is also possible to compare different classes through inter-class analyses. To compare gels in a class or within different classes, the gels must be matched together. This means that they must belong to the same match set.

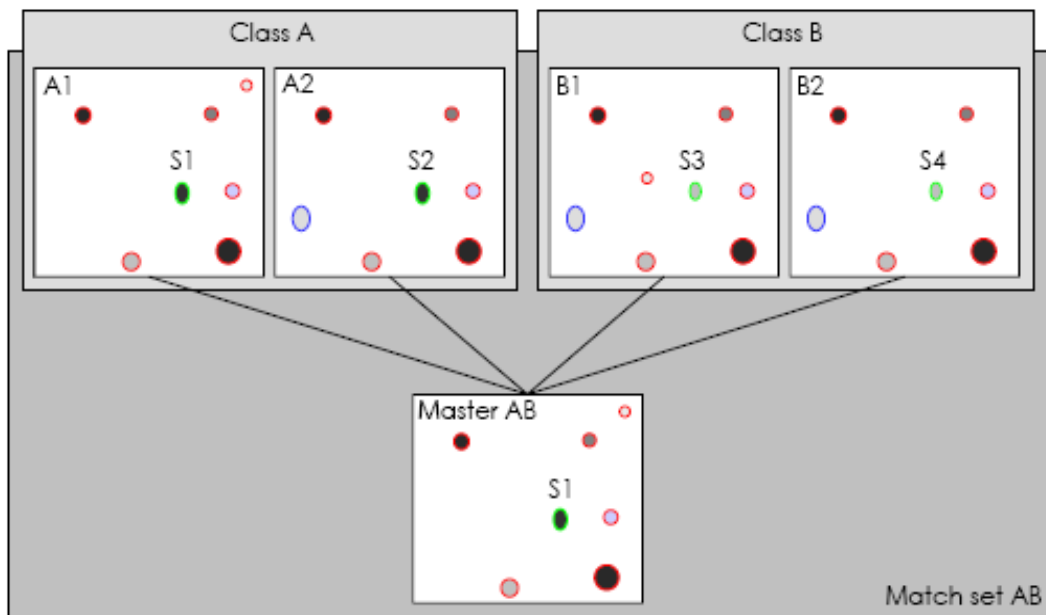
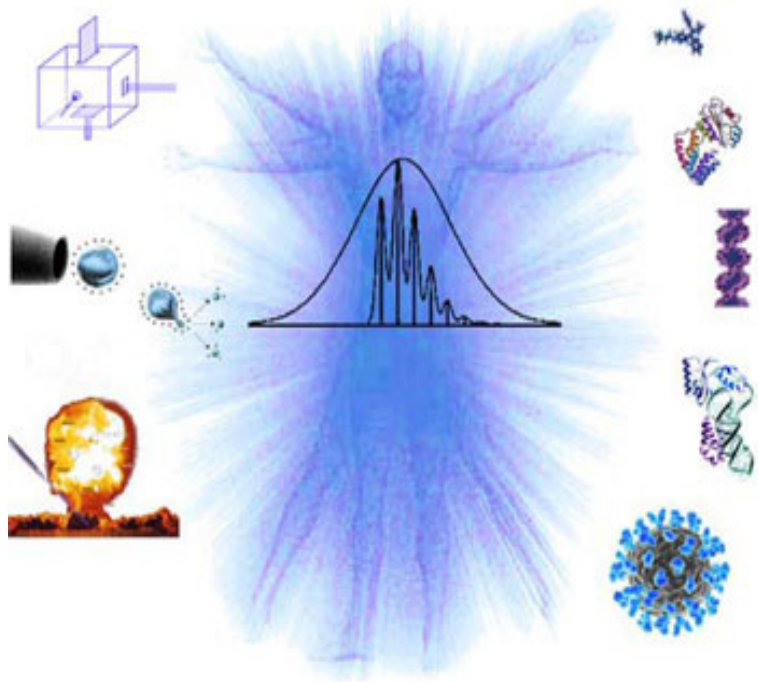


Figure 3. Definition of matches, match sets and classes. Spots S1, S2, S3, and S4 together form a match. Note that the spot in Master AB has the same number as the corresponding spot in A1. This is because A1 is the reference image for Match set AB, on which the Master AB is based. The Match set AB contains all the gels to be matched (A1, A2, B1 and B2), and is represented by a master image (Master AB). A class regroups gels from a particular biological state for comparison with another such state. The spots in the selected match (green) are under-expressed in Class B with respect to Class A.

This statistical relation between all the compared spots intensity may be obtained, therefore the choice of the most interesting spot to be identified becomes easier.

1.2.3 Protein Identification by mass spectrometry

In proteomics Mass Spectrometry, together with two-dimensional gel electrophoresis, emerged as the leading technology, due to its high sensitivities and the ability of generating data rapidly. Thus it has a great potential for high-throughput analysis



required by this kind of approach. The ability to identify proteins rapidly using mass spectrometry data has catalyzed the development of methods for large scale protein analysis as well as the development of new approaches to analyze protein mixtures and complexes (32, 33, 34,).

The growing utility of mass spectrometry in biological research derives from the development of two extraordinary methods for ionizing biomolecules, matrix-assisted laser desorption/ionization (MALDI) and electrospray ionization (ESI). These techniques enable the determination of the molecular mass of peptides and proteins with high accuracy and speed.

Atomic resolution structure determinations of proteins are formidable multidisciplinary undertakings encompassing tasks such as protein cloning, expression and purification procedures, crystallization trials, phase determination and model building. The mass spectrometry can greatly facilitate these obligate tasks (35, 36). It can be used for assaying the correctness and purity of target protein constructs, due to its unsurpassed accuracy and speed for measuring mass, mass spectrometry allows to quickly test whether a given protein has been faithfully expressed. The

measurement allows for detection of PCR errors, mistranslation errors, unwanted modifications, and major protein impurities. Additional information concerning the nature of the error/modification can be obtained by MS peptide mapping.

A mass spectrometer consists of an ion source, a mass analyser that measures the mass-to-charge ratio (m/z) of the ionized analytes, and a detector that registers the number of ions at each m/z value.

MALDI-MS is normally used to analyze peptide mixtures, whereas integrated liquid-chromatography ESI-MS systems (LC-MS) are preferred for the analysis of complex samples.

There are four basic types of mass analyser currently used in proteomics research. These are the ion trap, time-of-flight (TOF), quadrupole and Fourier transform ion cyclotron (FT-MS) analysers. They are very different in design and performance, each with its own strength and weakness. These analysers can be stand alone or, in some cases, put together in tandem to take advantage of the strengths of each.

Two mass spectrometric methods for rapid identification of proteins are now in widespread use: one of these methods (MALDI) uses the characteristic distribution of peptide masses obtained by chemical or enzymatic hydrolysis of proteins (37, 38). A number of computer programs are available for using the observed peptide masses to search gene sequence databases for proteins that fit the mass fingerprint (39, 40, 41).

For this method the combination of the high resolution power of 2DE and the rapidity of MALDI analysis is the best combination. MALDI in fact may be considered the fastest technique for peptide analysis.

The other method for protein identification uses sequence tags (42, 43); i.e., partial amino acid sequence information. Searching of gene sequence databases is again used to identify the protein at the gene level.

The outcome of the experiment is the identity of the peptides and therefore the proteins making up the purified protein population. Often MS/MS instruments are classified in one or two categories: tandem in space or tandem in time. Tandem in space instruments require a distinct analyser for each stage (isolation and fragmentation) of MS/MS. Today, almost all tandem in space MS-MS instruments are either triple quadrupole (QqQ) or

hybrid instruments quadrupole/time-of-flight (Q/TOF). Trapping instruments are typically tandem in time. The various stages of MS-MS are performed in the same analyzer but separated in time.

Peptide Sequence analysis

The technique of tandem mass spectrometry (MS-MS) is an important factor in the contributions of the application of mass spectrometry to biological compounds. As the name implies, MS/MS involves two stages of MS. In the first stage of MS-MS, ions of a desired m/z are isolated from the rest of the ions coming from the ion source. These isolated ions (termed parent ions) are then induced to undergo a reaction that increases the internal energy of the ions, leading to dissociation. The ions resulting from the various reactions are termed product ions, and these are analyzed with the second stage of MS-MS. The representation of this can be summarized in reaction in which m_p^+ is the parent ion, m_d^+ is the product or fragment ion and m_n the neutral fragment or another product ion if the parent ion is multiply charged:



With some instrument, it's possible to repeat this process, leading to what is termed an MS^n experiment, where n is equal to the number of stages of MS performed. A crucial aspect of the MS-MS experiment is the reaction that occurs between the two MS stages. By far the most frequent reaction is unimolecular dissociation, which is generally enhanced by some form of ion activation. The ion activation is necessary to increase the internal energy of the parent ion so that it will dissociate before analysis by MS^2 . In practice, the activation cannot be separated from the dissociation, so the ion activation techniques are typically referred to as dissociation methods. The dissociation method almost universally used is collision-induced dissociation (CID) (44, 45). In CID, the parent ion collides with a neutral target (collision) gas and some of the kinetic energy of the parent ion can be converted to internal energy. High energy CID spectra (keV) tend to be

dominated by fragment ions formed by charge-remote mechanism, while low energy CID spectra (< 100 eV) often show intense fragment ions formed by abundant neutral losses. The CID spectra of peptides recorded at low collision energy tend to show abundant fragment ions formed by cleavage of the peptide bonds, while high-energy CID spectra often contain fragment ions formed by other backbone and also side-chain cleavages .

Peptide sequence identification by mass spectrometry involves fragmentation of a peptide to produce smaller m/z fragments; ideally, measured m/z values of these pieces can be assembled to produce the original sequence. Cleavage is commonly accepted to occur predominantly through charge-directed pathways.

A nomenclature exists to describe the fragment ion types that are produced by cleavage of different bonds along the peptide backbone and/or side chain. Cleavage of the backbone typically occurs at the peptide bond to produce b ions, if the amino terminal fragment retains the charge, or y ions, if the carboxy-terminal fragment retains the charge (fig. 4). In the case of multiply charged ions, a charge separation can occur to produce complementary ion pairs. Both partners of the complementary pair are not always detected in equal abundance, because they are not equally stable against further fragmentation or because instrument discrimination may enhance or diminish one partner of the pair. Although b and y ions are considered to be the most useful sequence ion types, because they correspond to cleavage of the amide bond, other ion types are observed and used in spectral interpretation. These include a ions which correspond formally to loss of CO from b ion; a m/z difference of 28 between two peaks suggests an a-b ion pair and is useful in identifying the ion series to which the peaks belong. The y series is sometimes accompanied by peaks formally corresponding to loss of NH_3 from the y ions, allowing designation of the higher m/z ion each $\Delta 17$ pair as belonging to the y ion series. Ions that correspond to immonium ions, or fragments of immonium ions, of individual amino acid residues in a peptide are often detected, even for residues from the internal portion of the sequence (86).

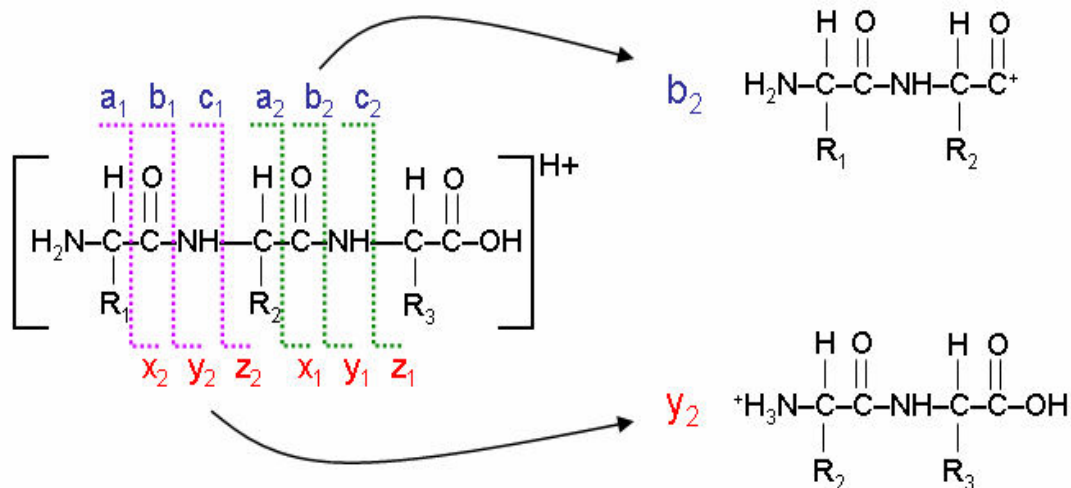


Fig.4 Schematic representation of nomenclature for fragmentation of peptide ions.

MALDI mass fingerprinting

The term matrix-assisted laser desorption ionization (MALDI) was coined in 1985 by Franz Hillenkamp, Michael Karas and their colleagues (46). These researchers found that the amino acid alanine could be ionized more easily if it was mixed with the amino acid tryptophan and irradiated with a pulsed 266 nm laser. The tryptophan was absorbing the laser energy and helping to ionize the non-absorbing alanine. Peptides up to the 2843 Da (melittin) could be ionized when mixed with this kind of “matrix” (46,47,48). The breakthrough for large molecule laser desorption ionization came in 1987 when Koichi Tanaka of Shimadzu Corp. and his co-workers used what they called the “ultra fine metal plus liquid matrix method” that combined 30 nm cobalt particles in glycerol with a 337 nm nitrogen laser for ionization (46). Using this laser and matrix combination, Tanaka was able to ionize biomolecules as large as the 34,472 Da protein carboxypeptidase-A. Tanaka received one-quarter of the 2002 Nobel Prize in Chemistry for demonstrating that, with the proper combination of laser wavelength and matrix, a protein can be ionized (49). Karas and Hillenkamp were subsequently able to ionize the 67 kDa protein albumin using a nicotinic acid matrix and a 266 nm laser (46)

. Further improvements were realized through the use of a 355 nm laser and the cinnamic acid derivatives ferulic acid, caffeic acid and sinapinic acid as the matrix (50). The availability of small and relatively inexpensive nitrogen lasers operating at 337 nm wavelength and the first commercial instruments introduced in the early 1990s brought MALDI to an increasing number of researchers (51,52). Today, mostly organic matrices are used for MALDI mass spectrometry.

Matrix-assisted laser desorption/ionization (MALDI) is a soft ionization technique used in mass spectrometry, allowing the analysis of biomolecules (biopolymers such as proteins, peptides and sugars) and large organic molecules (such as polymers, dendrimers and other macromolecules), which tend to be fragile and fragment when ionized by more conventional ionization methods. It is most similar in character to electrospray ionization both in relative softness and the ions produced (although it causes much fewer multiply charged ions).

The ionization is triggered by a laser beam (normally a nitrogen laser). A matrix is used to protect the biomolecule from being destroyed by direct laser beam and to facilitate vaporization and ionization

The matrix consists of crystallized molecules, of which the three most commonly used are 3,5-dimethoxy-4-hydroxycinnamic acid (sinapinic acid), α -cyano-4-hydroxycinnamic acid (alpha-cyano or alpha-matrix) and 2,5-dihydroxybenzoic acid (DHB). A solution of one of these molecules is made, often in a mixture of highly purified water and an organic solvent (normally acetonitrile (ACN) or ethanol). Trifluoroacetic acid (TFA) may also be added. A good example of a matrix-solution would be 20 mg/mL sinapinic acid in ACN:water:TFA (50:50:0.1).

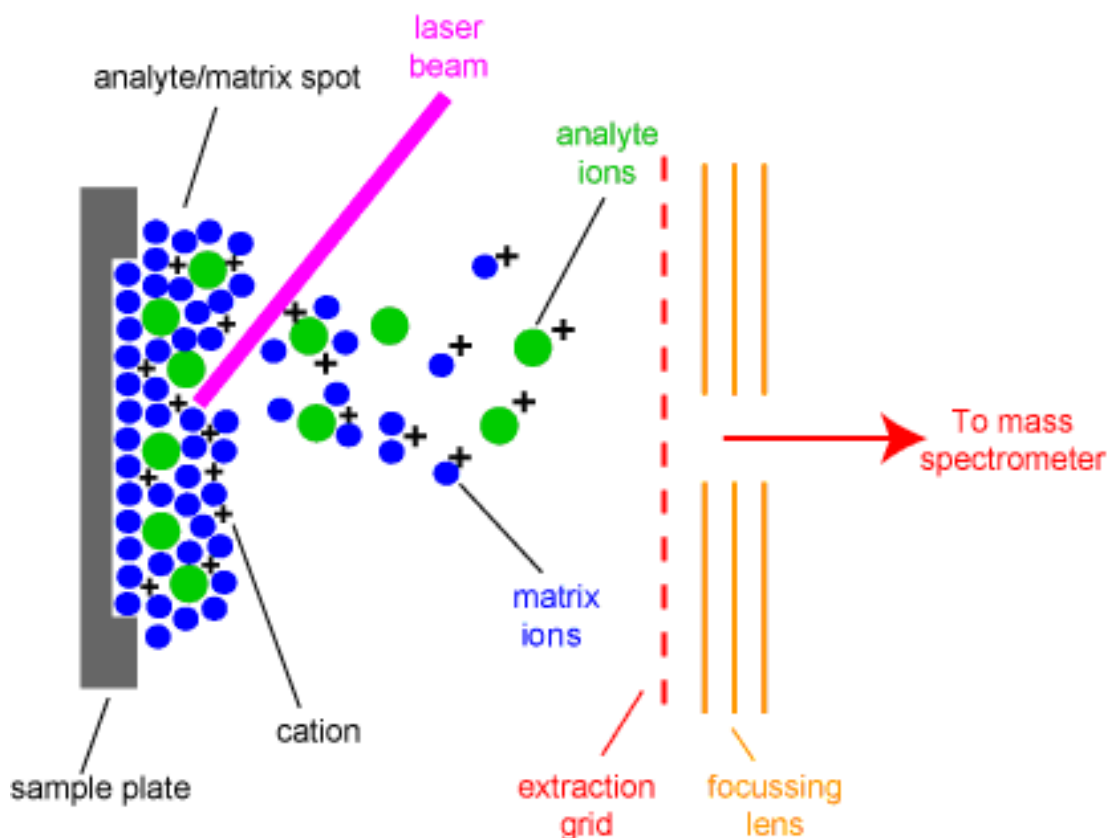


Fig 5. Matrix-assisted laser desorption ionization depicted with matrix in blue and analyte in green

The identity of suitable matrix compounds is determined to some extent by trial and error, but they are based on some specific molecular design considerations:

- They are of a fairly low molecular weight (to allow facile vaporization), but are large enough (with a high enough vapour pressure) not to evaporate during sample preparation or while standing in the spectrometer.
- They are acidic, therefore act as a proton source to encourage ionization of the analyte; a matrix molecule have a strong optical absorption in the UV, so that they rapidly and efficiently absorb the laser irradiation.

The matrix solution is mixed with the analyte (e.g. protein-sample). The organic solvent allows hydrophobic molecules to dissolve into the solution, while the water allows for water-soluble (hydrophilic) molecules to do the same. This solution is spotted onto a MALDI plate (usually a metal plate designed for this purpose). The solvents vaporize, leaving only the

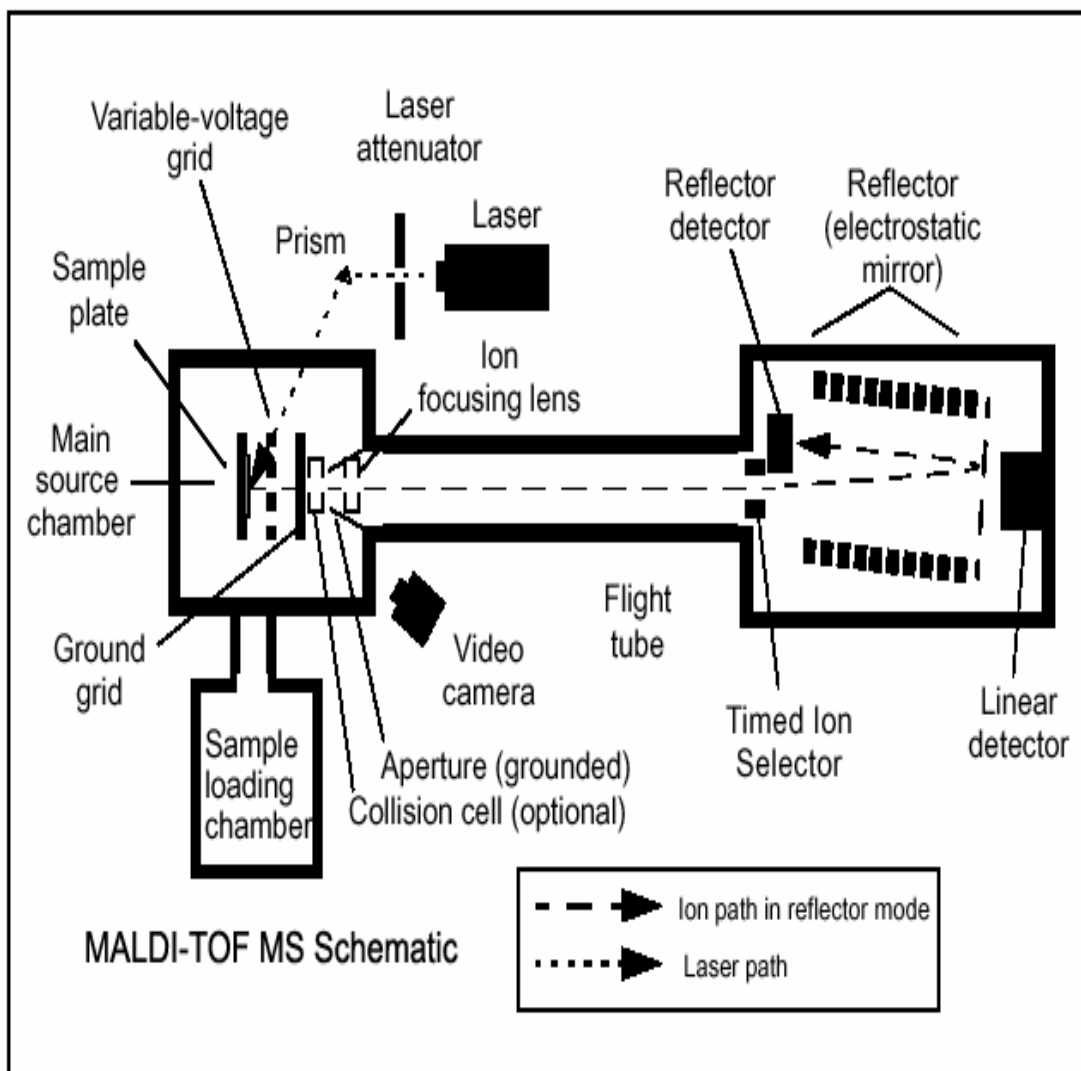
recrystallized matrix, but now with analyte molecules spread throughout the crystals. The matrix and the analyte are said to be co-crystallized in a MALDI spot.

The laser is fired at the crystals in the MALDI spot. The spot absorbs the laser energy and it is thought that primarily the matrix is ionized by this event. The matrix is then thought to transfer part of its charge to the analyte molecules (e.g. protein), thus ionizing them while still protecting them from the disruptive energy of the laser. Ions observed after this process are quasimolecular ions that are ionized by the addition of a proton to $[M+H]^+$, or other cation such as sodium ion $[M+Na]^+$, or the removal of a proton $[M-H]^-$ for example. MALDI generally produces singly-charged ions, but multiply charged ions ($[M+nH]^{n+}$) can also be observed, usually in function of the matrix used and/or of the laser intensity, voltage. Note that these are all even-electron species. Ion signals of radical cations can be observed eg. in case of matrix molecules and other stable molecules.

Lasers Used for MALDI		
Laser	Wavelength (nm)	Reference
<u>Nitrogen laser</u>	337	(Tanaka 1988)
<u>Nd:YAG</u>	355, 266	(Karas 1985)
<u>Er:YAG</u>	2940	(Overberg 1990)
<u>CO₂</u>	10,600	(Overberg 1991)

Time Of Flight analyzer

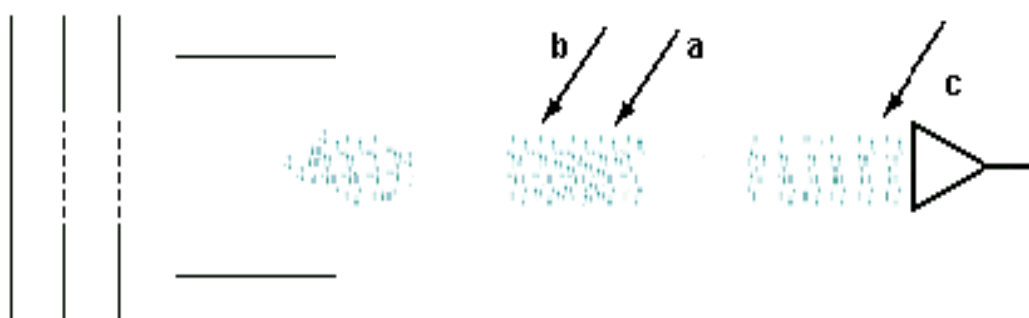
The most widely used analyzer is the TOF (time-of-flight mass spectrometer), mainly due to its large mass range. The TOF measurement procedure is also ideally suited to the MALDI ionization process since the pulsed laser takes individual 'shots' rather than working in continuous operation. MALDI-TOF instruments are typically equipped with an "ion mirror", deflecting ions with an electric field, thereby doubling the ion flight path and increasing the resolution. Commercial reflector TOF instruments reach today a resolving power $m/\Delta m$ of well above 20'000 FWHM (full-width half-maximum, Δm defined as the peak width at 50% of peak height).



The flight tube is usually a vacuum enclosure, free of electrical fields, between the ion source and the detector. It is sometimes referred to as a “field free drift region”.

The ions which are under study exit the ion source and enter the flight tube with the proper velocity and direction to arrive at the detector. The flight tube does not usually interact with the ion packets along their flight path. If the ions are created at a positive voltage and accelerated to ground potential, the flight tube can be a simple pipe.

Fig. 6



Ions are pulsed into the flight tube in short, well defined packets. All the ions are given the same energy in the source. Since the light ones were pushed just as hard as the heavy ones, they will travel faster.

Since they are travelling at different velocities, the ion packets become strung out as they travel down the flight tube. The light ions (Fig 6, a) in front, and the heavier ones (Fig 6, b) in back. Given sufficient flight time, the ions become separated into individual packets (Fig 6, c) by mass number. The detector amplifies them sequentially, and each packet becomes a mass peak.

The equation governing TOF separation is:

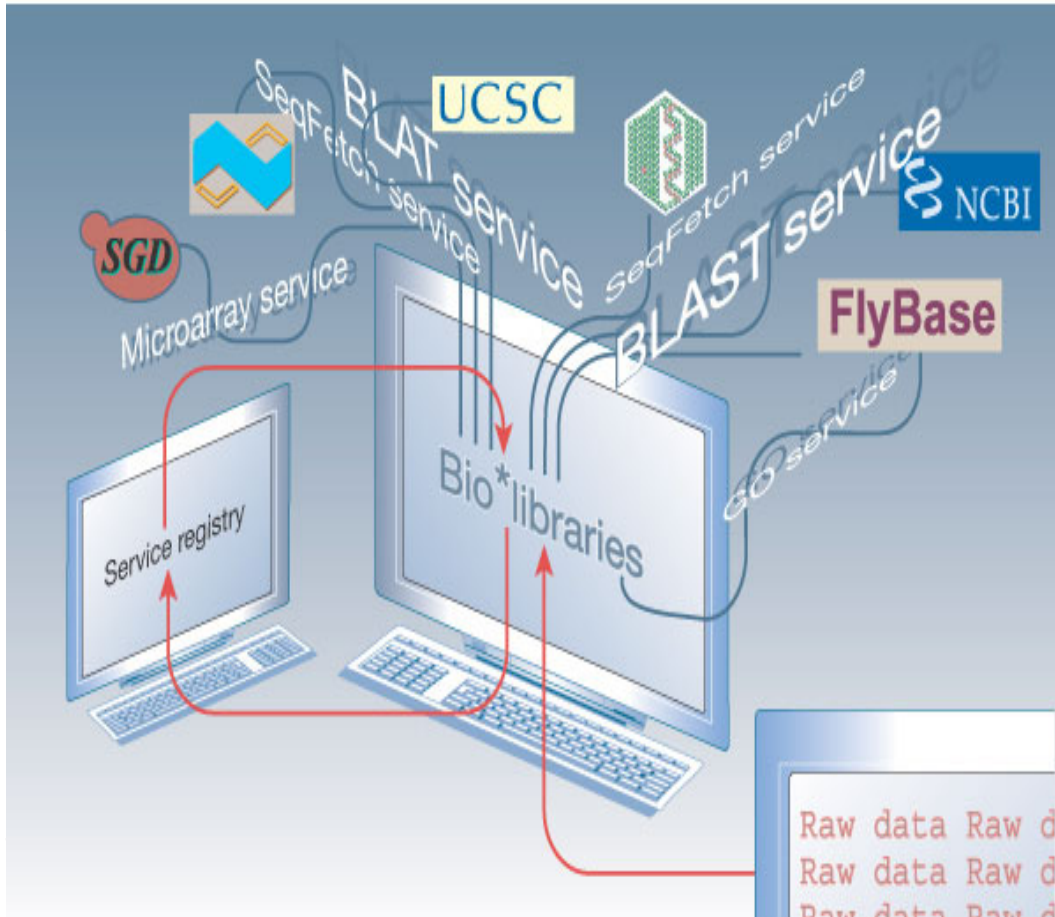
$$\frac{m}{z} = 2eEs \left(\frac{t}{d} \right)^2$$

m/z is mass-to-charge ratio of the ion
E is the extraction pulse potential
s is the length of flight tube over which E is applied
d is the length of field free drift zone
t is the measured time-of-flight of the ion

The initial MS spectrum determining the molecular masses of all of the components in the digest mixture can often provide sufficient information to search a database using just several of the molecular weights from this peptide map, the so called *Peptide Mass Fingerprinting* (PMF) of a protein. Peptide Mass Fingerprinting (PMF) is a technique used to identify proteins by matching their constituent fragment masses (peptide masses) to the theoretical peptide masses generated from a protein or DNA database. The first step in PMF is that an intact, unknown protein is cleaved with a proteolytic enzyme to generate peptides. With PMF, heterogeneity is most commonly imparted to the unknown protein with a trypsin digestion. A PMF database search is usually employed following MALDI TOF mass analysis. The premise of peptide mass finger printing is that every unique protein will have a unique set of peptides and hence unique peptide masses. Identification is accomplished by matching the observed peptide masses to the theoretical masses derived from a sequence database. PMF identification relies on observing a large number of peptides, 5+, from the same protein at high mass accuracy. This technique does well with 2D gel spots where the protein purity is high. PMF protein identification can run into difficulties with complex mixtures of proteins. Low level ID also becomes difficult due to commonplace contamination by keratin.

1.2.4 Software and bioinformatics

The terms bioinformatics and computational biology are often used interchangeably.



informatics more properly refers to the creation and advancement of algorithms, computational and statistical techniques, and theory to solve formal and practical problems inspired from the management and analysis of biological data. Computational biology, on the other hand, refers to hypothesis-driven investigation of a specific biological problem using computers, carried out with experimental or simulated data, with the primary goal of discovery and the advancement of biological knowledge. More simply, bioinformatics is concerned with the information while computational biology is concerned with the hypotheses. A similar distinction is made by National Institutes of Health (U.S.A.) in their working definitions of Bioinformatics and Computational Biology, where it is further emphasized that there is a tight coupling of developments and knowledge

between the more hypothesis-driven research in computational biology and technique-driven research in bioinformatics.

A common thread in projects in bioinformatics and computational biology is the use of mathematical tools to extract useful information from data produced by high-throughput biological techniques such as genome sequencing. A representative problem in bioinformatics is the assembly of high-quality genome sequences from fragmentary "shotgun" DNA sequencing. Other common problems include the study of gene regulation using data from microarrays or mass spectrometry.

Software tools

First generation bioinformatics tools consisted of applications, usually with a text-based interface, which performed a specific task well. The computational biology tool best-known among biologists is probably BLAST, an algorithm for searching large databases of protein or DNA sequences. The National Center for Biotechnology Information (NCBI) at the National Institutes of Health (NIH) provides a popular web-based implementation that searches their massive sequence databases.

Also fairly early on, due to the amassing of sequence and annotation data, keyword search engines which were able to resolve gene and protein synonyms were important. Computer scripting languages such as Perl (for its regular expressions handling facilities) and Python are often used to interface with biological databases and parse output from bioinformatics programs written in languages such as C or C++. Communities of bioinformatics programmers have set up free open source bioinformatics projects to develop and distribute the tools and modules they produce.

As the data sources expanded and diversified, both in content and geography, bioinformatics search engines, such as sequence profiling tools, to help in finding relevant information from several databases.

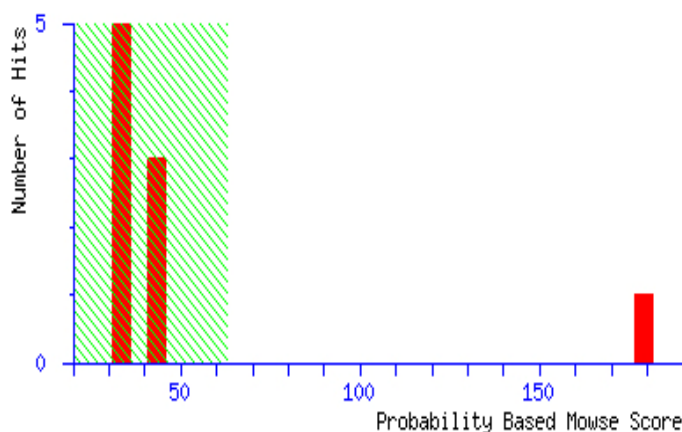
More recently, SOAP-based (Service Oriented Architecture Protocol)

{MATRIX} *{SCIENCE}* Mascot Search Results

User : maria agata catino
Email : macmail@netgroup.it
Search title : banda B
Database : NCBI nr 20031116 (1542172 sequences; 504050046 residues)
Taxonomy : Homo sapiens (human) (108205 sequences)
Timestamp : 17 Nov 2003 at 15:07:43 GMT
Top Score : 179 for **gi|18645167**, ANXA2 protein [Homo sapiens]

Probability Based Mowse Score

Score is $-10 \cdot \log(P)$, where P is the probability that the observed match is a random event. Protein scores greater than 63 are significant ($p < 0.05$).



interfaces have been developed for a wide variety of bioinformatics applications allowing an application running on one computer in one part of the world to use algorithms, data and computing resources on servers in other parts of the world. A large availability of these SOAP-based bioinformatics web services, along with the open source bioinformatics collections, lead to the next generation of bioinformatics tools: the integrated bioinformatics platform. These tools range from a collection of standalone tools with a common data format under a single, slick standalone or web-based interface, to integrative and extensible bioinformatics workflow development environments.

One of the crucial steps in Proteomic investigations is the correct use of software capable of identifying proteins starting from empirical data.

Produced by Matrix Science, Mascot is a powerful search engine, which uses mass spectrometry (MS) data to identify proteins from primary sequence databases.

The protein informatics range follows the researcher's workflow, including experiment set-up, 2D gel image analysis, data-mining and MS-based protein identification. Generally, to identify an unknown protein the target is subjected to protease treatment and the peptide mass fingerprint is recorded by a mass spectrometer (MALDI or ESI/MS). The peptide masses are then used to perform a pattern search in all available databases, mass tolerance is another criterion to increase the stringency in the search. Mascot does the job of matching a list of given masses to the MSDB (Mass Spec Database), specifically designed for peptide mass searches.

These different search methods can be divided as follows:

- Peptide Mass Fingerprint in which the only experimental data are peptide mass values,
- Sequence Query in which peptide mass data are combined with amino acid sequence and composition information. A super-set of a sequence tag query,
- MS/MS Ion Search using uninterpreted MS/MS data from one or more peptides.

The first stage of a molecular weight search (MOWSE) peptide-mass database (53) is to compare the calculated peptide masses for each entry in the sequence database with the set of experimental data. Each calculated value which falls within a given mass tolerance of an experimental value counts as a match. A molecular weight range for the intact protein can be used as a pre-filter.

Rather than just counting the number of matching peptides, Mowse uses empirically determined factors to assign a statistical weight to each individual peptide match. The matrix of weighting factors is calculated during the database build stage, as follows:

A frequency factor matrix, F , is created, in which each row represents an interval of 100 Da in peptide mass, and each column an interval of 10 kDa in intact protein mass. As each sequence entry is processed, the appropriate matrix elements $f_{i,j}$ are incremented so as to accumulate statistics on the size distribution of peptide masses as a function of protein mass. The elements of F are then normalised by dividing the elements of each 10 kDa column by the largest value in that column to give the Mowse factor matrix M :

$$m_{i,j} = \frac{f_{i,j}}{\left| f_{i,j} \right|_{\max \text{ in column } j}}$$

After searching the experimental mass values against a calculated peptide mass database, the score for each entry is calculated according to:

$$\text{Score} = \frac{50,000}{M_{\text{Prot}} \times \prod_n m_{i,j}}$$

Where M_{Prot} is the molecular weight of the entry and the product term is calculated from the Mowse factor elements for each match between the experimental data and peptide masses calculated from the entry.

Mascot incorporates a probability based implementation of the Mowse algorithm. The Mowse algorithm is an excellent starting point because it accurately models the behaviour of a proteolytic enzyme. By casting the Mowse score into a probabilistic framework, we gain a number of additional benefits:

1. A simple rule can be used to judge whether a result is significant or not.
2. Different types of matching (peptide masses and fragment ions) can be combined in a single search.
3. Scores from different searches and on different databases can be compared.
4. Search parameters can be optimised more readily by iteration.

Matches using mass values (either peptide masses or MS/MS fragment ion masses) are always handled on a probabilistic basis. The total score is the absolute probability that the observed match is a random event. Reporting probabilities directly can be confusing. Partly because they encompass a very wide range of magnitudes, and also because a "high" score is a "low" probability, which can be ambiguous. For this reason, we report scores as $-10 \cdot \log_{10}(P)$, where P is the absolute probability. A probability of 10⁻²⁰ thus becomes a score of 200.

Given an absolute probability that a match is random, and knowing the size of the sequence database being searched, it becomes possible to provide an objective measure of the significance of a result. A commonly accepted threshold is that an event is significant if it would be expected to occur at random with a frequency of less than 5%. This is the value which is reported on the master results page.

The master results page for typical peptide mass fingerprint search reports that "Scores greater than 67 are significant ($p < 0.05$)".

The sequence databases that can be searched on this server are:

- MSDB is a comprehensive, non-identical protein sequence database maintained by the Proteomics Department at the Hammersmith Campus of Imperial College London. MSDB is designed specifically for mass spectrometry applications.
- NCBI nr is a comprehensive, non-identical protein database maintained by NCBI for use with their search tools BLAST and Entrez. The entries have been compiled from GeneBank CDS translations, PIR, SWISS-PROT, PRF, and PDB.
- SwissProt is a high quality, curated protein database. On this server, the database has been expanded using the Swissknife VARSPLIC utility. This parses the annotation text and creates new entries for any splice variants, sequence variants, or sequence conflicts. Original entries have a standard Swiss-Prot accession string, such as P13813. New entries, created by varsplc, have accession numbers in the form P13744-00-00-01. The title

line describes the nature of the differences between the new entry and the parent entry.

The result of the search appears in another web page, which automatically gives a short description of the protein and offers the option of a longer detail analysis of the protein that is matched.

1.3 Ageing and Apoptosis

Apoptosis (Greek: apo - from, ptosis - falling) was distinguished from traumatic cell death in 1972 by Andrew H. Wyllie while studying tissues with electron microscopes (54). He called this process of natural cell death apoptosis, from the use of this word in an ancient Greek poem to mean "falling off" and its connotations of leaves falling from a tree (54).

Apoptosis is a process of deliberate life relinquishment by a cell in a multicellular organism. It is one of the main types of programmed cell death (PCD), and involves an orchestrated series of biochemical events leading to a characteristic cell morphology and death. The apoptotic process is executed in such a way as to safely dispose of cell corpses and fragments.

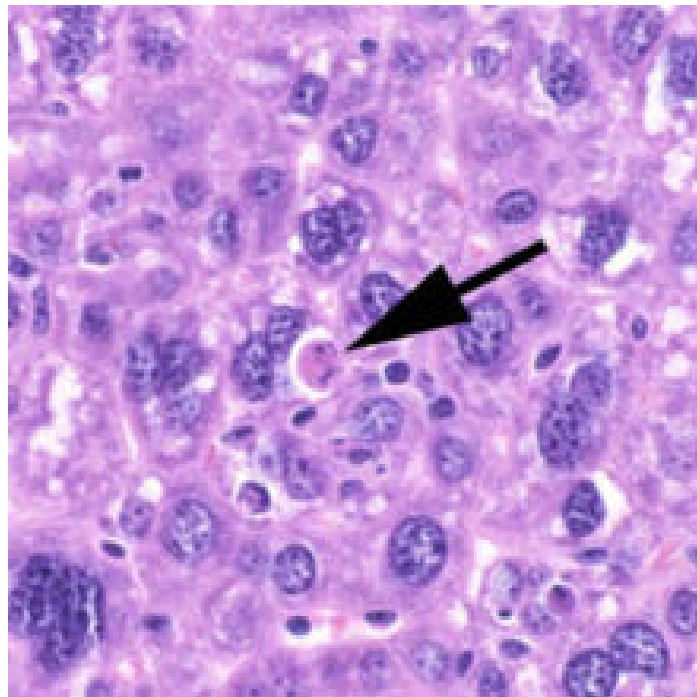


Fig .7 A section of mouse liver showing an apoptotic cell indicated by an arrow

In contrast to necrosis, which is a form of traumatic cell death that results from acute cellular injury, apoptosis is carried out in an orderly process that generally confers advantages during an organism's life cycle. For example, the differentiation of fingers and toes in a developing human embryo requires cells between the fingers to initiate apoptosis so that the digits can separate. Between 50 billion and 70 billion cells die each day due to

apoptosis in the average human adult. For an average child between the ages of 8 to 14, approximately 20 billion to 30 billion cells die a day. In a year, this amounts to the proliferation and subsequent destruction of a mass of cells equal to an individual's body weight.



Fig.8 Incomplete differentiation in two toes (syndactyly) due to lack of apoptosis

Research on apoptosis has increased substantially since the early 1990s. In addition to its importance as a biological phenomenon, defective apoptotic processes have been implicated in an extensive variety of diseases. Excessive apoptosis causes hypotrophy, such as in ischemic damage, whereas an insufficient amount results in uncontrolled cell proliferation, such as cancer.

Apoptosis can occur when a cell is damaged beyond repair, infected with a virus, or undergoing stress conditions such as starvation or ageing. DNA damage from ionizing radiation or toxic chemicals can also induce apoptosis via the actions of the tumour-suppressing gene p53. The "decision" for apoptosis can come from the cell itself, from the surrounding tissue, or from a cell that is part of the immune system. In these cases apoptosis functions to remove the damaged cell, preventing it from sapping further nutrients from the organism, or to prevent the spread of viral infection.

Apoptosis also plays a role in preventing cancer; if a cell is unable to undergo apoptosis, due to mutation or biochemical inhibition, it can continue dividing and develop into a tumour. For example, infection by papillomaviruses causes a viral gene to interfere with the cell's p53 protein, an important member of the apoptotic pathway. This interference in the

apoptotic capability of the cell plays a critical role in the development of cervical cancer.

1.3.1 Homeostasis

In adult organism, the number of cells is kept relatively constant through cell death and division. Cells must be replaced when they become diseased or malfunctioning; but proliferation must be compensated by cell death (55). This balancing process is part of the homeostasis required by living organisms to maintain their internal states within certain limits. Some scientists have suggested homeodynamics as a more accurate term (56, 57). The related term allostasis reflects a balance of a more complex nature by the body.

Homeostasis is achieved when the rate of mitosis (cell division) in the tissue is balanced by cell death. If this equilibrium is disturbed, one of two potentially fatal disorders occurs:

- The cells are dividing faster than they die, effectively developing a tumour.
- The cells are dividing slower than they die, which results in a disorder of cell loss.
- The organism must orchestrate a complex series of controls to keep homeostasis tightly controlled, a process which is ongoing for the life of the organism and involves many different types of cell signalling. Impairment of any one of these controls can lead to a diseased state: for example, deregulation of hedgehog signalling has been implicated in several forms of cancer. The hedgehog pathway, which conveys an anti-apoptotic signal, has been found to be activated in pancreatic adenocarcinoma tissues.

Programmed cell death is an integral part of both plant and animal tissue development. Development of an organ or tissue is often preceded by the

extensive division and differentiation of a particular cell, the resultant mass is then "pruned" into the correct form by apoptosis. Unlike cellular death caused by injury, apoptosis results in cell shrinkage and fragmentation. This allows the cells to be efficiently phagocytosed and their components reused without releasing potentially harmful intracellular substances into the surrounding tissue.

During development, apoptosis is tightly regulated and different tissues use different signals for inducing apoptosis. In birds, bone morphogenetic proteins (BMP) signaling is used to induce apoptosis in the interdigital tissue. In *Drosophila* flies, steroid hormones regulate cell death. Developmental cues can also induce apoptosis, such as the sex-specific cell death of hermaphrodite specific neurons in *C. elegans* males through low TRA-1 transcription factor activity (TRA-1 helps prevent cell death).

The process of apoptosis is controlled by a diverse range of cell signals which may originate either extracellularly (extrinsic inducers) or intracellularly (intrinsic inducers). Extracellular signals may include hormones, growth factors, nitric oxide (58, 59, 60, 61) or cytokines, and therefore must either cross the plasma membrane or transduce to effect a response. These signals may positively or negatively induce apoptosis; in this context the binding and subsequent initiation of apoptosis by a molecule is termed positive, whereas the active repression of apoptosis by a molecule is termed negative.

Intracellular apoptotic signalling is a response initiated by a cell in response to stress, and may ultimately result in cell suicide. The binding of nuclear receptors by glucocorticoids, heat, radiation, nutrient deprivation, viral infection and hypoxia are all factors which can lead to the release of intracellular apoptotic signals by a damaged cell (62). A number of cellular components, such as poly ADP ribose polymerase, may also help regulate apoptosis (63).

Before the actual process of cell death is carried out by enzymes, apoptotic signals must be connected to the actual death pathway by way of regulatory proteins. This step allows apoptotic signals to either culminate in cell death, or be aborted should the cell no longer need to die. Several proteins are involved, however two main methods of achieving regulation

have been identified; targeting mitochondria functionality, or directly transducing the signal via adapter proteins to the apoptotic mechanisms. The whole preparation process requires energy and functioning cell machinery.

1.3.2 Mitochondrial regulation

The mitochondria are essential to multicellular life, without them a cell ceases to respire aerobically and quickly dies - a fact exploited by some apoptotic pathways. Apoptotic proteins which target mitochondria affect them in different ways; they may cause mitochondrial swelling through the formation of membrane pores, or they may increase the permeability of the mitochondrial membrane and cause apoptotic effectors to leak out (64). There is also a growing body of evidence which indicates that nitric oxide (NO) is able to induce apoptosis by helping to dissipate the membrane potential of mitochondria and therefore make it more permeable (65).

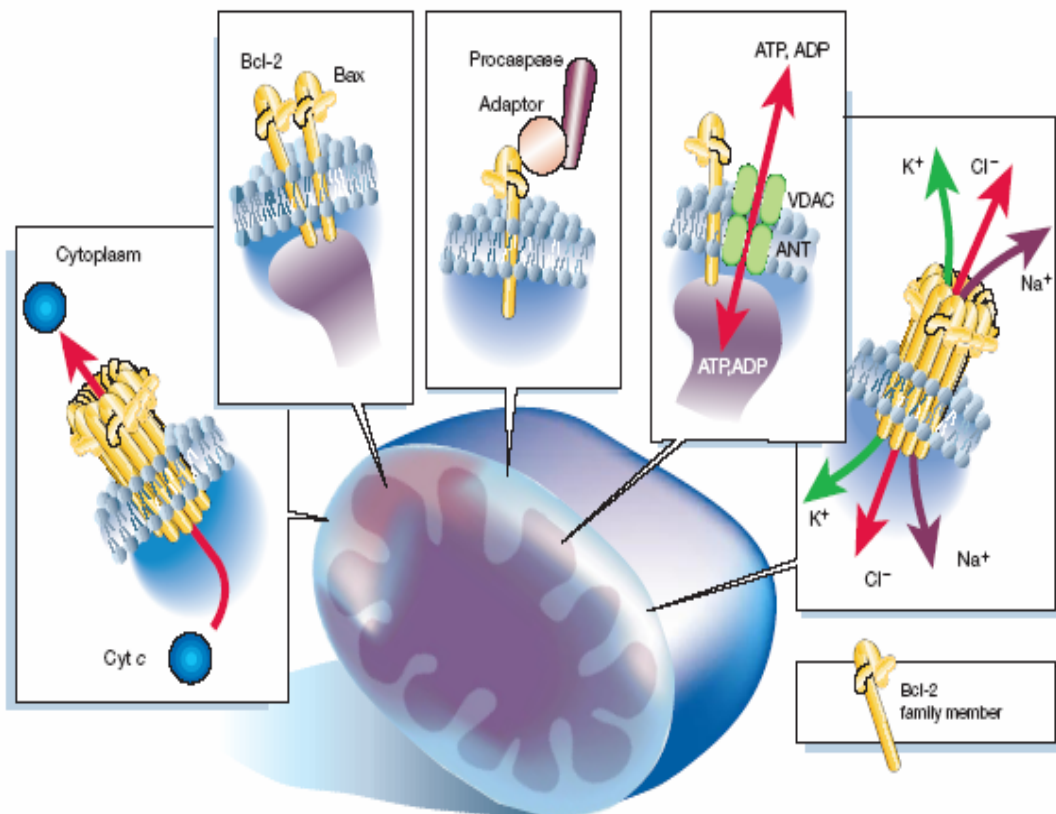


Fig 9. Mitochondrial regulation

Mitochondrial proteins known as SMACs (second mitochondria-derived activator of caspases) are released into the cytosol following an increase in permeability. SMAC binds to inhibitor of apoptosis proteins (IAPs) and inhibits them, preventing the IAPs from arresting the apoptotic process and therefore allowing apoptosis to proceed. IAP also normally suppresses the activity of a group of cysteine proteases called caspases (66), which carry out the degradation of the cell, therefore the actual degradation enzymes can be seen to be indirectly regulated by mitochondrial permeability.

Cytochrome c is also released from mitochondria due to increased permeability of the outer mitochondrial membrane, and serves a regulatory function as it precedes morphological change associated with apoptosis (67). Once cytochrome c is released it binds with Apaf-1 and ATP, which then bind to pro-caspase-9 to create a protein complex known as an apoptosome. The apoptosome cleaves the pro-caspase to its active form of caspase-9, which in turn activates the effector caspase-3.

The mitochondrial permeability is itself subject to regulation by various proteins, such as those encoded by the mammalian Bcl-2 family of anti-apoptotic genes, the homologs of the ced-9 gene found in *C. elegans* (68). Bcl-2 proteins are able to promote or inhibit apoptosis by either direct action on mitochondrial permeability, or indirectly through other proteins. Importantly, the actions of some Bcl-2 proteins are able to halt apoptosis even if cytochrome c has been released by the mitochondria (67).

Two important examples of the direct initiation of apoptotic mechanisms in mammals include the TNF-induced (tumour necrosis factor) model and the Fas-Fas ligand-mediated model, both involving receptors of the TNF receptor (TNFR) family (69) coupled to extrinsic signals.

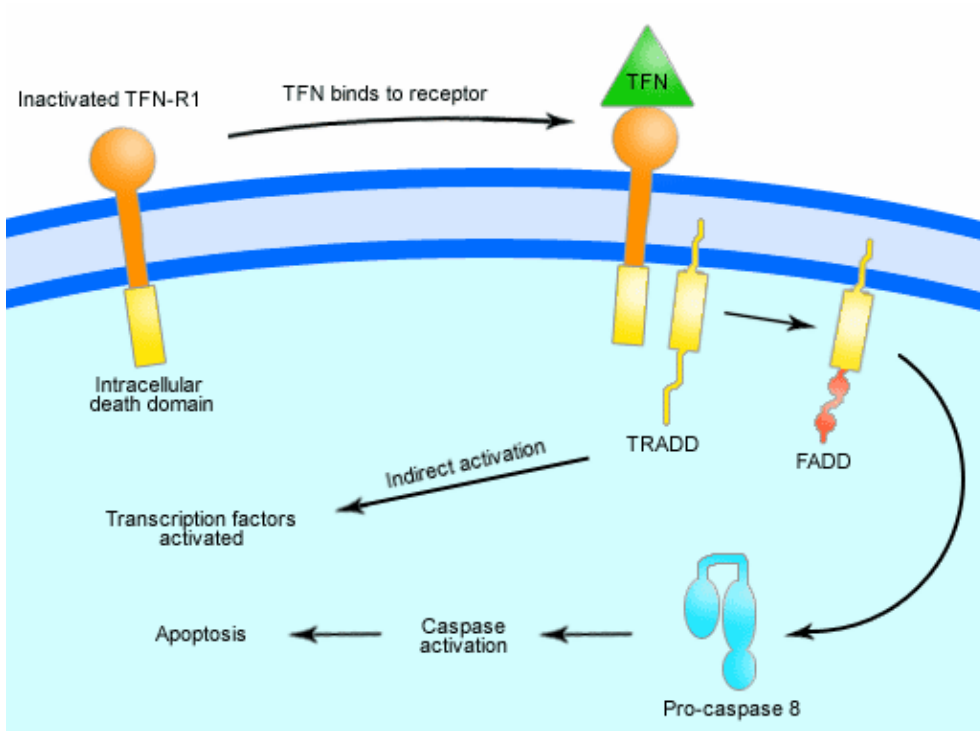


Fig.10 Overview of TNF signaling in apoptosis, an example of direct signal transduction

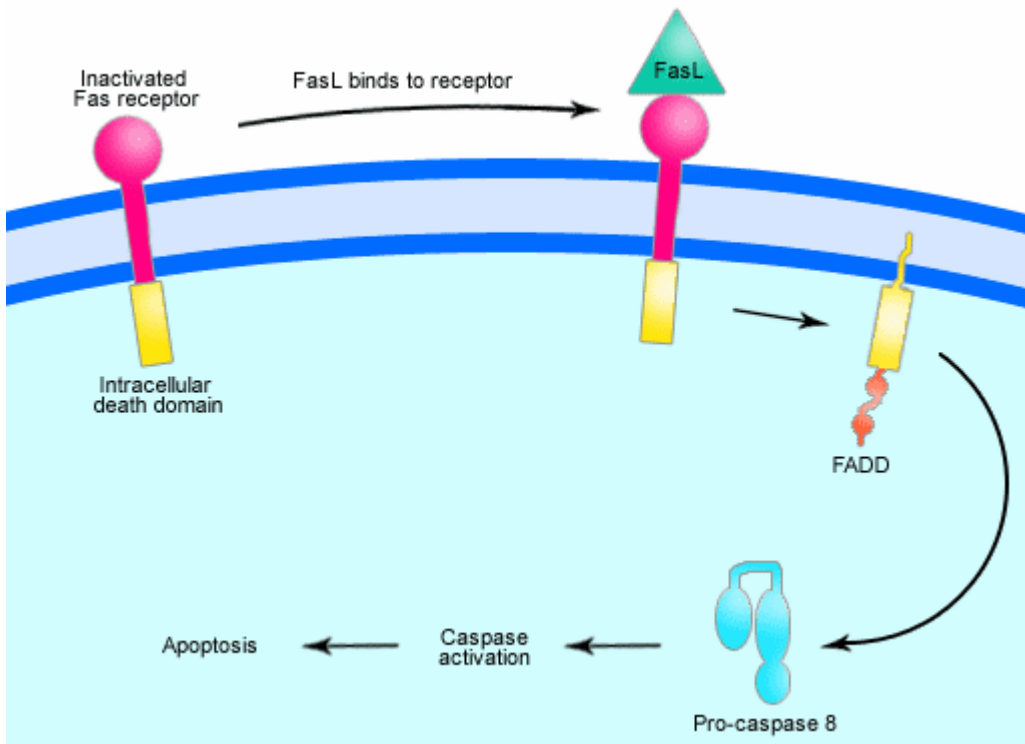


Fig. 11 Overview of Fas signaling in apoptosis, an example of direct signal transduction

TNF is a cytokine produced mainly by activated macrophages, and is the major extrinsic mediator of apoptosis. Most cells in the human body have

two receptors for TNF: TNF-R1 and TNF-R2. The binding of TNF to TNF-R1 has been shown to initiate the pathway that leads to caspase activation via the intermediate membrane proteins TNF receptor-associated death domain (TRADD) and Fas-associated death domain protein (FADD) (70). Binding of this receptor can also indirectly lead to the activation of transcription factors involved in cell survival and inflammatory responses (71). The link between TNF and apoptosis shows why an abnormal production of TNF plays a fundamental role in several human diseases, especially in autoimmune diseases.

The Fas receptor (also known as Apo-1 or CD95) binds the Fas ligand (FasL), a transmembrane protein part of the TNF family (72). The interaction between Fas and FasL results in the formation of the death-inducing signaling complex (DISC), which contains the FADD, caspase-8 and caspase-10. In some types of cells (type I), processed caspase-8 directly activates other members of the caspase family, and triggers the execution of apoptosis. In other types of cells (type II), the Fas-DISC starts a feedback loop that spirals into increasing release of pro-apoptotic factors from mitochondria and the amplified activation of caspase-8 (73).

Following TNF-R1 and Fas activation in mammalian cells a balance between pro-apoptotic (BAX [17], BID, BAK, or BAD) and anti-apoptotic (Bcl-Xl and Bcl-2) members of the Bcl-2 family is established. This balance is the proportion of pro-apoptotic homodimers that form in the outer-membrane of the mitochondrion. The pro-apoptotic homodimers are required to make the mitochondrial membrane permeable for the release of caspase activators such as cytochrome c and SMAC. Control of pro-apoptotic proteins under normal cell conditions of non-apoptotic cells is incompletely understood, but it has been found that a mitochondrial outer-membrane protein, VDAC2, interacts with BAK to keep this potentially-lethal apoptotic effector under control (74). When the death signal is received, products of the activation cascade displace VDAC2 and BAK is able to be activated.

1.3.3 Execution

Although many pathways and signals lead to apoptosis, there is only one mechanism which actually causes the death of the cell in this process; after the appropriate stimulus has been received by the cell and the necessary controls exerted, a cell will undergo the organised degradation of cellular organelles by activated proteolytic caspases. A cell undergoing apoptosis shows a characteristic morphology that can be observed with a microscope:

Cell shrinkage and rounding due to the breakdown of the proteinaceous cytoskeleton by caspases.

The cytoplasm appears dense, and the organelles appear tightly packed. Chromatin undergoes condensation into compact patches against the nuclear envelope in a process known as pyknosis, a hallmark of apoptosis (75).

The nuclear envelope becomes discontinuous and the DNA inside it is fragmented in a process referred to as karyorrhexis. The nucleus breaks into several discrete chromatin bodies or nucleosomal units due to the degradation of DNA (76).

The cell membrane shows irregular buds known as blebs.

The cell breaks apart into several vesicles called apoptotic bodies, which are then phagocytosed.

Apoptosis progresses quickly and its products are quickly removed, making it difficult to detect or visualize. During karyorrhexis, endonuclease activation leaves short DNA fragments, regularly spaced in size. These give a characteristic "laddered" appearance on agar gel after electrophoresis. Tests for DNA laddering differentiate apoptosis from ischemic or toxic cell death.

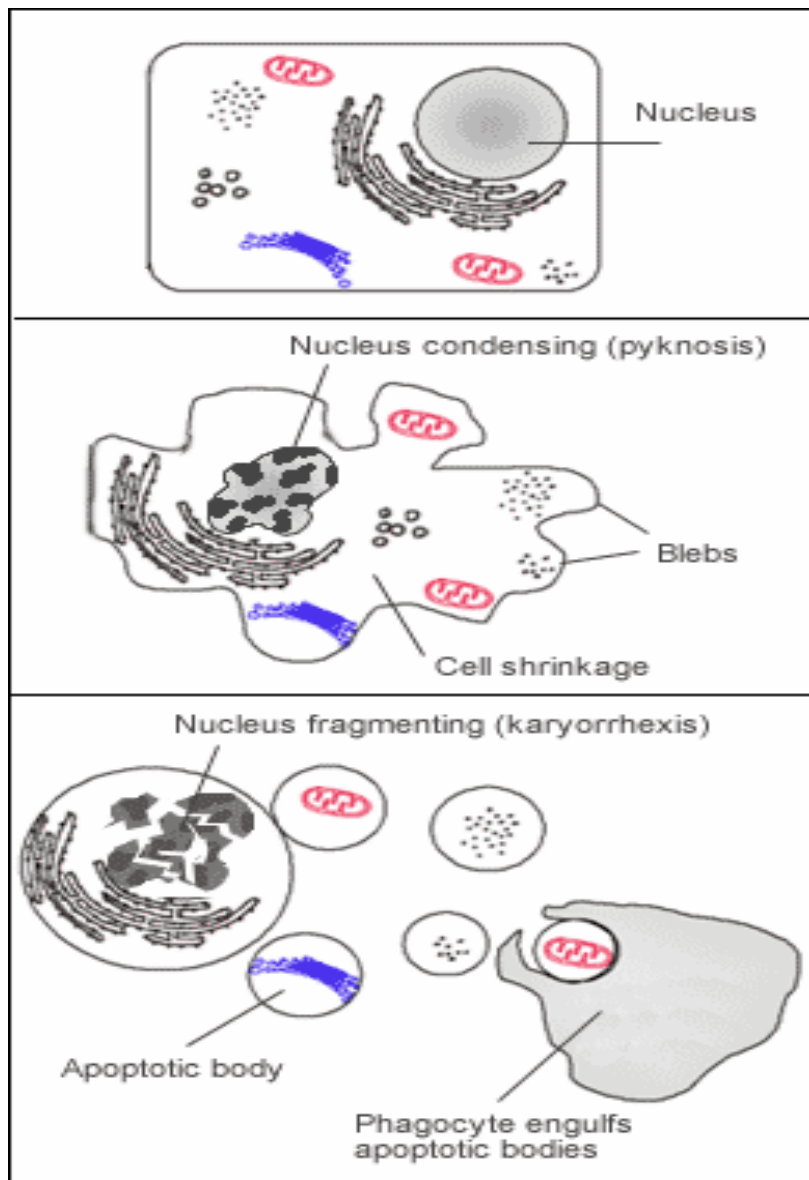


Fig 12. Execution of Apoptosis and dead cells removal

1.3.4 Removal of dead cells

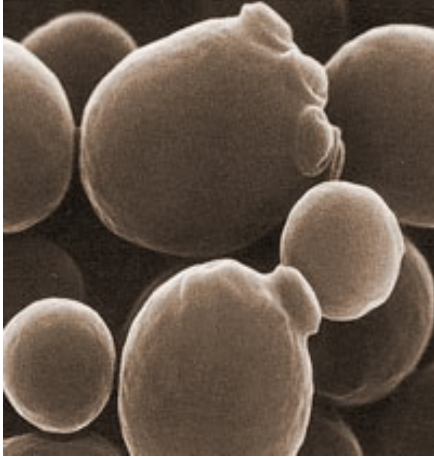
Dying cells that undergo the final stages of apoptosis display phagocytotic molecules, such as phosphatidylserine, on their cell surface. Phosphatidylserine is normally found on the cytosolic surface of the plasma membrane, but is redistributed during apoptosis to the extracellular surface by a hypothetical protein known as scramblase (77). These molecules mark the cell for phagocytosis by cells possessing the appropriate receptors, such as macrophages (78). Upon recognition, the phagocyte

reorganizes its cytoskeleton for engulfment of the cell. The removal of dying cells by phagocytes occurs in an orderly manner without eliciting an inflammatory response.

The many different types of apoptotic pathways contain a multitude of different biochemical components, many of them not yet understood. As a pathway is more or less sequential in nature it is a victim of causality; removing or modifying one component leads to an effect in another. In a living organism this can have disastrous effects, often in the form of disease or disorder. A discussion of every disease caused by modification of the various apoptotic pathways would be impractical, but the concept overlying each one is the same: the normal functioning of the pathway has been disrupted in such a way as to impair the ability of the cell to undergo normal apoptosis. This results in a cell which lives past its "use-by-date" and is able to replicate and pass on any faulty machinery to its progeny, increasing the likelihood of the cell becoming cancerous or diseased.

A recently described example of this concept in action can be seen in the development of a lung cancer called NCI-H460 (79). The X-linked inhibitor of apoptosis protein (XIAP) is overexpressed in cells of the H460 cell line. XIAPs bind to the processed form of caspase-9, and suppress the activity of apoptotic activator cytochrome c, therefore overexpression leads to a decrease in the amount of pro-apoptotic agonists. Consequently, the balance of anti-apoptotic and pro-apoptotic effectors is upset in favour of the former and the damaged cells continue to replicate despite being told to die.

1.3.5 Yeast and metazoan ageing



Yeast provides a simple and powerful model for the study of cellular complex mechanisms such as apoptosis caused by ageing, due to the presence of simplified regulatory pathways, comparing to more complex organisms, such as *Homo sapiens*.

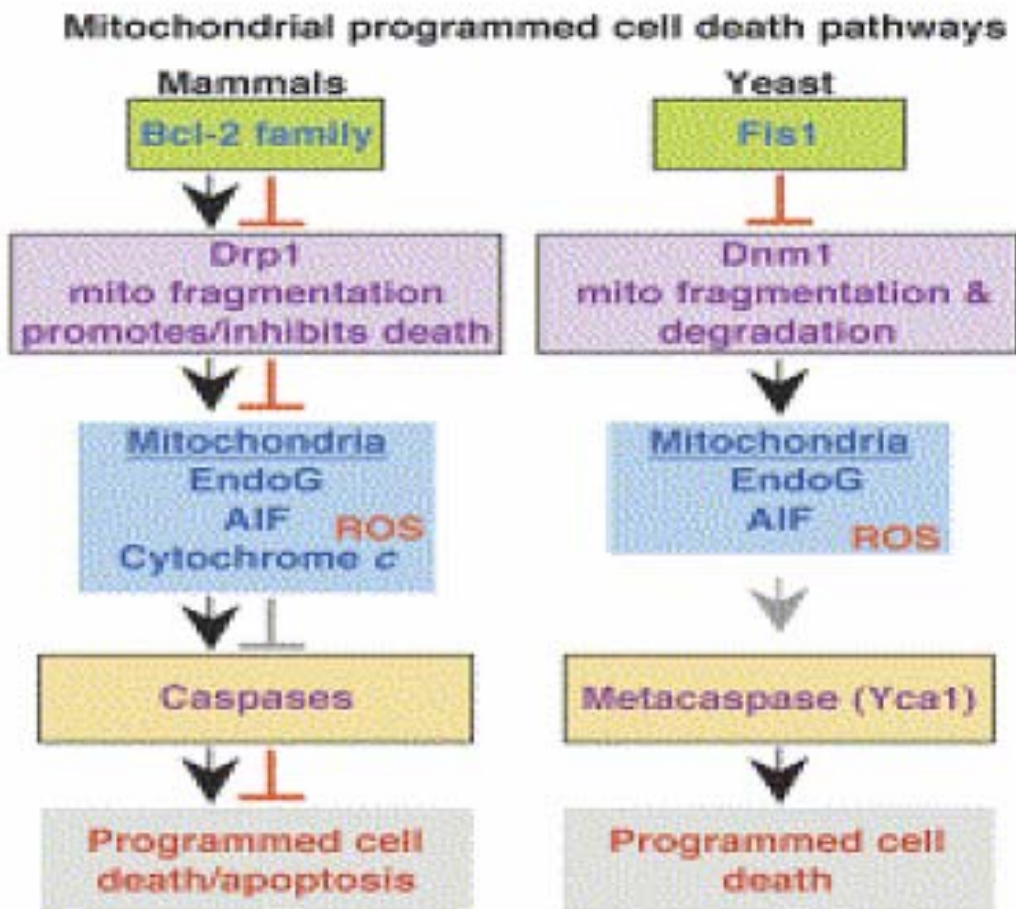
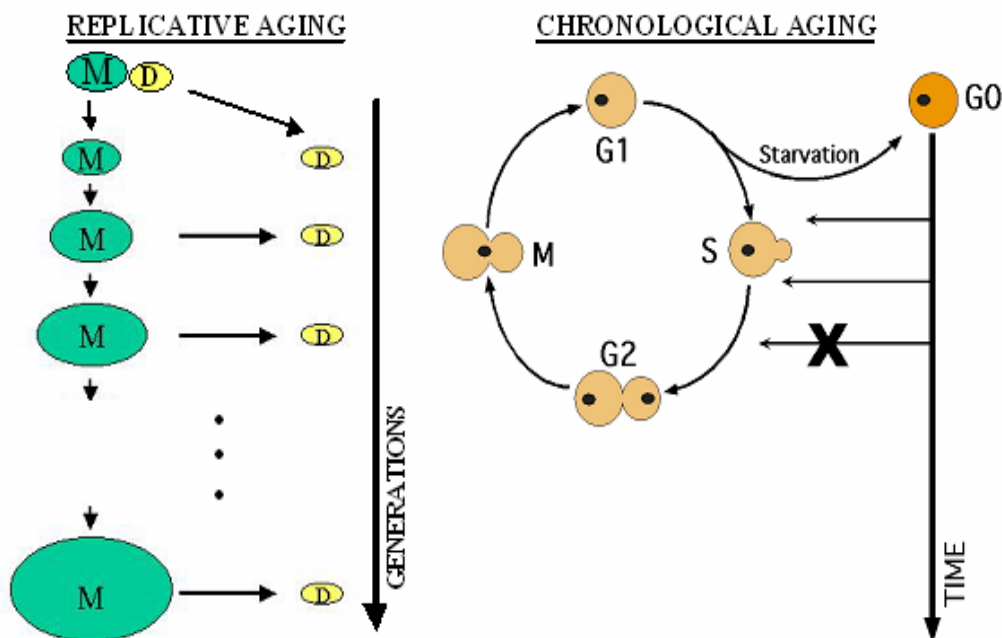


Fig 13 simplified pathways in yeast

In yeast, two different forms of aging processes are studied: one is mother cell-specific aging in which only the mother cell ages, while the daughter cell resets the clock to zero.

Age in this case is measured by cell generations, not by calendar time. The daughter cells remain in the stem cell pool while the other cell has made the first step towards differentiation. Resetting the clock is also known as “rejuvenation”, a process which is absolutely necessary for survival of the yeast strain.

Fig. 14 Scheme of yeast ageing forms



The second process of aging that can be studied in yeast is chronological aging of postmitotic cells. This aging process simply is the process of deterioration and loss of viability of cells during stationary phase. Again, like in mother cell-specific replicative aging, chronological aging is a process of genetically controlled cell differentiation. To give an example, the cell wall of stationary cells undergoes genetically controlled structural changes and remodelling. The chronological lifespan measures the ability of stationary (G0) phase yeast cultures to maintain viability over time (80, 81, 82). It is the a model of ageing in nondividing cells. (80,81,82,83). An increase in intracellular oxidative stress, in ROS and in “death factors”

seems to be common to the two aging processes as reported by many authors.

Reactive oxygen species generated by aerobic metabolism cause oxidative damage to cell macromolecules such as proteins, DNA and lipids inducing structure alteration and in many cases loss of function. It is now widely accepted that accumulation of these dysfunctional molecules during lifespan of the cell plays a key role in ageing process and degenerative diseases.

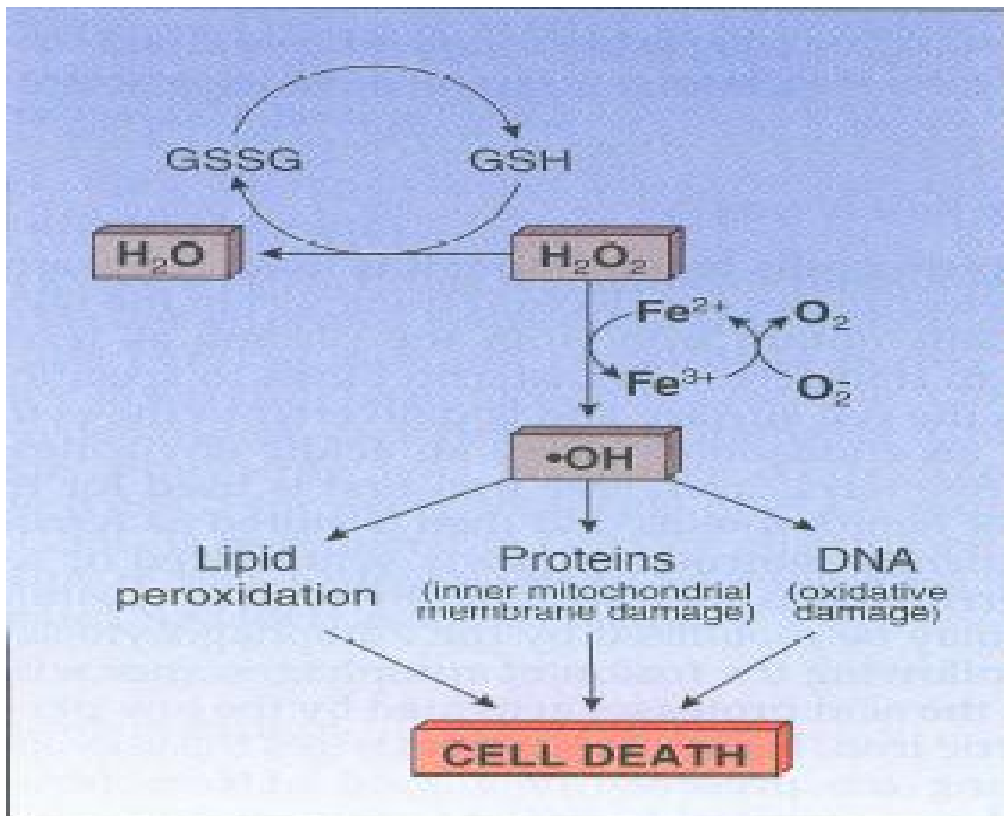


Fig.15 effect of H₂O₂ on cellular macromolecules

Harman's "free radical theory of aging" is now fifty years old; today although ROS are believed as the major cause of ageing many questions

remains opened. In particular is not clear the relationship between metabolism rate and ROS production. Furthermore, although many molecules are found in oxidized state during cell senescence, is not clear which are the relevant targets of oxidation and how their modification can affect lifespan.

In both forms of ageing, the terminal yeast cells execute apoptosis. This may elucidate some questions about the oxygen theory of ageing in mammalian cells. The involvement of oxygen toxicity in the ageing processes of cells as widely divergent as human and yeast leads to the proposal to use the powerful system of yeast molecular genetics to study the role of oxygen toxicity as a mechanism of ageing.

It has become clear through recent studies of yeast and human cells, that apoptosis is not only a mechanism to prevent ageing of a tissue by removing irreversibly damaged cells which can then be replaced by regeneration.

Yeast cells are also an excellent system to test other current theories of ageing. Prominent among them are the theory according to which an ageing signal is produced by critically short telomeres and the theory according to which unrepaired DNA damage leads to premature ageing and apoptosis.

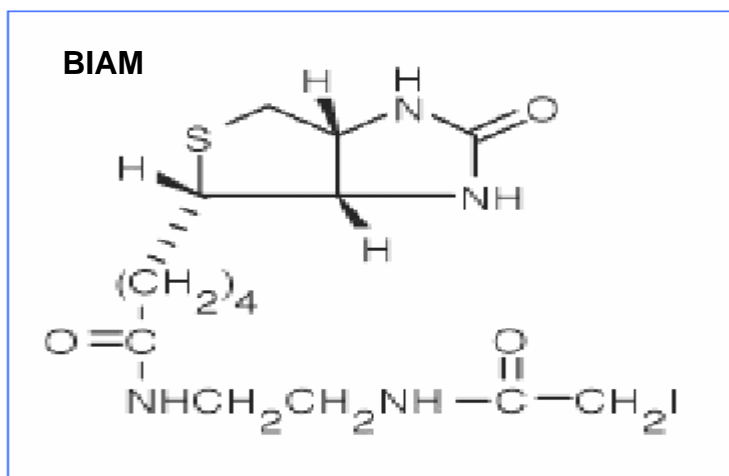
In non-dividing cells, essential components that become damaged cannot be diluted out through cell division but must, of necessity, be turned over and renewed. By elevating stress resistances, many of the activities needed for such renewal should be elevated with commensurate reduction in the steady-state levels of damaged cell components. Therefore, chronological lifespan in particular might be expected to relate to stress resistance. For yeast to attain a full chronological lifespan requires the expression of the general stress response. It is more important, though, that the cells should be efficiently adapted to respiratory maintenance, since it is culture grown to stationary phase on respiratory media that usually display the longest chronological lifespan. For this reason, respiration-adapted cells potentially provide a better model of chronological ageing than cultures pre-grown on glucose. (84)

2. Aim of the project

The proteomic approach offers all the instruments to deeply understand the mechanisms of this phenomenon. The high capacity of the analytical technique used in proteomics to resolve complex mixture of proteins extracted from a cell and the very sensitive techniques used to identify them, led in the last few years to a better understanding of apoptosis.

A procedure for detecting proteins that contain oxidation-sensitive cysteine residues, as a means to study protein oxidation from different growth conditions in yeast cells, was the main goal of this project.

The procedure is based on the fact that biotin-conjugated iodoacetamide



(BIAM) selectively reacts with free thiols in cysteine residues (Fig.16).

The decrease in proteins labelling with BIAM can be monitored by western blot analysis.

Thiol (SH) groups play a broad range of roles in the cell, since their redox state can affect the activity and the structure of enzymes, receptors and transcription factors.

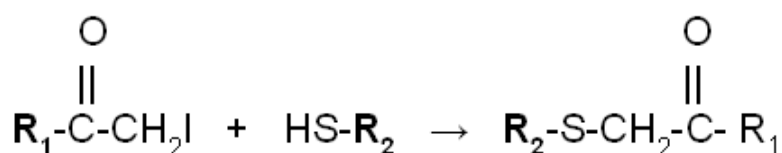


Fig. 16 Reaction between BIAM and cysteine thiol group

In this study we evaluated the redox state of proteins combining a selective method for labelling proteins containing reduced cysteine residues and mono/two dimensional electrophoresis followed by mass spectrometry. In fact cysteine residues can react with ROS and can function as detector of redox status of the cells. In particular we compared yeast cells exponentially growing with cells during chronological ageing. The experiments were performed in complete synthetic medium (SC) containing three different carbon source: glucose 2%, glucose 0,5% and 3% glycerol. SC plus 2% glucose is the standard medium used from many authors to study the chronological aging features. In this condition yeast cells initially obtain energy through fermentation pathway and approximately after 10 hours, when the glucose concentration reaches very low level, yeasts switch to respiration pathway. This switch is called "diauxic shift" and then yeast enter in the post-diauxic phase. In this phase cells grow slowly until about 48 hours and then stop dividing but the metabolic rate remain high until approximately one week (80). SD plus 0,5% glucose is the medium used to mimic caloric restriction; in this condition yeast cells show an increase of life span probably through a decrease in ROS production although the mechanism involved in this reduction is still debated. For the first time we also tested a role of a poor fermentable carbon source as glycerol on yeast chronological aging.

3. Material and Methods

The strain used in this study is W303-A (MATa leu2-3,112ura3-1 trp1-92 his3-11, 15 ade2-1 can1, 100, GAL SUC mal). Yeast cells were grown at 30°C in complete SC medium (0,17% yeast nitrogen base without aminoacid) supplemented with complete dropout and a four-fold excess of leucine, tryptophan, adenine, histidine, and uracil. These supplements were added in excess to prevent any growth limitation due to the auxotrophies of the W303. 2% glucose, 0,5% glucose or 3% glycerol were used as carbon sources. YEPD solid medium (1% yeast extract, 2% peptone, 2% w/v glucose, 2% w/v agar used as carbon sources) was used to perform viability assay.

Cells viability assay

Cell viability was measured by plating serial dilution of treated and untreated cells on YEPD plates. The percentage of colony-forming units (c.f.u.) of cells treated was obtained by relating the c.f.u. counts of treated cells to those untreated which were considered to be 100%. Viability is defined as the ability of a single cell to form a colony within 2 days.

Cystein residues labelling

Cells grown in SC medium supplemented with glucose 2%, glucose 0,5% or 3% glycerol were harvested in exponential phase (0,8 O.D./ml) and after 24, 48, 72 hours and one week. For 1D electrophoresis 1 O.D. of cells were broken in RIPA buffer (25 mM Tris-HCl pH 7.6, 150 mM NaCl, 1% NP-40, 1% Sodium deoxycholate and 0.1 % SDS) containing 40 µM biotinylated iodoacetamide, BIAM (Molecular Probes) with glass beads in a Fastprep instrument (Savant) and protein extracts were clarified by centrifugation at 8000g for 10 minutes. For 2D electrophoresis cells were broken 8M urea, 4% CHAPS, 200 µM BIAM and Tris-HCl pH7. In both cases the labelling reaction was stopped with 10mM DTT.

Affinity chromatography

After cysteine residues labelling yeast extract sample was submitted to a purification protocol using immobilized avidin resin. This is a chromatographic procedure based on affinity between avidin and biotin: proteins labelled with BIAM binds resin making their isolation possible.

Resin had been equilibrated by 0,1 M phosphate, 0,15 M sodium chloride, pH7,2 buffer washing . Cellular extracts had been incubated with resin over night at 4°C. After washing procedure by washing buffer, in order to remove non BIAM containing proteins, samples were eluted by 30% Acetonitrile, 0,4% TFA

Electrophoresis and western blot.

For 1D electrophoresis labelled samples were prepared as previously described, separated on SDS-PAGE and transferred on PVDF membrane (Millipore). 2D electrophoresis IEF (first dimension) was carried out on non-linear wide-range immobilized pH gradients (pH 3-10; 18 cm long IPG strips; GE Healthcare, Uppsala, Sweden) and achieved using the Ettan IPGphor system (GE Healthcare, Uppsala, Sweden). Analytical-run IPG-strips were rehydrated with 60µg of total proteins in 350µl of lysis buffer and 0,2% (v/v) carrier ampholyte for 1h at 0 V and for 8h at 30 V, at 16°C. The strips were then focused according to the following electrical conditions at 16°C: 200 V for 1h, from 300 V to 3500 V in 30 min, 3500 V for 3h, from 3500 V to 8000 V in 30 min, 8000 V until a total of 80000 Vh was reached. For preparative gels 400µg of total proteins were used. After focusing, analytical and preparative IPG strips were equilibrated for 12 min in 6 M urea, 30% (V/V) glycerol, 2% (w/V) SDS, 0.05 M Tris-HCl, pH 6.8, 2% (w/V) DTE, and subsequently for 5 min in the same urea/SDS/Tris buffer solution but substituting the 2% (w/V) DTE with 2.5% (w/V) iodoacetamide. The second dimension was carried out on 9-16% polyacrylamide linear gradient gels (18 cm x 20 cm x 1.5 mm) at 40 mA/gel constant current and 10°C until the dye front reached the bottom of the gel, according to Laemmli *et al* and Hochstrasser *et al*. Analytical gels were stained with ammoniacal silver nitrate as previously described [ref]; while MS-preparative gels were stained with colloidal comassie. For western blot

of 2D gels 150 µg of total proteins were transferred on PDVF membrane overnight at 4°C using a constant current of 100mA.

In all cases the blots were incubated at least four hours with blocking buffer (PBS, 2% non-fat dry milk, 0.1% v/v Tween-20). Biotinylated proteins were detected incubating PVDF membrane with streptavidine conjugated horse radish peroxidase (Biorad). The chemiluminescence immunodetection system (GE Healthcare) was used for signal development.

Image analysis

Gels and western blot images were acquired with an Epson expression 1680 PRO scanner. Computer-aided 2-D image analysis was carried out using the MELANIE 4.0 software (GeneBio, Geneva, Switzerland). Relative spot volumes (%V) ($V = \text{integration of OD over the spot area}$; $\%V = V \text{ single spot} / V \text{ total spot}$) were used for quantitative analysis in order to decrease experimental errors. The normalized intensity of spots on three replicate 2-D gels was averaged and standard deviation was calculated for each condition. A two-tailed non-paired Student's T-test was performed using ORIGIN 6.0 (Microcal Software, Inc.) to determine if the relative change was statistically significant. Reported pI and Mr (Da) values were experimentally determined by comigration with human serum as internal standard.

Protein identification by Mass Spectrometry

TPCK-treated Trypsin, dithiothreitol, and alfa-cyano-4-hydroxycinnamic acid were from Sigma-Aldrich (St. Louis, MO, USA). All other reagents and solvents were of the highest purity available from Carlo Erba (Milan, Italy).

In situ digestion

The analysis was performed on the Coomassie blue-stained spots excised from gels. The excised spots were washed first with ACN and then with 0.1M ammonium bicarbonate. Protein samples were reduced by incubation in 10mM dithiothreitol (DTT) for 45 min at 56°C. The cysteines were alkylated by incubation in 5mM iodoacetamide for 15 min at room

temperature in the dark. The gel particles were then washed with ammonium bicarbonate and ACN.

Enzymatic digestion was carried out with trypsin (12.5ng/μl) in 50mM ammonium bicarbonate pH 8.5 at 4°C for 4 hours. The buffer solution was then removed and a new aliquot of the enzyme/buffer solution was added for 18 hours at 37°C. A minimum reaction volume, enough for the complete rehydration of the gel was used. Peptides were then extracted washing the gel particles with 20mM ammonium bicarbonate and 0.1% TFA in 50% ACN at room temperature and then lyophilised.

MALDI-TOF Mass spectrometry

Positive Reflectron MALDI spectra spectra were recorded on a Voyager DE STR instrument (Applied Biosystems, Framingham, MA). The MALDI matrix was prepared by dissolving 10 mg of alpha cyano in 1 mL of acetonitrile / water (90:10 v/v). Typically, 1 uL of matrix was applied to the metallic sample plate and 1 uL of analyte was then added. Acceleration and reflector voltages were set up as follow: target voltage at 20 kV, first grid at 95% of target voltage, delayed extraction at 600 ns to obtain the best signal-to-noise ratios and the best possible isotopic resolution with multipoint external calibration using peptide mixture purchased from Applied Biosystems. Each spectrum represents the sum of 1500 laser pulses from randomly chosen spots per sample position.

Raw data were analyzed using the computer software provided by the manufacturers and are reported as monoisotopic masses.

nanoLC Mass Spectrometry

A mixture of peptide solution was analysed by LCMS analysis using a 4000Q-Trap (Applied Biosystems) coupled to an 1100 nano HPLC system (Agilent Technologies). The mixture was loaded on an Agilent reverse-phase pre-column cartridge (Zorbax 300 SB-C18, 5x0.3 mm, 5 μm) at 10 μl/min (A solvent 0.1% formic acid, loading time 5 min). Peptides were separated on a Agilent reverse-phase column (Zorbax 300 SB-C18, 150 mm X 75μm, 3.5 μm), at a flow rate of 0.3 μl/min with a 0% to 65% linear gradient in 60 min (A solvent 0.1% formic acid, 2% ACN in MQ water; B

solvent 0.1% formic acid, 2% MQ water in ACN). Nanospray source was used at 2.5 kV with liquid coupling, with a declustering potential of 20 V, using an uncoated silica tip from New Objectives (O.D. 150 μm , I.D. 20 μm , T.D. 10 μm). Data were acquired in information-dependent acquisition (IDA) mode, in which a full scan mass spectrum was followed by MS/MS of the 5 most abundant ions (2 s each). In particular, spectra acquisition of MS-MS analysis was based on a survey Enhanced MS Scan.(EMS) from 400 m/z to 1400 m/z at 4000 amu/sec. This scan mode was followed by an Enhanced Resolution experiment (ER) for the five most intense ions and then MS² spectra (EPI) were acquired using the best collision energy calculated on the bases of m/z values and charge state (rolling collision energy) from 100 m/z to 1400 m/z at 4000 amu/sec. Data were acquired and processed using Analyst software (Applied Biosystems).

MASCOT analysis

Spectral data were analyzed using Analyst software (version 1.4.1) and MS-MS centroid peak lists were generated using the MASCOT.dll script (version 1.6b9). MS-MS centroid peaks were threshold at 0.1% of the base peak. MS/MS spectra having less than 10 peaks were rejected. MS/MS spectra were searched against NCBI nr database using the licensed version of Mascot 2.1 version (Matrix Science), after converting the acquired MS-MS spectra in mascot generic file format. The Mascot search parameters were: taxonomy *Saccharomyces cerevisiae*; allowed number of missed cleavages 2; enzyme trypsin; variable post-translational modifications, methionine oxidation, pyro-glu N-term Q; peptide tolerance 200ppm and MS/MS tolerance 0.5 Da; peptide charge, from +2 to +3 and top 20 protein entries. Spectra with a MASCOT score <25 having low quality were rejected. The score used to evaluate quality of matches for MS-MS data was higher than 30. However, spectral data were manually validated and contained sufficient information to assign peptide sequence and BIAM labelled Cysteine.

Confocal microscopy analysis and mitochondria function assay

Cells grown in SD complete medium were harvested at the indicated time. 1 O.D. of cells were washed twice in 10 mM HEPES buffer containing 5% glucose and resuspended in the same buffer with 100nM Rhodamine B hexyl ester or 2,5 μ M dihydrorhodamine 123 (both 123 from Molecular Probes) in order to evidence mitochondrion structure and ROS production respectively. The cells were incubated at 30° C in the dark for 45 minutes for rhodamine B hexyl ester staining and for 2 hours for dihydrorhodamine 123 staining. The treated cells washed twice in 10mM Hepes buffer, 5% glucose were visualized on Laika

Cytochrome spectra and respiration

Each cytochrome is characterized by a peak of absorption at a specific wavelength: cytochrome aa₃ = 602 nm (cytochrome c oxidase); cytochrome b = 560 nm; cytochrome c = 550 nm. Differential spectra between reduced and oxidized cells were recorded at room temperature, using a Cary 219 spectrophotometer, following the absorption of cellular samples from 630 nm to 540 nm. The height of each peak relative to the baseline of each spectrum is an index of cytochrome content (Dequard et al., 1980).

Oxygen uptake rate was measured at 30°C using a Hansatech Oxygraph. 100 μ l of a suspension of cells were added in the respiration buffer (0.1M K-Phthalate, pH 5.0). The rate of decreasing in oxygen content related to the amount of cells (dry weight) is an index of the respiratory ability of the analysed strain (Foury, 1989).

4. RESULTS

4.1 Calorie restriction and glycerol increase chronological life span.

S. cerevisiae cells were grown in complete synthetic medium (SC) containing three different carbon source: 2% glucose, 0.5% glucose and 3% glycerol. SC plus 2% glucose (SCD) constitutes the standard medium used to study chronological ageing features (2), whereas the reduction of glucose content in the media from 2% to 0.5% is a model for caloric restriction (CR) in yeast (12). When the glucose level is limited, respiration is preferred to fermentation and carbon is directed to the mitochondria increasing electrons transport and respiration. Finally, the non-fermentable substrate glycerol (SCG) drives the energy metabolism toward respiration as the unique way to produce ATP.

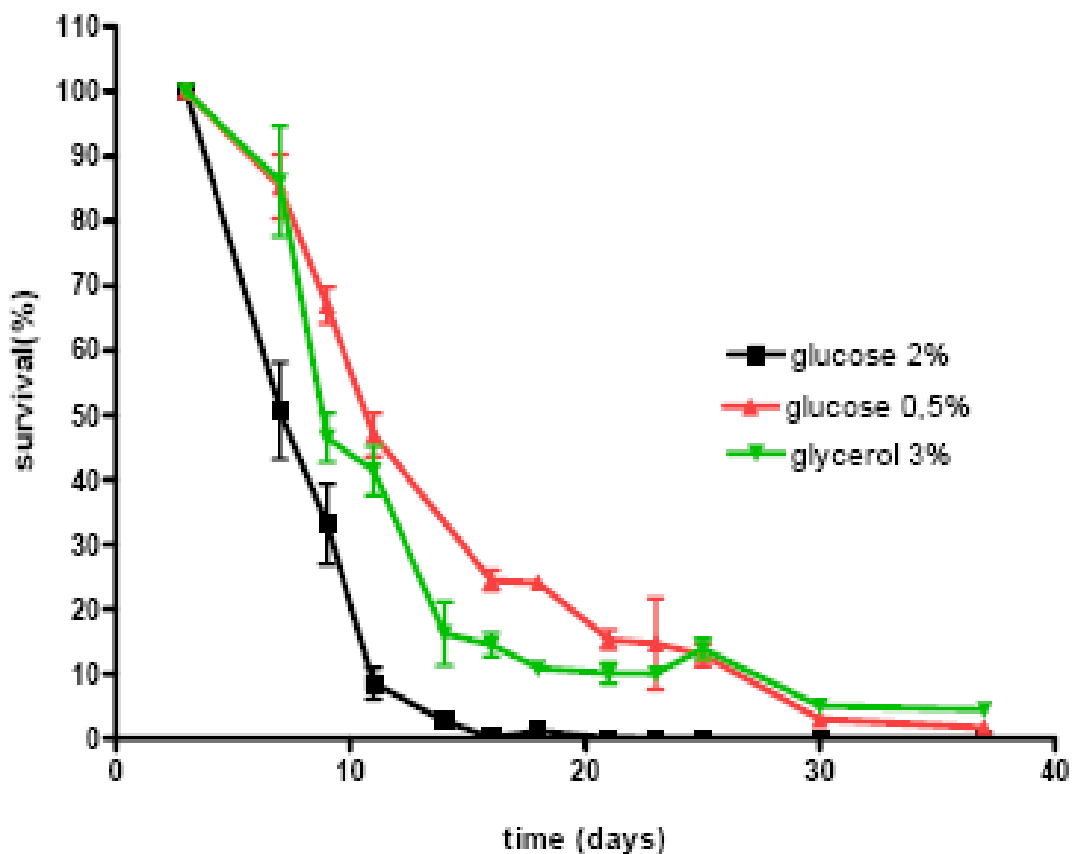


Fig17. Cell viability on different carbon sources. The percentage of colony-forming units (c.f.u.) of yeast cells was obtained by relating the c.f.u. counts of cells during ageing to those at the beginning of stationary phase which were considered to be 100%. The graphic is representative of three different independent experiment.

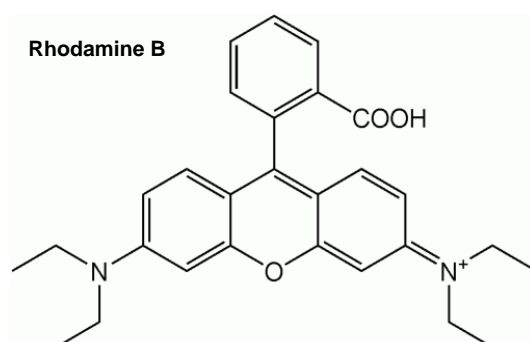
The ability of 3% glycerol (SCG) and/or caloric restriction (CR) to extend chronological lifespan of yeast cells was firstly examined (Fig. 17). Cell viability on different carbon sources was determined by measuring the percentage of colony-forming units (c.f.u.) of yeast cells during ageing. Figure 17 shows that the viability of yeast strains varies dramatically in different media conditions. When *S. cerevisiae* was grown in SCD, less than 10% of the cells were viable after 10 days whereas more than 50% of the cells were still viable after the same period when the cells were cultured in CR. Moreover, growing on a respiratory substrate as SCG yielded more than 40% of the yeast cells viable after 10 days.

According to these results, yeast cells grown for 72h (3 days) were selected as a model for chronologically aged cells during all the experiments as in these conditions the yeast cells in late stationary growth phase (non-dividing cells) gradually senesce but they are still alive.

4.2 ROS production, and mitochondria phenotypes during chronological aging in different carbon source.

Cellular ageing results in oxidative stress caused by the accumulation of oxygen-containing free radicals (81,82,83,84).

The relationship between ageing and oxidative stress was then verified in the three different carbon sources (SCD, SCG and CR) by evaluating the amount of ROS production with dihydrorhodamine (DHR) 123 during the growth. DHR123 is a nonfluorescent dye able to enter into the cells where it is oxidized by oxidative species or the cellular redox system to the fluorescent rhodamine 123 that accumulates in the mitochondrial membranes.



A relatively low and comparable ROS production was observed in yeast cells in the exponential growth phase independently from the different carbon source (data not shown). However, the growth medium greatly affected ROS production during ageing. When the ROS level was compared in chronologically aged cells (72h), oxidation of DHR resulted to be considerably higher in yeast grown on SCD in comparison to CR or SCG. Figure 18 panel A shows that about 70% of the cells were stained with fluorescent DHR after 72h of growth in SCD indicating a high level of ROS production. On the contrary, the percentage of fluorescent cells after the same period of growth was less than 20% when CR or SCG were used as

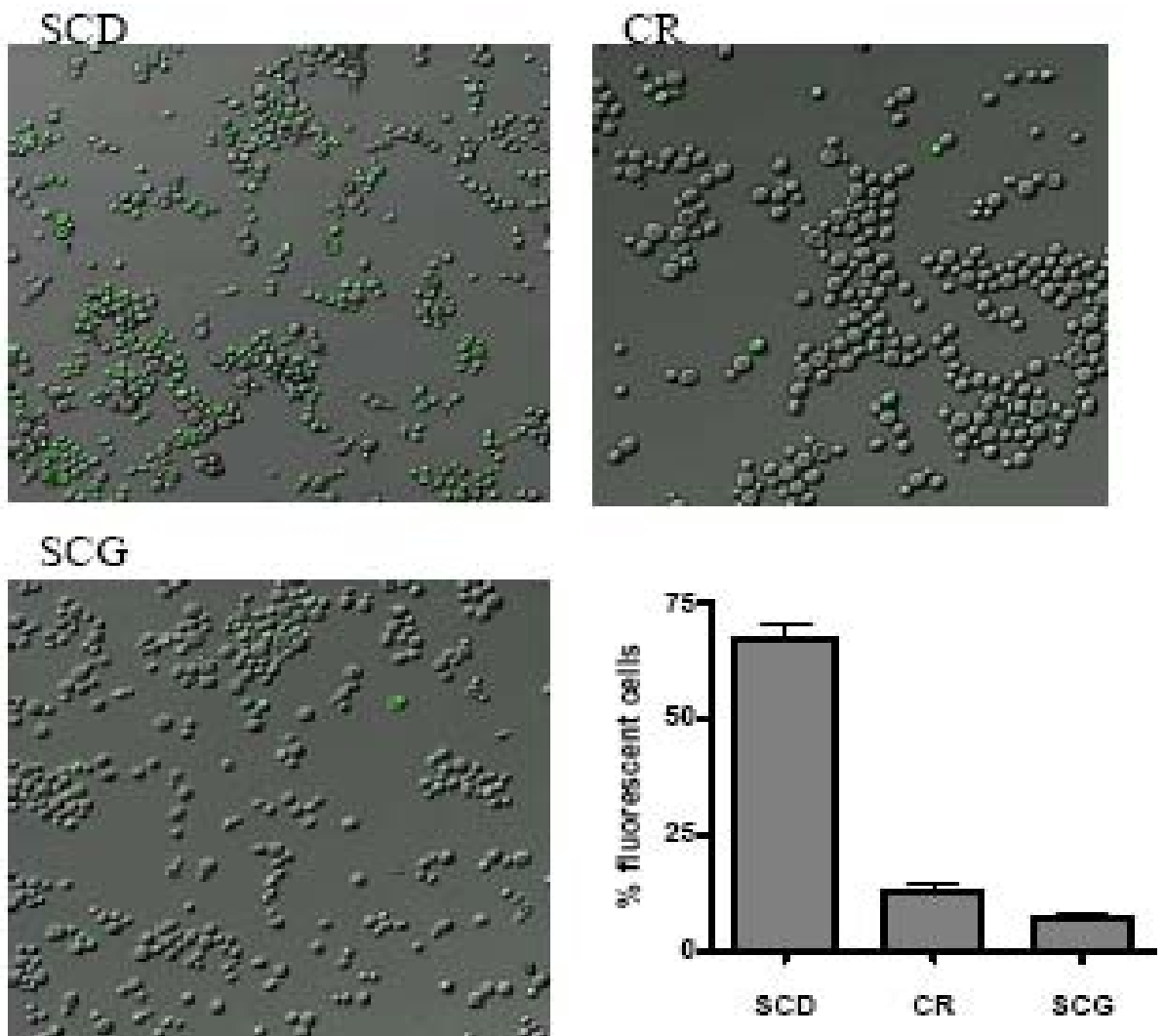
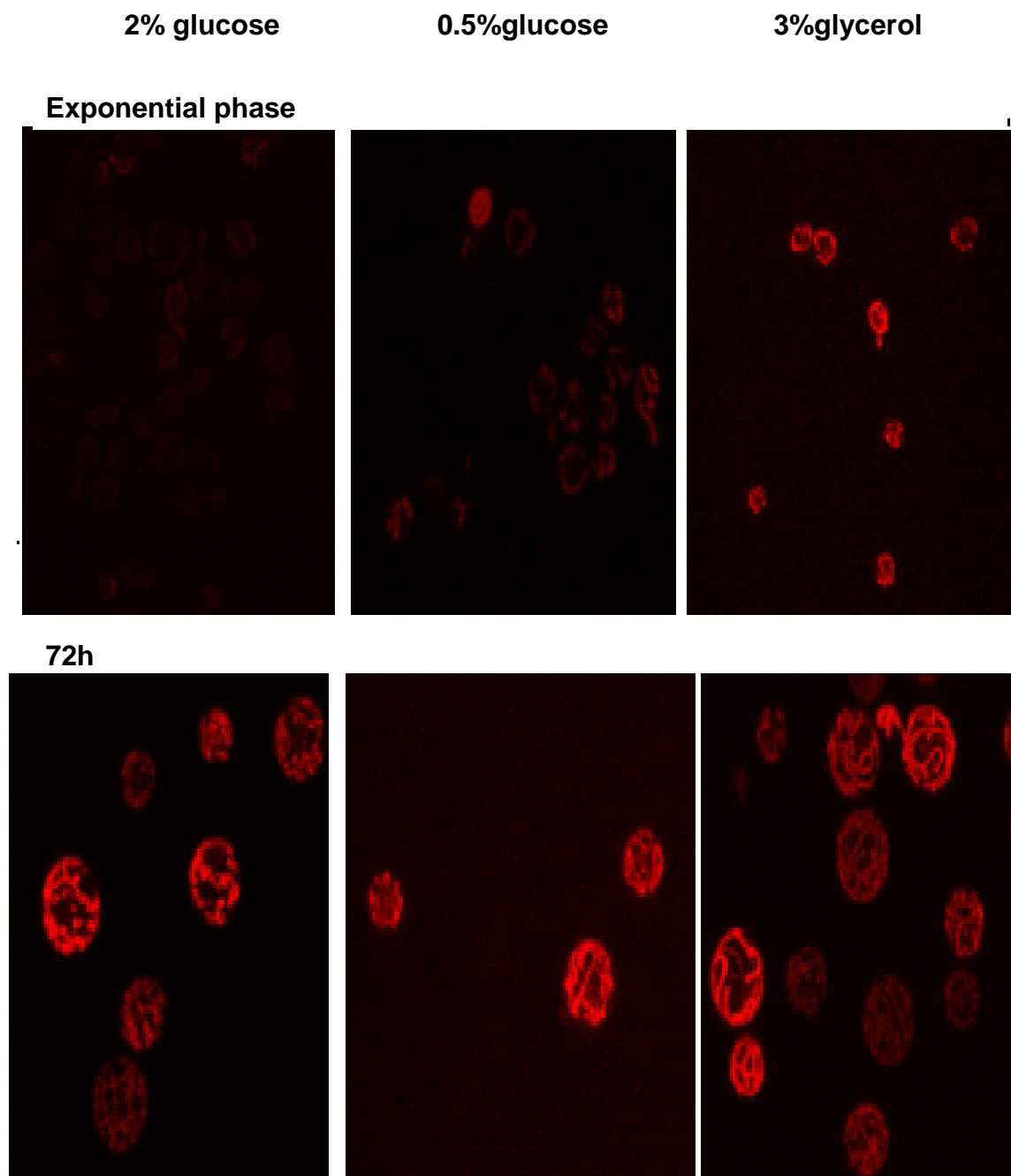


Fig.18 Panel A

used as carbon source, suggesting a reduced level of ROS accumulation.

Since mitochondria constitute the major source of ROS generation in the cell, the morphology of mitochondria in aged cells was analyzed using the plasmid pYX232-mtGFP that allows GFP to be specifically located into the organelles. Figure 18B shows that during ageing the morphology of SCD mitochondria became similar to those of CR and SCG (magnified images in Fig 18B) according to the switch to a derepressed state characteristic of low



glucose level after 72h of growth. It is interesting to note that the number of GFP-labelled yeast cells drastically decreased during ageing in SCD in comparison with the other two conditions, as shown in Fig. 18B. This decrease is clear just at 24 hours likely indicating that the aged cells in SCD are not proficient to retain or to correctly reproduce functional mitochondria. Moreover, growth conditions differently affected the mitochondria structure. In the exponential phase, yeast cells growing on CR and particularly on SCG showed a large number of small mitochondria whereas few, large and branched organelles (described as mitochondria reticula) were detected in cells growing in a reach glucose medium. These observations confirmed previous data from by Vissel et al. who extensively analysed the reticula morphology in different growth conditions Fleury et al., 2002.

4.3 O₂ consumption and cytochrome content during cronological life span in different carbon source

As yeast cells grown on different carbon sources showed different ROS release, the ability of the yeast to respire in the different conditions was measured by evaluating the rate of mitochondrial oxygen consumption after 24 and 72 hours of growth. As shown in Fig. 19A, at 24 hours similar values of oxygen consumption rate were observed for the cells independently from the growth conditions. However, after 72 hours of growth the oxygen consumption decreased to 30% for the cells in SCD while a lower decrease

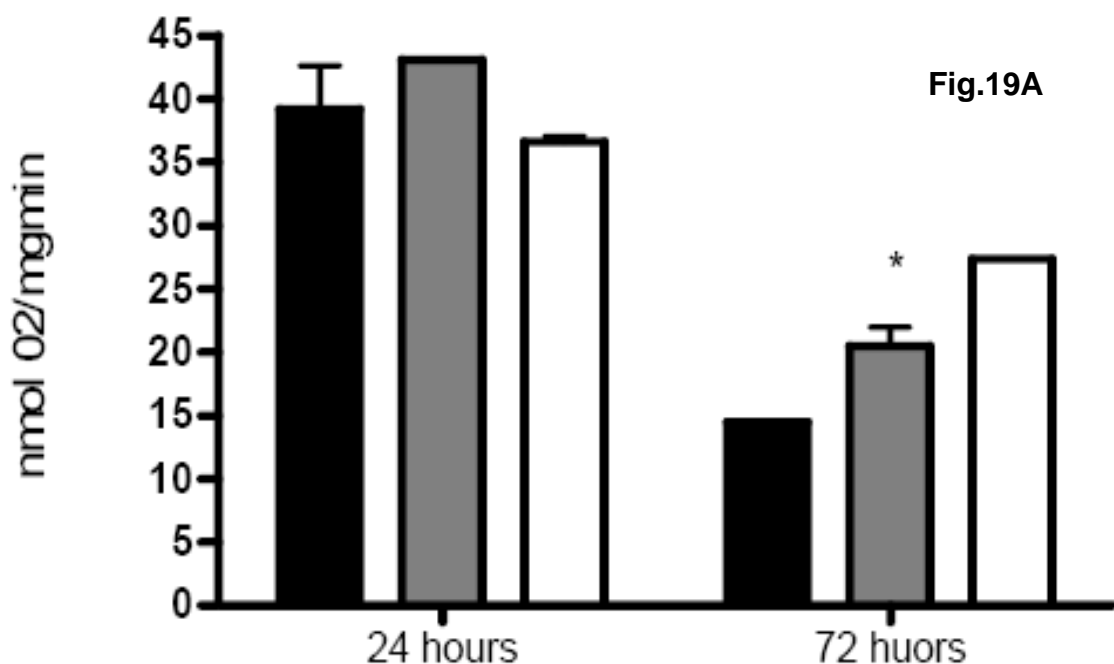


Fig. 19 A. O₂ consumption in SCD (black bars), CR (squared bars) and SCG (white bars) growth conditions. Oxygen uptake rate was measured at 30°C using a Hansatech Oxygraphas described in Material and Methods. After 72 hours of growth O₂ consumption in SCG and CR is significant higher than in SCD.

was observed for those in SCG and CR with a reduction of about 50% of the consumption rate measured at 24 hours.

The decrease in respiration observed in yeast grown in 2% glucose might have been related to an alteration on the amount of the various cytochromes. A linear relationship between the respiratory rate and the amount of each kind of cytochrome, in fact, exists indicating that respiratory rate is mostly controlled by the amount of respiratory chain components. The mitochondrial cytochromes content in the strains under consideration was then assessed in different carbon sources and growth phases by spectroscopic analyses. As shown in Fig. 19B, at 24 h the cytochromes a, a₃, b, c₁ and c are present in the yeast grown in all the medium analyzed. However, the amount of cytochrome c was lower in the yeast grown in SCD in comparison to SCG and CR, with this deficiency increasing at 72h as indicated by the relative heights of the peaks corresponding to the cytochrome c, c₁ and b. The cytochrome c deficiency suggests a non proper functioning of mitochondria in the presence of 2% glucose both at 24h and in chronological ageing.

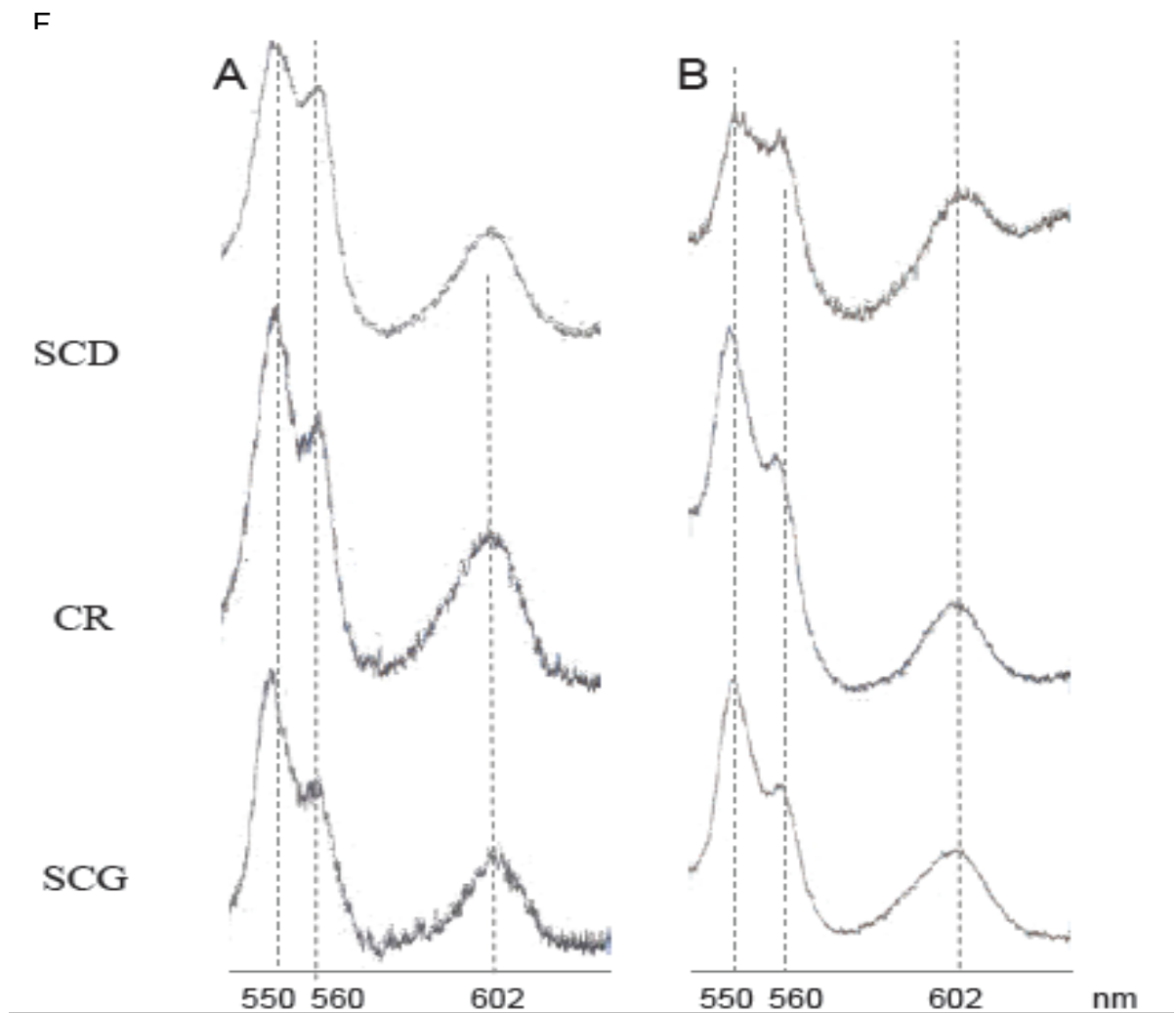


Fig.19B Oxidized versus reduced cytochrome spectra of W303 strain cultured in SDC medium supplemented with the indicated carbon source after (A) 24h and (B) 72h of grown at 28°C. The peaks at 550, 560 and 602 nm (vertical bars) correspond to cytochromes c, b and aa3, respectively. The height of each peak relative to the baseline of each spectrum is an index of cytochrome content.

4.4 Detection of oxidation-sensitive cysteine during chronological aging in different carbon sources.

The redox status of cysteine residues might be involved in the regulation of protein function but it also represents a signal of oxidative damage. ROS are able to oxidize cysteine residues in protein to cysteine sulfenic acid (P-SOH) or disulfide that are readily reduced back to reduced cysteine by cellular reductants. These modifications could play a regulative role, i.e.

modification of enzyme activity or protein localization, and in this view the oxidation is not a negative or harmful event.

Oxidation of protein cysteines in yeast cells grown in different conditions was then investigated by using the BIAM [N-(Biotinoyl)-N'(iodoacetyl)ethylenediamine] labelling protocol [11]. This procedure is based on the ability of BIAM to react with reduced cysteine residues whereas oxidized Cys are not modified by the reagent leading to a selective biotinylation of proteins that contain ROS-sensitive Cys residues. These experiments can easily be monitored by western blot analyses taking advantage of the high interaction of biotin with streptavidin that in turn can be used to selectively isolate and to identify the labelled proteins by immunotechniques.

We first investigated whether BIAM was really able to react with free cysteine. Thus proteins were extracted in lysis buffer (RIPA) at pH 7, as described in material and methods. Cell lysate were incubated for 30 min at room temperature with 40 μ M BIAM, a procedure that results in the rapid biotinylation of proteins containing low- pK_a Cys residues. The BIAM-labeled reaction mixtures and the control (cell lysate not incubated with BIAM) were subjected to affinity chromatography using streptavidin modified agarose beads as described in Material and Methods section. Eluted samples were separated by monodimensional SDS-PAGE and protein bands were blotted on a nitrocellulose membrane and detected with streptavidin HRP.

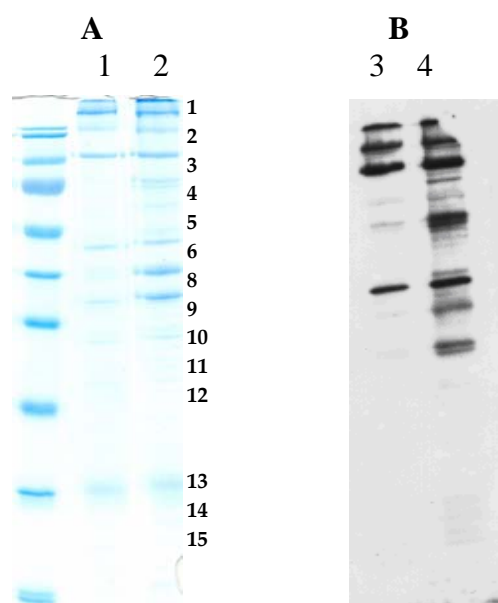


Fig. 20 Mono dimensional SDS PAGE (A) and Western Blot analysis (B) of Cell lysate after BIAM labelling (lane 2 and 4) and not labelled with BIAM (lane 1 and 3)

Blot analysis of the cell lysates revealed many proteins labeled with BIAM in exponential phase (Fig 20); many signals may be observed in the control too, but these might be due to endogenous biotin containing proteins.

Protein bands which gave positive signal to Western Blot analysis were submitted to an identification procedure by *in situ* hydrolysis, MALDI analysis of peptide mixtures and data bank interrogation, the results are summarized in table 1.

Tab.1

BIAM # 1	Mass = 250881	ACETIL-Co A CARBOXYLASE
BIAM # 2	Mass = 131624	PIRUVATE CARBOXYLASE
BIAM # 3	Mass = 122542	Ric 1p
BIAM # 4	Mass = 75872	Hda 3p
BIAM # 5	Mass ₁ = 54575 Mass ₂ = 54942	<ul style="list-style-type: none"> ● ORFX ● IMMEDIATELY UPSTREAM OF PPR1
BIAM # 6	Mass = 52297	YGR110W
BIAM # 8	Mass = 42442	G4p1
BIAM # 9/10	Mass = 37125	ALCOOL DEHYDROGENASE I
BIAM # 11	Mass = 35780	YGR192C GLYCERALDEIDE-3- PHOSPHATE DEHYDROGENASE 2
BIAM # 12	Mass = 27933	40S RIBOSOMAL PROTEIN S0-A
BIAM # 13	Mass = 18763	Hit1p
BIAM # 14	Mass = 26412	40S RIBOSOMAL PROTEIN S3
BIAM # 15	Mass = 24949	40S RIBOSOMAL PROTEIN S5
BIAM # 16	Mass = 14408	HYPOTETICAL 14.4 kDa PROTEIN IN RPL30-CWH41
BIAM # 17	Mass = 31270	PinX1

Peptide spectra from *in situ* hydrolysis of the protein bands after proteins identifications, were manually analyzed in order to identify those signals which could be attributed to BIAM linked peptides.

As an example, figure 21 shows partial peptide MALDI spectra of band 1 corresponding to acetyl CoA carboxylase. The signal at m/z 1757.92 was attributed to 988-998 peptide carrying one BIAM group linked to Cys 993.

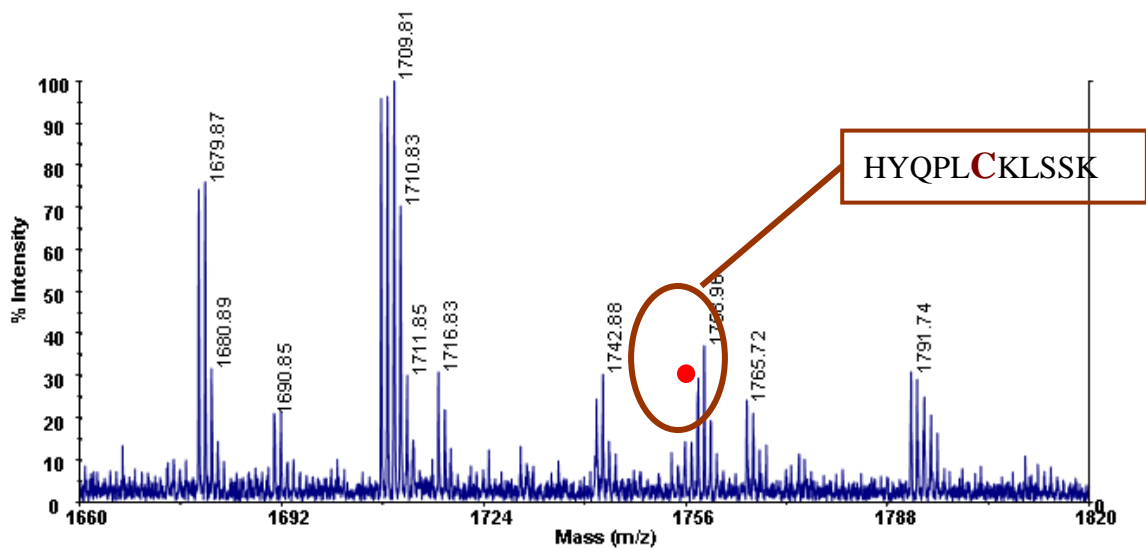


Fig.21

However Tab. 1 shows, in some cases, the identification of more than one protein in a single band; therefore we decided to increase the resolute power of the separation technique, therefore after BIAM labelling protein extracts were separated by bi-dimensional electrophoresis avoiding affinity purification step.

Optimized protocol was therefore used to investigate whether at pH 7, the BIAM-labeled proteins amount change on different carbon source and during chronological aging. Yeast cells grown in SCD, CR and SCG were harvested in exponential phase and at different time during chronological aging (24h and 72h) see figure 22.

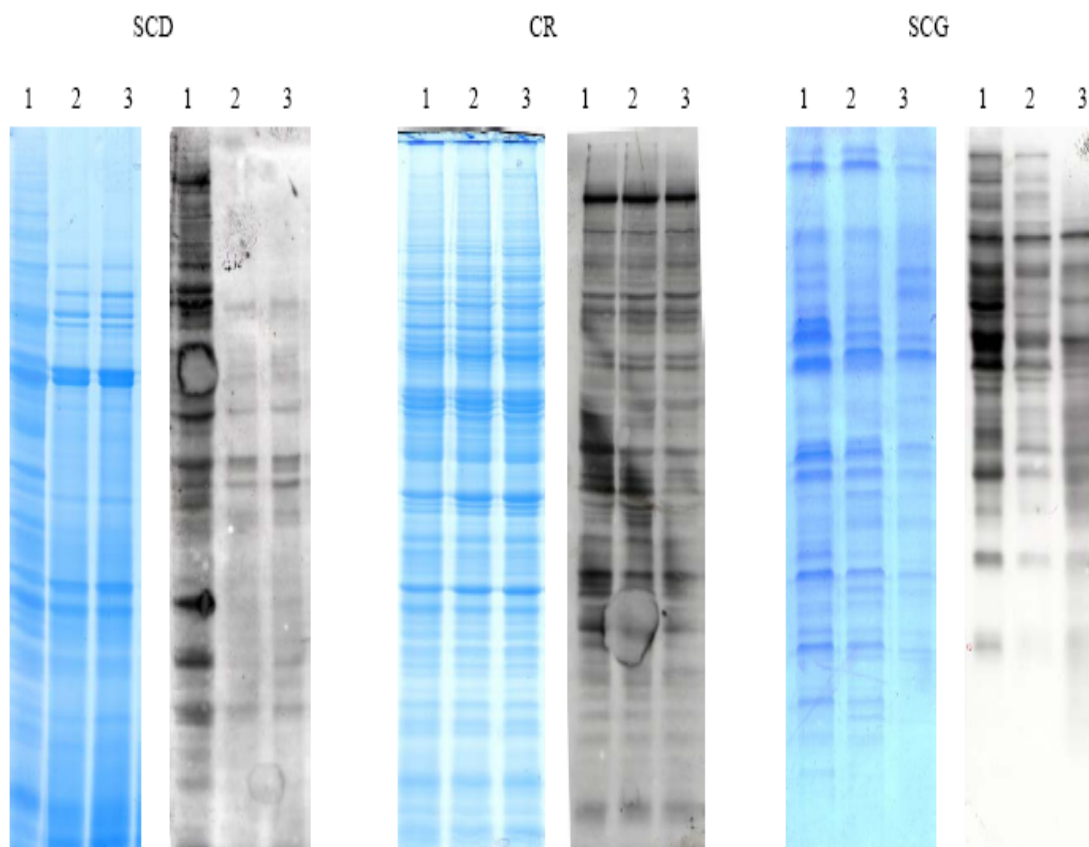
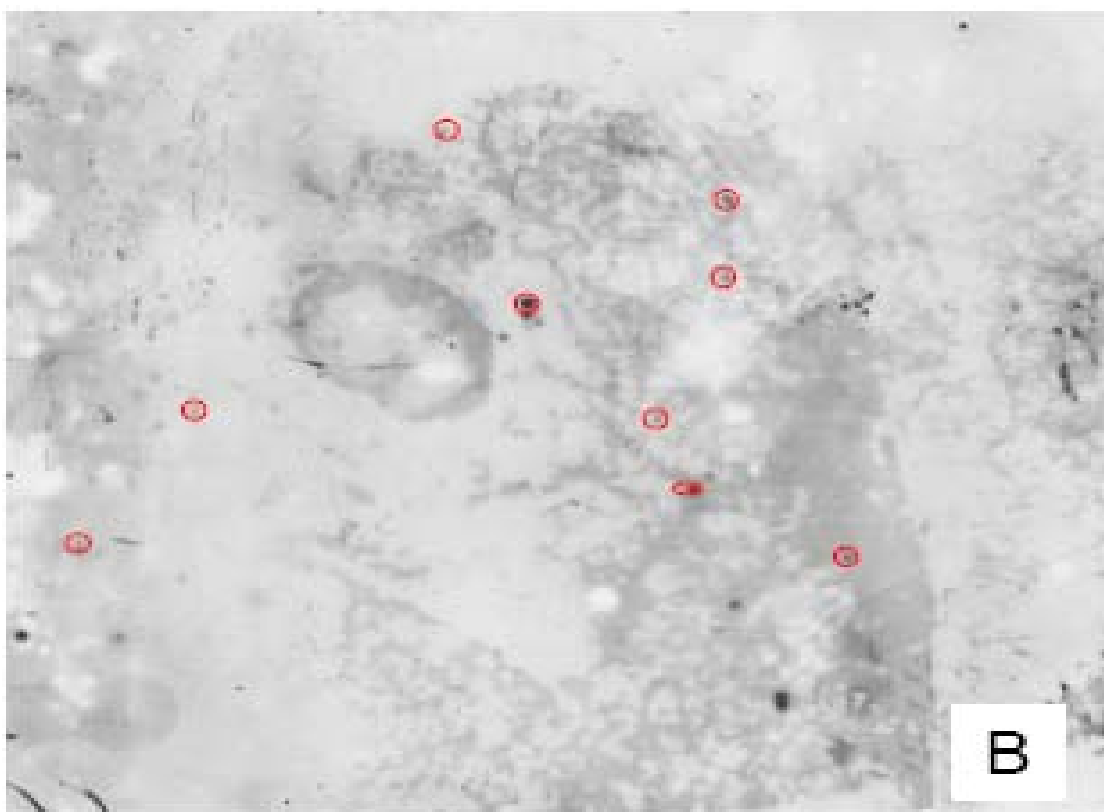
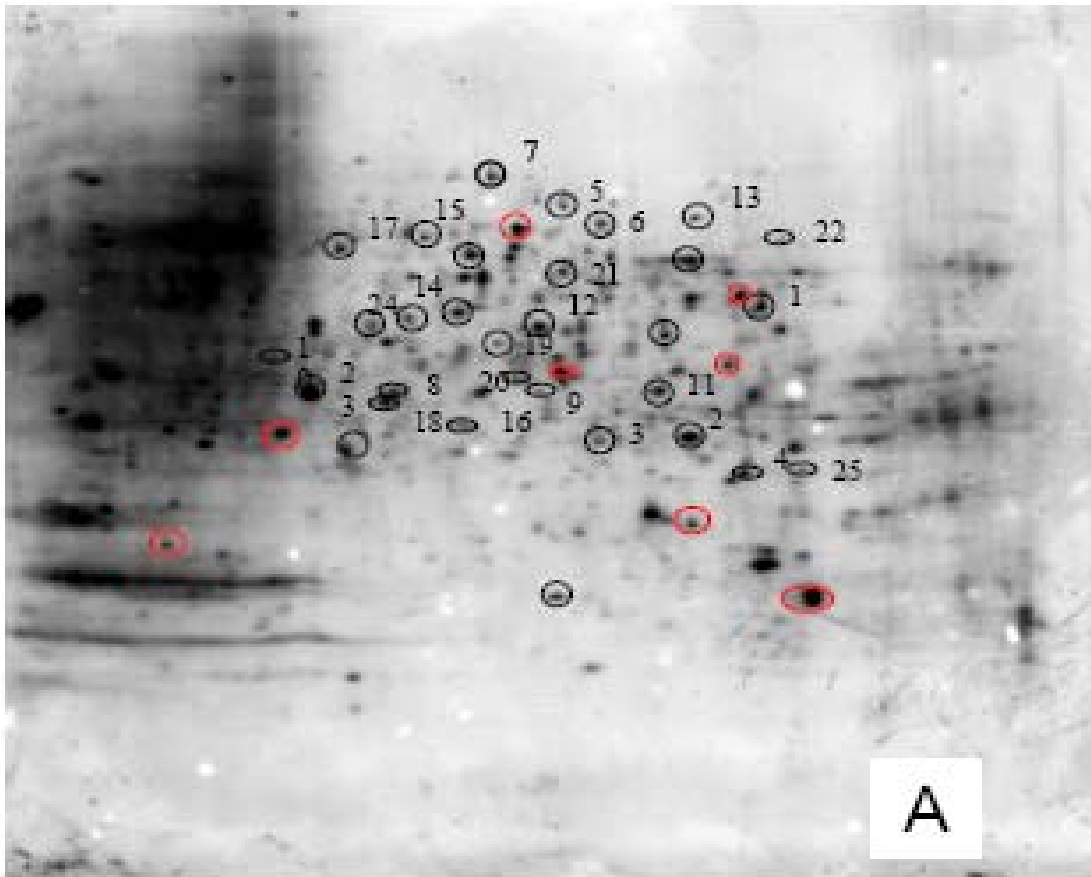


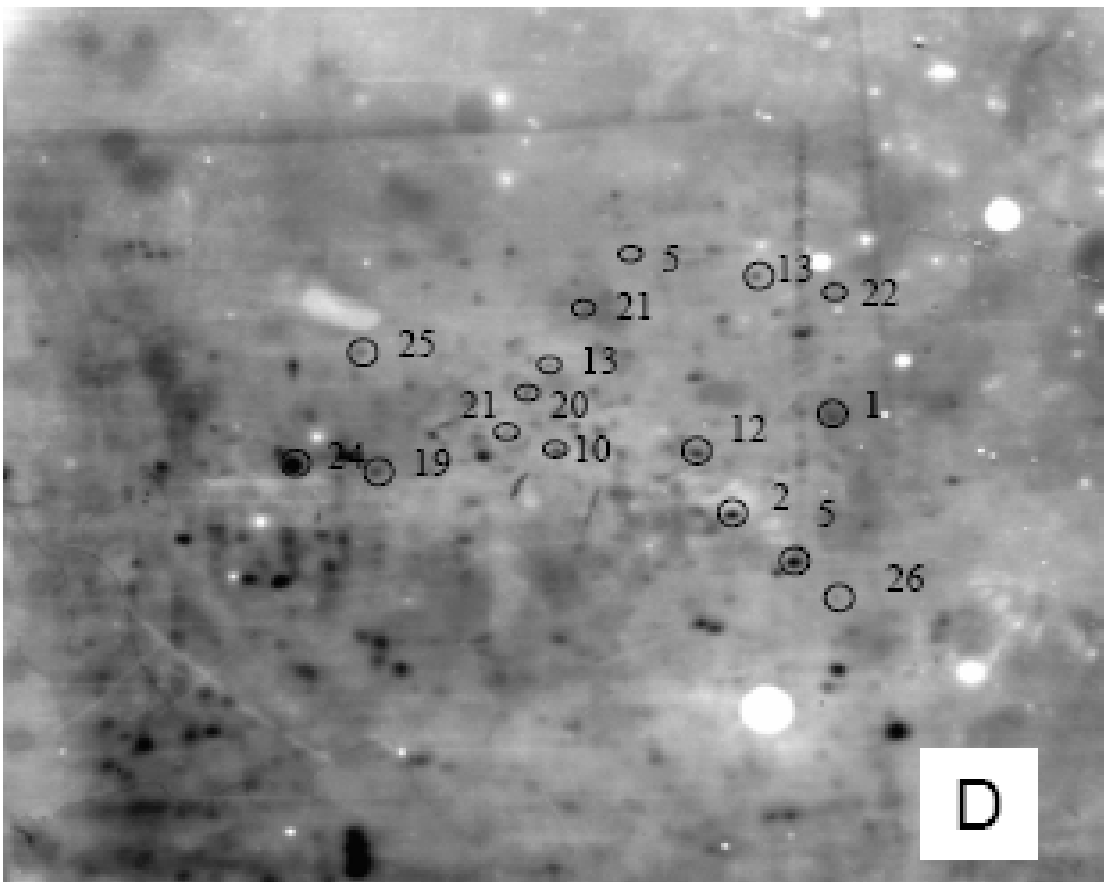
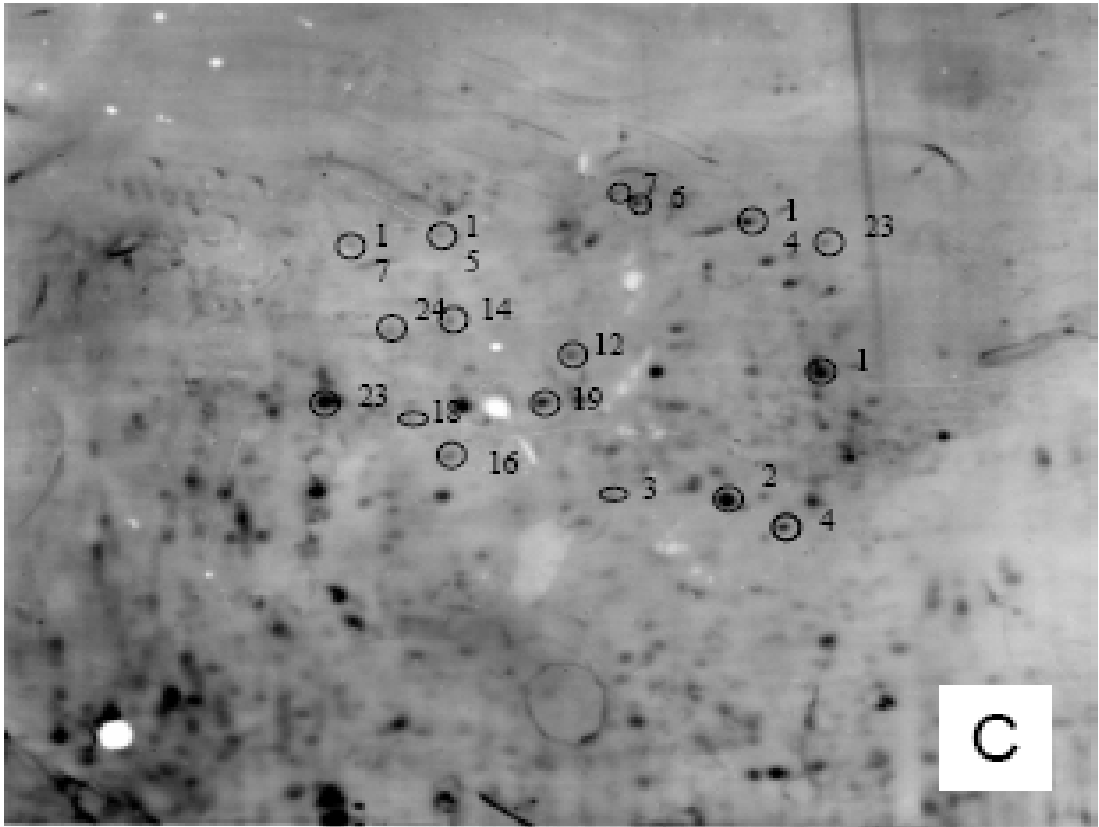
Fig.22 Comassie staining and blot analysis with HRP-conjugate streptavidin of protein extract from yeast grown in SCD, CR and SCG. Yeast cells were harvest in exponential phase (lane 1), and after 24 and 72 hours of growth (lane 2 and 3 respectively)

Growth in SCD resulted in a time–depending decrease in the extent of BIAM labelling of these proteins. In fact after 24 hours, BIAM-linked proteins profile, of yeast growth in SCD, is drastically reduced. In contrast during growth in CR or in SCG is evident the BIAM-labeled protein level is only weakly modified during all the time of analysis indicating a prevalence of reduced form of cystein during aging. In order to better evaluate the cysteine oxidation process in chronological ageing in SCD, protein lysates were prepared from cells in the exponential phase and after 72 h growth and incubated with BIAM. Proteins were separated by 2D-gel electrophoresis and the BIAM-labelled proteins revealed by Western blot. The results shown in figure 23 indicates that many proteins are in a reduced form (BIAM-linked) during exponential phase (Figure 23A) whereas at 72h a dramatically decrease of the BIAM labeled proteins is evident indicating a prevalence of oxidized cysteine residues (Figure 23B). Since we previously

observed that chronological aged cells on SCG or in CR present a reduction of ROS level and a reduction on oxidized proteins as evaluated with BIAM labelling by 1D electrophoresis (Fig.22) we performed the same experiment separating the lysates by 2D electrophoresis. Western blot with HRP-conjugated streptavidin and ECL of 2D-gels from cells grown for 72 h in CR or SCG showed an increase in BIAM-labelling (Figure 23C and 23D respectively) in comparison to the same experiment from cells grown in SCD (Figure 23B).

Fig.23





4.5 Image analysis and Identification of major proteins oxidized on cysteine residues.

Streptavidin immunostained gels of protein lysates from yeast cells grown in SCD both in the exponential phase and during ageing (72 h) were compared by using the MELANIE 4.0 software. We were also able to compare different gels, in order to localize spots corresponding to proteins with an alteration in cysteine redox state during cell chronological ageing in different growth conditions.

During growth in exponential phase in SCD about 50 spots corresponding to BIAM-linked proteins were clearly detected in repeated trials (Figure 23A). Among these, 9 spots correspond to proteins that are still reduced on cysteine residues after 72h in SCD (Figure 23A and 23B red circles). Moreover 10 spots corresponded to proteins that were not visible during ageing even when the gels were silver stained suggesting that these proteins might not be expressed at detectable level in the late stationary phase (data not shown).

Finally, the image analysis identified 31 spots (indicated by black circles) 25 (indicated by black circles and number in Figure 23A) and the redox status of these spots were analysed, by BIAM-labelling, in chronological aged cells growth in CR (Figure 23C) and in SCG (Figure 23D) respectively.

The locations of the identified spots were marked with numbers in a representative gel shown in Figure 24 where proteins were visualized by silver staining.

Proteins excised from the gel, were reduced, alkylated and *in situ* digested with trypsin and the resulting peptide mixtures were directly analysed by MALDI/MS according to the peptide mass fingerprinting procedure. Peaks detected in the MALDI spectra were used to search for a non redundant sequence database using the in house MASCOT software, taking advantage of the specificity of trypsin and the taxonomic category of the samples. The set of experimental mass values was compared to the theoretically predicted peptides from the proteins in the explored database.

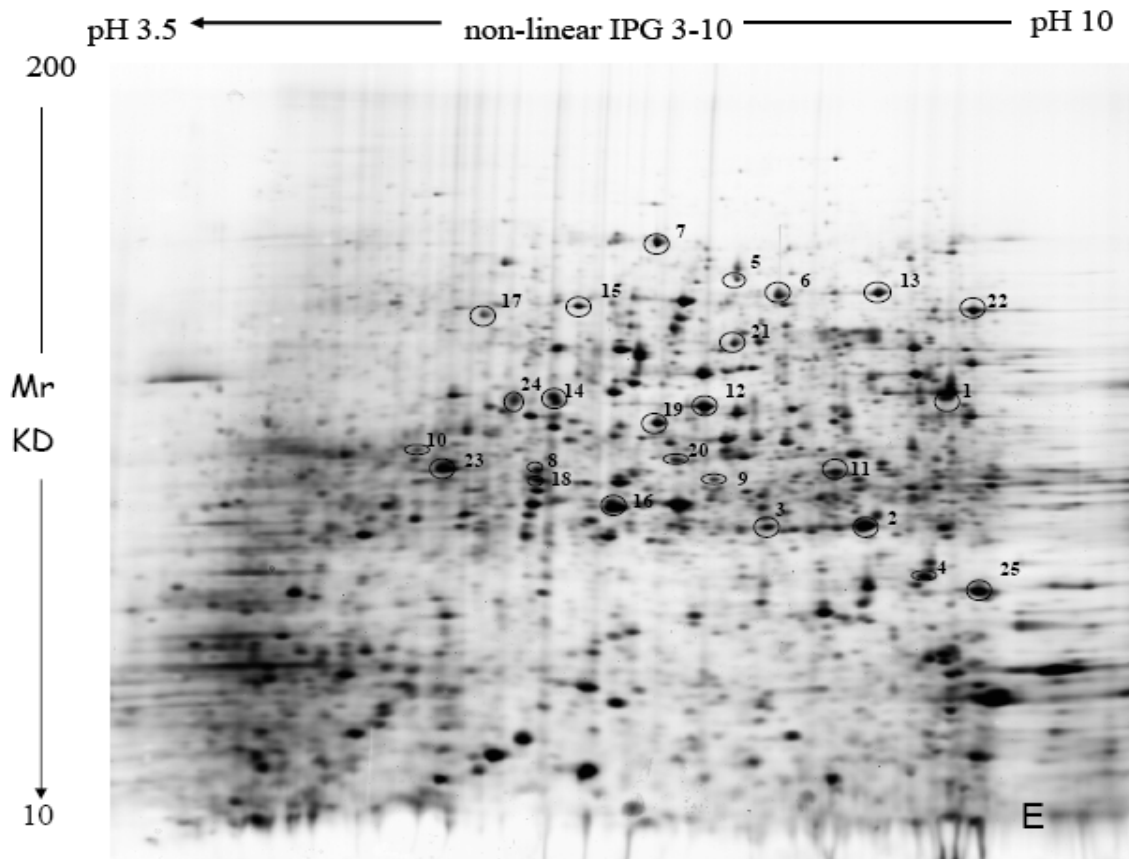


Fig. 24 2D-electrophoresis of total proteins from yeast cells grown in 2% glucose. Circles represent biotinylated protein in exponential phase (figure 6 panel A) that undergo to oxidation during chronological aging in 2% glucose²⁰⁰

The number of measured masses that matched within the given mass accuracy of 200 ppm was recorded and the proteins that received the highest number of peptide matches were examined. The probability score of the second best candidate identified by the program was several orders of magnitude lower. This approach was employed for the identification of all protein bands indicated and a summary of the results is reported in Table I. Sequences coverage of most relevant protein spot obtained mass spectral analyses are summarised in Table II. As indicated in the Tables II and III, several spots occurring at different molecular mass and isoelectric point were identified as corresponding to the same protein even if the peptides identified by MASCOT software clustered in different regions within amino acids sequence. This might be due to a proteolytic processing occurred during sample manipulation. It should be underlined that the spectra revealed the occurrence of some signals that could not be interpreted on the basis of the aminoacidic sequence by MASCOT software. These signals

were then manually interpreted “*a posteriori*” as arising by the addition of one or more BIAM moieties to Cys-containing peptides. As an example Figure 24 shows the partial MALDI spectrum of spot 1 corresponding to GAPDH. The signals at m/z 2159.11 and 2613.35 were attributed to 144-160 peptide carrying one and two BIAM groups respectively, linked to Cys 150 and 154. Additional data were obtained by nanoLC/MS/MS experiments. As indicated in Table II, several spots gave no confident identification by peptide mass fingerprinting. Thus the peptide mixtures were fractionated by nanoHPLC and sequence information were obtained by tandem mass spectrometry on an 4000QTrap linear ion trap instrument leading to the unambiguous identification of the protein candidate as reported in Table I. As evident from the Table I most of the enzymes from the glycolytic and fermentative pathways became oxidized in cysteine residues under chronological aging in media containing high glucose concentration, meanwhile cells grown

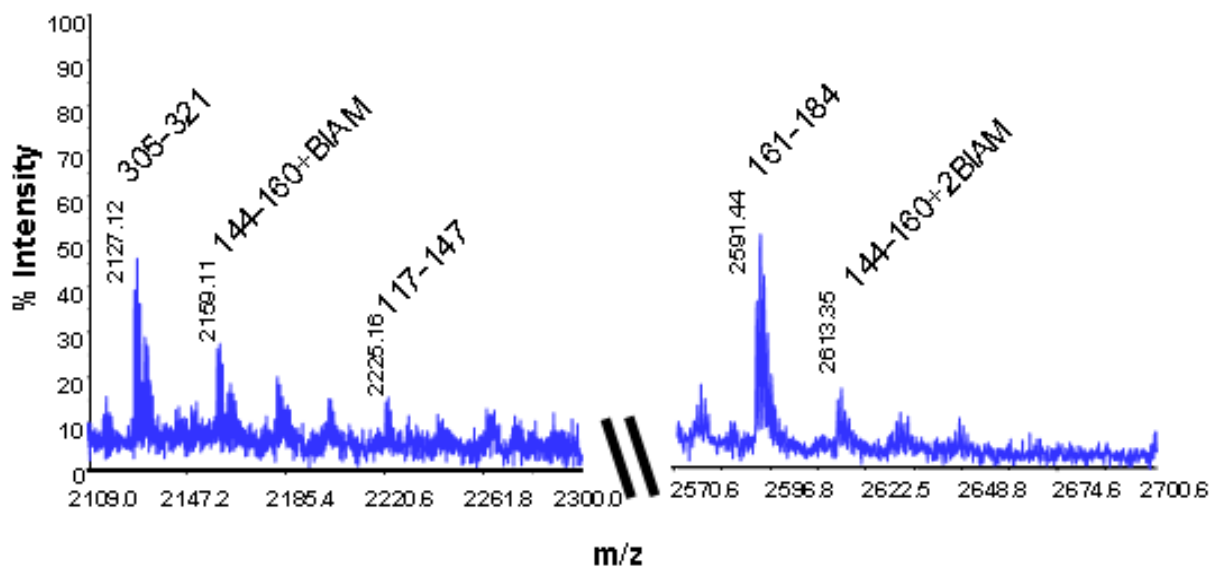


Fig.24 Partial MALDI spectrum of spot 1

in CR or SCG, showed lower levels of protein oxidation on their cysteines. Several major spots from 1 to 4 correspond to glyceraldehyde 3-phosphate dehydrogenase 3 (GAPDH 3) an enzyme involved in glycolysis and gluconeogenesis. Six spots identified in western blot from cells grown on CR or SCG as BIAM-labelled, correspond to a major of three pyruvate decarboxylase isozymes (spots from 6 to 11). Enolase 1 (Spots 13 and 14) and Enolase 2 (spots 12, 15 and 16) are phosphopyruvate hydratases involved in the conversion of 2-phosphoglycerate to phosphoenolpyruvate during glycolysis and the reverse reaction during gluconeogenesis. Two proteins identified as unique spots belong to glycolysis or gluconeogenesis namely phosphoglycerate kinase (spot 22) and fructose-1,6-bisphosphate aldolase (spot 24). Spots 17 and 18 resulting in identification of actin, and spots 20 and 21 are MS identified as mannose-1-phosphate guanylttransferase, two proteins both required for normal cell wall structure. Actin is a structural protein involved in many cytoskeletal functions like cell wall organization and biogenesis and mannose-1-phosphate guanylttransferase is an enzyme responsible of cell wall biosynthesis.

Spot	pI/MW(Da) teor.	pI/MW(KDa) 2DE	Mascot score	N° of peptides	Sequence coverage (%)	Protein	Accessi on number
1*	6.49/3570 7	6.8/32.77	470	33	69	glyceraldehyde-3- phosphate dehydrogenase 3	P00359
2*	6.49/3570 7	6.5/21.01	321	23	46	glyceraldehyde-3- phosphate dehydrogenase 3	P00359
3*	6.49/3570 7	6.25/20.92	127	12	22	glyceraldehyde-3- phosphate dehydrogenase 3	P00359
4 [#]	6.49/3580 7	6.72/19.73	423	VLPELQ GK VVDLVEHVAKAK AVGKVLPELQ GK TASGNIIPSSTGAAK LNKETTYDEIKK GGRTASGNIIPSSTGAAK TASGNIIPSSTGAAKAVG K IVSNASCTTNCLAPLAK		glyceraldehyde-3- phosphate dehydrogenase 2	P00358
5*	5.98/4856 8	6.29/45.53	134	13	30	protein MET17includes: O- acetylhomoserine sulfhydrylase	P06106
6*	5.8/61554	6.15/48.86	238	24	46	pyruvate decarboxylase isozyme 1	P06169
7*	5.8/61554	6.0/56.62	447	56	56	pyruvate decarboxylase isozyme 1	P06169
8 [#]	5.8/61554	5.41/25.65	54		Q-trap	pyruvate decarboxylase isozyme 1	P06169
9*	5.8/61554	6.09/25.02	73	17	7	pyruvate decarboxylase isozyme 1	P06169
10 [#]	5.8/61554	5.09/27.47	291	LLTTIADA AK NATFPGVQMK TPANA AVPASPLK NPVILADACCSR DAKNPVILADACCSR		pyruvate decarboxylase isozyme 1	P06169
11	5.80/6155 4	6.46/25.51	82	8	21	pyruvate decarboxylase isozyme 1	P06169
12*	5.67/4681 1	6.06/31.49	205	17	32	Enolase 2	P00925
13*	6.17/4669 9	6.59/45.69	392	42	65	Enolase 1	P00924
14 [#]	5.67/4681 1	5.5/32.04	467	AAAAEKNVPL YQHLADLSK IGSEVYHNLK IGLDCASSEFFK NVPLYQHLADLSK AVDDFLLSLDGTANK		Enolase 1	P00924
15*	5.67/4681 1	5.66/44.04	345	27	47	Enolase 2	P00925
16 [#]	5.67/4681 1	5.82/22.87	350	TFAEAMR IGSEVYHNLK IGLDCASSEFFK NVPLYQHLADLSK IGSEVYHNLKSLTK AVDDFLLSLDGTANKSK		Enolase 2	P00925
17*	5.44/4189 1	5.24/42.28	138	11	27	Actin	P60010
18 [#]	5.44/4189 1	5.34/25.14	206		Q-trap	Actin	P60010

19*	6.26/3703 4	6.0/29.83	92	5	27	Alcohol dehydrogenase I	P00331
20*	5.95/3971 2	6.01/26.77	111	12	29	Mannose-1- phosphate guanyltransferase	P41940
21*	5.95/3971 2	6.15/37.56	143	12	32	Mannose-1- phosphate guanyltransferase	P41940
22*	7.10/4463 7	6.88/43.07	423	38	75	Phosphoglycerate kinase	P00560
23*	8.31/2373 4	5.15/25.94	434	33	72	Heat shock protein 26	P15992
24*	5.51/3975 0	5.03/32.04	180	19	31	fructose-1,6- bisphosphate aldolase	P14540
25 [#]	9.14/5040 0	6.89/19.03	169	IGGIGTVPVGR FQEIVKETSNIK VETGVIKPGMVVTFAPAG VTTEVK		Elongation factor 1- alpha	P02994

(*) see Table III

(#) identified by LC/MSMS analysis

TABLE II
Proteins identified

1	<p>1 VRVAINGFGR IGRVLMRIAL SRPNVEVVAL NDPFITNDYA AYMFKYDSTH 51 GRYAGEVSHD DKHIIVDGKK IATYQERDPA NLPWGSSNVD IAIDSTGVFK 101 ELDTAQKHID AGAKKVITA PSSTAPMFVM GVNEEKYTS D LKIVSNASCT 151 TNCLAPLAKV INDAFGIEEG LMTTVHSLTA TQKTVDGSPH KDWRGGRTAS 201 GNIIPSSGTA AKAVGKVLPE LQGLTGMAF RVPTVDVSVV DLTVKLNKET 251 TYDEIKKVVK AAAGKLGKGV LGYTEDAVVS SDFLGDSSH IFDASAGIQL 301 SPKFVKLVSW YDNEYGYSTR VVDLVEHVAK A</p>	15	<p>1 AVSKVYARSV YDSRGNPTVE VELTTEKGVF RSIVPSGAST GVHEALEMRD 51 EDKSKWMGKG VMNAVNNVNN VIAAAFVKAN LDVKDQKAVD DFLLSLDGTGTA 101 NKSKLGANAI LGVSMMAARA AAAEKNVPLY QHLADLSKSK TSPYVLPVFP 151 LNVLNGGSHA GGALALQEFM IAPTAKTFA EAMRIGSEVY HNLKSLTKKR 201 YGASAGNVGD EGGVAPNIQT AEEALDLIVD AIKAAGHDGK VKIGLDCASS 251 EFFKDGKYDL DFKNPESDKS KWLTVGVELAD MYHSLMKRYP IVSIEDPFAE 301 DDWEAWSHFF KTAGIQIVAD DLTVTNPARI ATAIEKKAAD ALLLKVNIQIG 351 TLSESIAAQ DSFAANWGMV VSHRSGETED TFIADLVVGL RTGQIKTGAP 401 ARSERLAKLN QLLRIEELG DKAVYAGENF HHGDKL</p>
2	<p>1 VRVAINGFGR IGRVLMRIAL SRPNVEVVAL NDPFITNDYA AYMFKYDSTH 51 GRYAGEVSHD DKHIIVDGKK IATYQERDPA NLPWGSSNVD IAIDSTGVFK 101 ELDTAQKHID AGAKKVITA PSSTAPMFVM GVNEEKYTS D LKIVSNASCT 151 TNCLAPLAKV INDAFGIEEG LMTTVHSLTA TQKTVDGSPH KDWRGGRTAS 201 GNIIPSSGTA AKAVGKVLPE LQGLTGMAF RVPTVDVSVV DLTVKLNKET 251 TYDEIKKVVK AAAGKLGKGV LGYTEDAVVS SDFLGDSSH IFDASAGIQL 301 SPKFVKLVSW YDNEYGYSTR VVDLVEHVAK A</p>	17	<p>1 MDSEVAALVI DNGSGMCKAG FAGDDAPRAV FFSIVGRPRH QGIMVGMGQK 51 DSYVGDQAQS KRGIILTRYP IEHGIVTNWD DMEKIWHHTF YNELRVAPEE 101 HPVLLTEAPM NPKSNREKMT QIMFETFNVP AFYVSIQAVL SLYSSGRITTG 151 IVLDSGDGVT HVVPIYAGS LPHAILRIDL AGRDLTDYLM KILSERGYSF 201 STTAEREIVR DIKEKLCYVA LDFEQEMQTA AQSSIEKSY ELPDQGVITI 251 GNERFRAPEA LFHPSVLGLE SAGIDQTTYN SIMKCDVDR KELYGNIVMS 301 GGTTFMPPGIA ERMQKEITAL APSSMKVKII APPERKYSVW IGGSLASLT 351 TFQQMWISKQ EYDESGPSIV HHKCF</p>
3	<p>1 VRVAINGFGR IGRVLMRIAL SRPNVEVVAL NDPFITNDYA AYMFKYDSTH 51 GRYAGEVSHD DKHIIVDGKK IATYQERDPA NLPWGSSNVD IAIDSTGVFK 101 ELDTAQKHID AGAKKVITA PSSTAPMFVM GVNEEKYTS D LKIVSNASCT 151 TNCLAPLAKV INDAFGIEEG LMTTVHSLTA TQKTVDGSPH KDWRGGRTAS 201 GNIIPSSGTA AKAVGKVLPE LQGLTGMAF RVPTVDVSVV DLTVKLNKET 251 TYDEIKKVVK AAAGKLGKGV LGYTEDAVVS SDFLGDSSH IFDASAGIQL 301 SPKFVKLVSW YDNEYGYSTR VVDLVEHVAK A</p>	19	<p>1 SIPETQKAI FYESNGKLEH KDIPVPKPKP NELLINVKYS GVCHTDLHAW 51 HGDWYLPPTKL PLVGGHEGAG VVGMGENVK GWKIGDYAGI KWLNGSCMAC 101 ECELGNESN CPHADLSGYT HDGFSQEYAT ADAVQAAPH QGTDLAEVAP 151 ILCAGITVYK ALKSANLRAG HWAASISGAAG GLGSLAVQYA KAMGYRVLGI 201 DGGPGKEELF TSLGGEVFD FTKEKDIVSA VVKATNGGAH GIINVSSEA 251 IAEASTRYCR ANGTVVVLVGL PAGAKCSSDV FNHVVKYSI VGSYVGNRAD 301 TREALDFAR GLVKSPIKVV GLSSLEPIEY KMEKQIAGR YVVDTSK</p>
5	<p>1 PSHFDTVQLH AGQENPGDNA HRSRAVPIYA TTSYVFENSK HGSQFLGLEV 51 PGVYYSRFQN PTSNVLEER! AALEGGAAL AVSSGQAAQT LAIQGLAHTG 101 DNIVSTSYLY GGTYNQFKIS FKRFGIEARF VEGDNPPEEFE KVFDETRKAV 151 YLETIGNPKY NVPDFEKVA IAHKHGIVPV VDNFTGAGGY FCQPIKYGAD 201 IVTHSATKWI GGHGTTIGGI IVDSGKFPWK DYPEKFPQFS QPAEGYHGTI 251 YNEAYGNLAY IVHVRTELLR DLGMLPNPFA SFLLLQGVET LSLRAERHGE 301 NALKLAKWLE QSPYVSWVSY PGLASHSHE NAKKYLNSGF GGVLSFGVKD 351 LPNADKETDP FKLSGAQVVD NLKLASNLAN VGDAKTLVIA PYFTTHKQLN 401 DKEKLAGSVD KDLIRVSVGI EFIDIIADF QQSFTVFAG QKP</p>	20	<p>1 MKGLILVGGY GTRLRPLTL VPKPLVEFGN RPMILHQIEA LANAGVTDIV 51 LAVNYRPEVM VETLKKYEKE YGVNITFSVE TEPLGTAGPL KLAEDVLKDD 101 NSPFFVLNSD VICEYPPKEL ADFHKAHGGK GTIVATKVE PSKYGVIVHD 151 IATPNLIDRF VEKPKFEVGN RINAGLYLN PEVIDLIEMK PTSIEKETFP 201 ILVEEKQLYS FDELFWMVDV GQPKDFLSGT VLYLNSLAKR QPKKLTAGAN 251 IVGNALIDPT AKISSTAKIG PDVVIQPNVT IGDGVRITRS VVLGNSTIKN 301 HSLVKSTIVG WNSTVGQWCR LEGVTVLGDD VEKDEIYIN GGVKPLHXS 351 SDNVPEKAI M</p>
6	<p>1 SEITLGKYL ERLKQVNVNT VFGLPGDFNL SLLDKIYEVE GMRWAGNANE 51 LNAAYAADGY ARIKGMSCII TTFVGELSA LNGIAGSYAE HVGVLHVGV 101 PSISAQAKQL LHHHTLGNDD FTVFHRMSAN ISETTAMITD IATAPAEIDR 151 CIRTTYVTQR PVYGLPANL VDLNVPKALL QTPIDMSLKP NDAESEKEVI 201 DTILALVKDA KNPVILADAC CSRHDVKAET KKLIDLTFQFP AVFTPMGKGS 251 IDEQHPRYGG VYVGLSKPE VKEAVESADL ILSVGLLSD FNTGSFSYSY 301 KTKNIVEFHS DHMKIRNATF PGVQMKFVLQ KLLTTIADAA KGYPVAVPA 351 RTPANAAPVA STPLKQEWMM NQLGNLFQEG DVVIAETGTS AFGINQTFP 401 NNTYGISQVL WGSIGFTTGA TLGAFAAEE IDPKKRVLIF IGDGSLQTV 451 QEISTMIRWG LKPYLVLNN DGYTIEKLIH GPKAQYNEIQ GWDHLSLLPT 501 FGAKDYETHR VATTGEWDKL TQDKSFNDNS KIRMIEMLP VFDAPQNLVE 551 QAKLTAATNA KQ</p>	21	<p>1 MKGLILVGGY GTRLRPLTL VPKPLVEFGN RPMILHQIEA LANAGVTDIV 51 LAVNYRPEVM VETLKKYEKE YGVNITFSVE TEPLGTAGPL KLAEDVLKDD 101 NSPFFVLNSD VICEYPPKEL ADFHKAHGGK GTIVATKVE PSKYGVIVHD 151 IATPNLIDRF VEKPKFEVGN RINAGLYLN PEVIDLIEMK PTSIEKETFP 201 ILVEEKQLYS FDELFWMVDV GQPKDFLSGT VLYLNSLAKR QPKKLTAGAN 251 IVGNALIDPT AKISSTAKIG PDVVIQPNVT IGDGVRITRS VVLGNSTIKN 301 HSLVKSTIVG WNSTVGQWCR LEGVTVLGDD VEKDEIYIN GGVKPLHXS 351 SDNVPEKAI M</p>
7	<p>1 SEITLGKYL ERLKQVNVNT VFGLPGDFNL SLLDKIYEVE GMRWAGNANE 51 LNAAYAADGY ARIKGMSCII TTFVGELSA LNGIAGSYAE HVGVLHVGV 101 PSISAQAKQL LHHHTLGNDD FTVFHRMSAN ISETTAMITD IATAPAEIDR 151 CIRTTYVTQR PVYGLPANL VDLNVPKALL QTPIDMSLKP NDAESEKEVI 201 DTILALVKDA KNPVILADAC CSRHDVKAET KKLIDLTFQFP AVFTPMGKGS 251 IDEQHPRYGG VYVGLSKPE VKEAVESADL ILSVGLLSD FNTGSFSYSY 301 KTKNIVEFHS DHMKIRNATF PGVQMKFVLQ KLLTTIADAA KGYPVAVPA 351 RTPANAAPVA STPLKQEWMM NQLGNLFQEG DVVIAETGTS AFGINQTFP 401 NNTYGISQVL WGSIGFTTGA TLGAFAAEE IDPKKRVLIF IGDGSLQTV 451 QEISTMIRWG LKPYLVLNN DGYTIEKLIH GPKAQYNEIQ GWDHLSLLPT 501 FGAKDYETHR VATTGEWDKL TQDKSFNDNS KIRMIEMLP VFDAPQNLVE 551 QAKLTAATNA KQ</p>	22	<p>1 SLSSKLSVQD LDLDKRVFI RVDVFNPLDG KKITSNQRIV AALPTIKYVL 51 EHPHYVYVLA SHLGRPNGER NEKYSLAPVA KELQSLGKD VTFLNDVCPV 101 EVEAAVKASA PGVILLENL RYHIEEESGR KVDGQKVKAS KEDVQKFRHE 151 LSSLADVYIN DAFGTAHRAH SSMVGFDPQ RAAGFLLKE KYFYKALEN 201 PTRFLAILG GAKVADKQL IDNLLDKVDS IIGGGMAFT FKKVENTEI 251 GDSIFDKAGA EIVPKLEKA KAGGVEVLP VDFIADAHS ADANTKTVD 301 KEGIPAGWQG LDNGPESRKL FAATVAKAKT IWVNGPPGVF EFEKFAAGT 351 ALLDEVVKS AAGNTVGG DGTATVAKKY GVTDKISHVS TGGGASLELL 401 EGKELPGAVF LSEKK</p>
12	<p>1 AVSKVYARSV YDSRGNPTVE VELTTEKGVF RSIVPSGAST GVHEALEMRD 51 EDKSKWMGKG VLVHAVKNVD VIAPAFVKAN IDVKDQKAVD DFLLSLDGTGTA 101 NKSKLGANAI LGVSMMAARA AAAEKNVPLY QHLADLSKSK TSPYVLPVFP 151 LNVLNGGSHA GGALALQEFM IAPTAKTFA EAMRIGSEVY HNLKSLTKKR 201 YGASAGNVGD EGGVAPNIQT AEEALDLIVD AIKAAGHDGK VKIGLDCASS 251 EFFKDGKYDL DFKNPESDKS KWLTVGVELAD MYHSLMKRYP IVSIEDPFAE 301 DDWEAWSHFF KTAGIQIVAD DLTVTNPARI ATAIEKKAAD ALLLKVNIQIG 351 TLSESIAAQ DSFAANWGMV VSHRSGETED TFIADLVVGL RTGQIKTGAP 401 ARSERLAKLN QLLRIEELG DKAVYAGENF HHGDKL</p>	23	<p>1 SFNSPFFDF DNINNEVDAF NRLLGEGGLR GYAPRRQLAN TPAKDSTGKE 51 VARPNNYAGA LYDPRDETLD DWFNDLSLF PSFGFPRRS AVPDILDHD 101 NNYELKVVVP GVKSQKDDI EYHQNKQIL VSGEIPSTLN EESKDKVVKV 151 ESSSGKVVV ITPDPYGVAD ADNIKADYAN GVLTLVTPKL KPQKDGKNHV 201 KKIEVSSQES WGN</p>
13	<p>1 AVSKVYARSV YDSRGNPTVE VELTTEKGVF RSIVPSGAST GVHEALEMRD 51 GDKSKWMGKG VLVHAVKNVD VIAPAFVKAN IDVKDQKAVD DFLLSLDGTGTA 101 NKSKLGANAI LGVSMMAARA AAAEKNVPLY QHLADLSKSK TSPYVLPVFP 151 LNVLNGGSHA GGALALQEFM IAPTAKTFA EAMRIGSEVY HNLKSLTKKR 201 YGASAGNVGD EGGVAPNIQT AEEALDLIVD AIKAAGHDGK VKIGLDCASS 251 EFFKDGKYDL DFKNPESDKS KWLTVGVELAD MYHSLMKRYP IVSIEDPFAE 301 DDWEAWSHFF KTAGIQIVAD DLTVTNPARI ATAIEKKAAD ALLLKVNIQIG 351 TLSESIAAQ DSFAAGWGMV VSHRSGETED TFIADLVVGL RTGQIKTGAP 401 ARSERLAKLN QLLRIEELG DNAVYAGENF HHGDKL</p>	24	<p>1 GVEQILKRKT GVIVGEDVHN LFTYAKEHKF AIPAINVTSS STAVAALEAA 51 RDSKSPILQ TSGGAAAYFA GKGISNEGQN ASIKGAIAAA HYRSIAPAY 101 GIPVVLHSDH CAKKLLPWFD GMLEADEAYF KEHGEPLFSS HMLDLSEEDT 151 EENISTCVKY FKRMAAMDQW LEMEIGITGG EEDGVNENNA DKEDLYTKPE 201 QVYVYKALH PISPNSIAA AFGNCHGLYA GDIALRPEIL AEHQYTRQ 251 VGCKEELPY LVFHGSGSST VQEFHTGIDN GVKVNLDTD CQAYLTGIR 301 DYVLLKDDYI MSPVGNPEK EKPKNKFFDP RVVWREGEKT MGAKITKSL 351 TRFTTNTL</p>

TABLE III
Sequence coverage of identified proteins

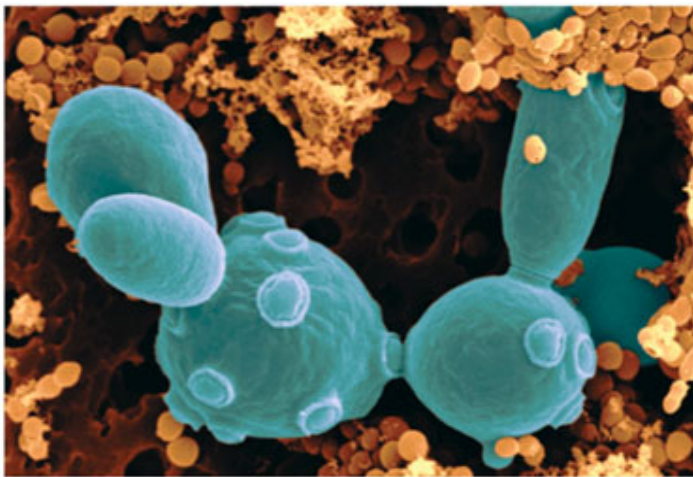
5.Discussion

In the complex field of biological processes, Proteomics offers the instruments to deeply understand the molecular mechanisms involved. However, the large amount of data produced needs to be interpreted and correlated in a very critical way. This research step requires a deeper study, and the analytical skills of the researcher must be accompanied by a sound biochemical background.

In this study we have tried to find correlations between cellular ageing (using cells in different growth conditions, i.e. different carbon sources) and apoptosis. Our interest was addressed to the identifications of the proteins involved, in order to understand the biochemical mechanisms at the basis of this phenomenon.

Apoptosis is a largely studied process with more than one thousand papers published only in the last year. This study constitutes a systematic approach to the investigation of ageing using the most modern analytical techniques.

Yeast is a versatile and simple eukaryotic model organism.



Budding (*S. cerevisiae*)

Although yeasts have greater genetic complexity than bacteria, containing 3.5 times more DNA than *Escherichia coli* cells, they share many of the technical advantages that permitted rapid progress in the molecular genetics of

prokaryotes.

Some of the properties that make yeast particularly suitable for biological studies include rapid growth, dispersed cells, the ease of replica plating and mutant isolation, a well-defined genetic system, and most important, a highly

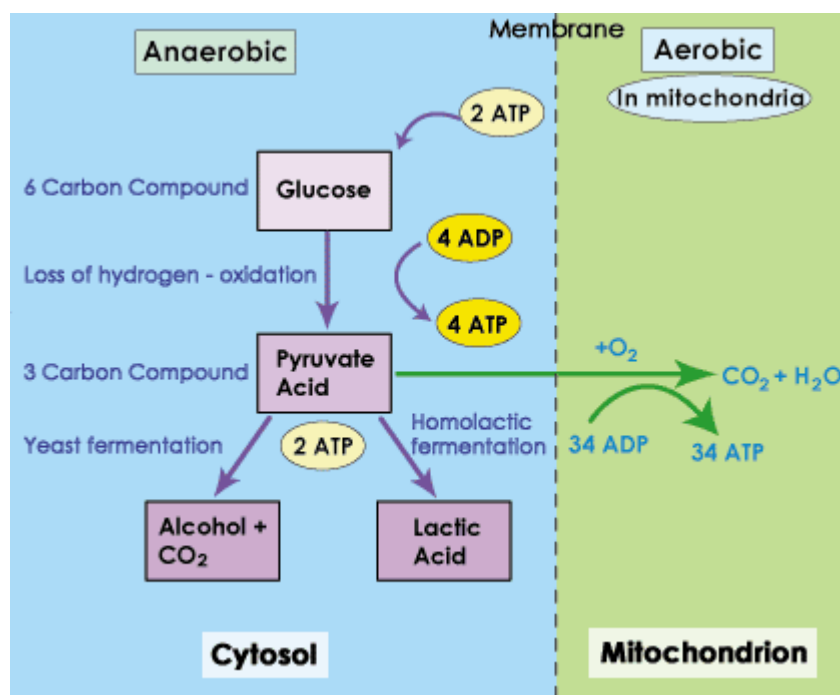
versatile DNA transformation system. Unlike many other microorganisms, *S. cerevisiae* is viable with numerous markers. Being non pathogenic, yeast can be handled with little precautions. Large quantities of normal bakers' yeast are commercially available and can provide a cheap source for biochemical studies.

Nevertheless yeast biochemical processes show many features with those occurring in complex eukaryotes, including humans.

The results reported showed that calorie restriction and respiration extend *S.cerevisiae* lifespan and that oxidative damage on cysteine residues in chronological-aged cells are different in cells grown on high glucose in comparison to cells grown in calorie restriction or in a respirable carbon source as glycerol. The viability of yeast strains varies dramatically in different media conditions. As reported by many authors, the growth in a reduced glucose media, extend life span relative to normal glucose. In our conditions when respiration is the only way to produce ATP, more than 40% of cells are viable after 10 days. Many authors have shown that an increase in the level of reactive oxygen species (ROS) lead to a shortening of life span. They propose that the increase of ROS production can depend on the nature of mitochondrial defects. It is well known that the increase of life span during chronological ageing depends on mitochondrial function. We demonstrated that the ROS production during exponential phase, is almost the same in all the media analyzed.

On the contrary we observed an increase in the ROS production in senescent cells grown on high glucose. We determined that the ROS production is less than 20% in senescent cells grown in CR or in a non-fermentable carbon source such as glycerol than in old cells grown on the high glucose medium. This reduction could be due to a more efficient electron transport in the mitochondrial respiratory chain or to a major protection of the cells against ROS or to a combination of both processes. In all the conditions and in old cells, the mitochondria display a typical morphology with extended tubular network located prevalently at the cell cortex showing a normal mitochondrial integrity. We suggest that a better mitochondrial metabolism occurring during respiration play a role in a life span-extending effect of CR and growth in a respiratory medium. We evaluated the mitochondrial function measuring the

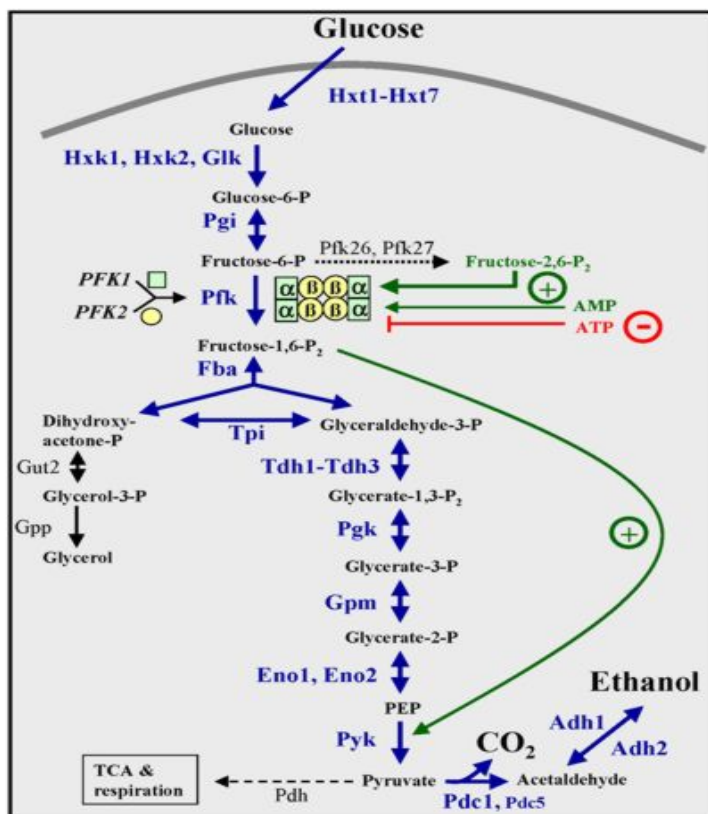
oxygen consumption of the young and old yeast in SCD, CR and SCG. In the young cells and in all the conditions of growth, the oxygen consumption rate had a similar value. We demonstrated a decreased routine respiration in senescent cells growth in high glucose in comparison to the cells growth on a non-fermentable carbon source. These observations suggest that yeast growth on a non-fermentable carbon source may contribute to a better activation of respiration increasing the rate of it. Plotting the respiratory rate against the amount of each kind of cytochrome, it is possible to see a linear relationship between these two parameters indicating that respiratory rate is mostly controlled by the amount of respiratory chain components. We showed that the cytochromes a_3 , b , c_1 and c are present in the yeast grown in all mediums analyzed in young cells even if the cytochrome c was lower in the yeast grown in SCD in comparison to SCG and CR. This reduction was more pronounced in senescent cells. All these evidence suggested that the growth in high glucose leads to a reduced mitochondrial efficiency in chronological aging. In contrast in CR and in SCG (a respirable carbon source) the level of cytochrome c content doesn't show any reduction from young to old cells and this is in agreement with a good efficiency of respiration due to an increase in capacity of the mitochondrial electron transport chain.



The results presented here revealed that these findings led to a decrease of ROS level and improved longevity during chronological ageing. We can conclude that, during respiration induced by calorie restriction or following a growth in a respirable carbon source, the well ageing is due to high metabolic activity of mitochondria but low ROS leakage from the respiratory chain. It is reported by many authors that restriction dietary intake increased the rate of oxygen consumption indicating an increase of mitochondrial respiration.

When the mitochondrial activity is inhibited, the effects of calorie restriction in abolished, showing that a reduction on calorie intake seems to increase mitochondrial activity probably because of a more efficient extraction of energy from a limited amount of food. Recently Antebi A. (87) reported the identification of two genes that mediate the increase in longevity by calorie restriction in worms *Caenorhabditis elegans*.

In this study we also suggest the possibility that increased and better mitochondrial activity might promote longevity triggering mechanisms that



**Carbohydrate
metabolism**

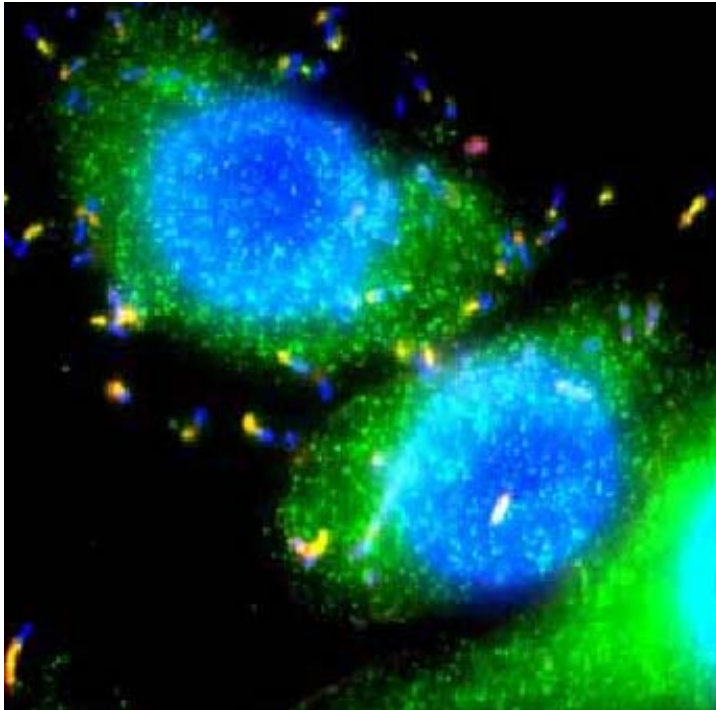
protect cells against oxidative stress or reduced the damage to cellular components like proteins. We described the oxidative damage caused by ROS generation on cysteine residues. We used a procedure based on the facts that: 1) Cys residues are selectively labelled with biotin-conjugated

iodoacetamide (BIAM), 2) oxidized cysteines are not labelled with BIAM and 3) the decrease in BIAM labelling, resulting from oxidation, can be monitored by western blot. The results obtained in this study indicated that many proteins were labelled with BIAM in exponential phase during growth in high glucose. In normal glucose the senescent cells showed a decrease in BIAM-labelled proteins showing a prevalence of oxidized form of cysteine residues. On the contrary the chronological aged cells on a reduced glucose level or in glycerol, present a reduction of cys-oxidized residues. These experiments suggest that cells grown with CR or SCG showed a very low level of cysteine oxidation. This result is consistent with the rule of CR and growth in non-fermentable carbon source extending chronological life span in yeast. It has been described that, in chronological aging, there was an increased protein carbonylation in comparison to young cells.

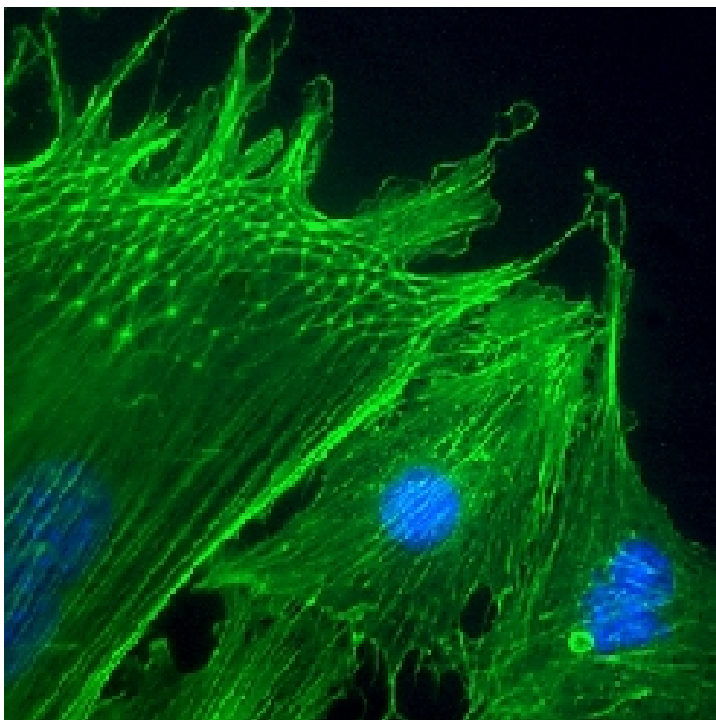
These proteins targets include enzymes involved in glucose metabolism and actin, explaining why the replication rate decrease in the passage through the stationary phase. Most of the enzymes of the glycolytic pathway such as GAPDHp, which we found to contain at least one Cys residue BIAM-labelled, Pdc1p, Eno1p and Eno2p, Pgc1p and Fba1p, were identified as targets for oxidation in old cells growth in high level of glucose.

On the contrary the old cells growth in calorie restriction or in glycerol, showed marked differences in protein labelling patterns in comparison to the same cells on normal glucose. The same proteins showed big differences in relative band intensity on the corresponding western-blot. It is interesting to observe that several spots corresponding to oxidized proteins on cysteine residues in SCD are not identified in western blots from cells grown in CR or SCG. Most of them are undetectable on the 2D-gel of the SCG cultures. One of these proteins corresponds to Pdc1. This enzyme is strongly expressed in fermenting yeast cells growing in a fermentative carbon source. This protein is expected to be low expressed upon a respiratory carbon source. Another of these protein correspond to alcohol dehydrogenase I the enzyme responsible for converting acetaldehyde to ethanol during fermentation. ADH1 is expected to be low expressed during growth in SCG a respiratory carbon source because it is specific for fermentation.

Actin (spot 17) has been found to be involved in many processes including transcription and chromatin structure. More recently has been demonstrated (88) that cysteines 285 and 374 of actin are important physiological sensors of intracellular oxidative stress and are regulators of programmed cell death during chronological aging. It is so evident that this protein is oxidized on cysteine residues after 72h in SCD. We evaluate the GSH level and



Interaction between DNA (blue) and actin (stained with fluorescein green)



Donald E. Ingber, "The Architecture of Life" Scientific American, Jan. 1998

our preliminary results indicate that growth on CR and SCG promote an increase on this peptide affecting the antioxidant defense of yeast cells. This observation could be due to the need of glutathione in the thiol redox system, although this question requires further study. In summary, respiration induced by caloric restriction or by a respirable carbon source reduces cysteine oxidative damage to proteins increasing life span in *S.cerevisiae* because in these conditions there is an increase in the capacity of the mitochondrial electron transport chain. Using the yeast *S. cerevisiae* as a model organism we showed a decrease in intracellular oxidation in old cells growth in low glucose or glycerol which results in better vitality of yeast cells.

6. References

- 1) Harry JL, Wilkins MR, Herbert BR, Packer NH, Gooley AA, Williams KL. *Electrophoresis*. 2000 Apr;21(6):1071-81.
- 2) Moller A, Soldan M, Volker U, Maser E. *Toxicology*. 2001 Mar 7;160(1-3):129-38.
- 3) Smoot LM, Smoot JC, Graham MR, Somerville GA, Sturdevant DE, Migliaccio CA, Sylva GL, Musser JM. *Proc Natl Acad Sci U S A*. 2001 Aug 28;98(18):10416-21.
- 4) Ronen M, Botstein D. *Proc Natl Acad Sci U S A*. 2006 Jan 10;103(2):389-94.
- 5) Hack N, Crawford N. *Biochem J*. 1984 Aug 15;222(1):235-46.
- 6) Holland JW, Deeth HC, Alewood PF. *Proteomics*. 2004 Mar;4(3):743-52.
- 7) Cecconi D, Scarpa A, Donadelli M, Palmieri M, Hamdan M, Astner H, Righetti PG. *Electrophoresis*. 2003 Jun;24(11):1871-8.
- 8) Marengo E, Robotti E, Righetti PG, Campostrini N, Pascali J, Ponzoni M, Hamdan M, Astner H. *Clin Chim Acta*. 2004 Jul;345(1-2):55-67.
- 9) Rappsilber J, Mann M. *Genome Biol*. 2002 Jul 31;3(8):
- 10) Monti M, Orru S, Pagnozzi D, Pucci P. *Clin Chim Acta*. 2005 Jul 24;357(2):140-50.
- 11) Monti M, Orru S, Pagnozzi D, Pucci P. *Biosci Rep*. 2005 Feb-Apr;25(1-2):45-56.
- 12) Andersen JS, Wilkinson CJ, Mayor T, Mortensen P, Nigg EA, Mann M. *Nature*. 2003 Dec 4;426(6966):570-4.
- 13) Righetti PG, Bossi A. *J Chromatogr B Biomed Sci Appl*. 1997 Oct 10;699(1-2):77-89.
- 14) Carboni L, Piubelli C, Righetti PG, Jansson B, Domenici E. *Electrophoresis*. 2002 Dec;23(24):4132-41.
- 15) Righetti PG, Bossi A. *J Chromatogr B Biomed Sci Appl*. 1997 Oct 10;699(1-2):77-89.
- 16) Righetti PG, Castagna A, Antonioli P, Boschetti E. *Electrophoresis*. 2005 Jan;26(2):297-319.

- 17) Rabilloud T, Kieffer S, Procaccio V, Louwagie M, Courchesne PL, Patterson SD, Martinez P, Garin J, Lunardi J. *Electrophoresis*. 1998 May;19(6):1006-14.
- 18) Pinder JC, Gratzer WB. *Biochim Biophys Acta*. 1970 Mar 31;200(3):429-32.
- 19) Kenrick KG, Margolis J. *Anal Biochem*. 1970 Jan;33(1):204-7.
- 20) Aebersold RH, Pipes G, Hood LE, Kent SB. *Electrophoresis*. 1988 Sep;9(9):520-30.
- 21) Shi R, Kumar C, Zougman A, Zhang Y, Podtelejnikov A, Cox J, Wisniewski JR, Mann M. *J Proteome Res*. 2007 Aug;6(8):2963-72.
- 22) Zhang X, Shi L, Shu S, Wang Y, Zhao K, Xu N, Liu S, Roepstorff P. *Proteomics*. 2007 Jul;7(14):2340-9.
- 23) Katz A, Waridel P, Shevchenko A, Pick U. *Mol Cell Proteomics*. 2007 Sep;6(9):1459-1472.
- 24) Gagne JP, Ethier C, Gagne P, Mercier G, Bonicalzi ME, Mes-Masson AM, Droit A, Winstall E, Isabelle M, Poirier GG. *Proteome Sci*. 2007 Sep 24;5(1):16
- 25) Blagoev B, Mann M. *Methods*. 2006 Nov;40(3):243-50
- 26) De Palma S, Ripamonti M, Viganò A, Moriggi M, Capitanio D, Samaja M, Milano G, Cerretelli P, Wait R, Gelfi C. *J Proteome Res*. 2007 May;6(5):1974-84.
- 27) Hunzinger C, Schratzenholz A, Poznanovic S, Schwall GP, Stegmann W. *J Chromatogr A*. 2006 Aug 11;1123(2):170-81.
- 28) Liu H, Yang C, Yang Q, Zhang W, Zhang Y. *J Chromatogr B Analyt Technol Biomed Life Sci*. 2005 Mar 5;817(1):119-26
- 29) Guerrier L, Thulasiraman V, Castagna A, Fortis F, Lin S, Lomas L, Righetti PG, Boschetti E. *J Chromatogr B Analyt Technol Biomed Life Sci*. 2006 Mar 20;833(1):33-40.
- 30) Lipkin LE, Lemkin PF. *Clin Chem*. 1980 Sep;26(10):1403-12.
- 31) Righetti PG. *Electrophoresis*. 2004 Jul;25(14):2111-27.
- 32) Shevchenko A, Tomas H, Havlis J, Olsen JV, Mann M. *Nat Protoc*. 2006;1(6):2856-60.
- 33) Rappsilber J, Mann M, Ishihama Y. *Nat Protoc*. 2007;2(8):1896-906.

- 34) Schwartz SA, Weil RJ, Thompson RC, Shyr Y, Moore JH, Toms SA, Johnson MD, Caprioli RM. *Cancer Res.* 2005 Sep 1;65(17):7674-81.
- 35) Andre M, Karas M. *Anal Bioanal Chem.* 2007 Oct;389(4):1047-53.
- 36) Pucci P, Siciliano R, Ferranti P, Malorni A, Marino G. *Biotechnol Appl Biochem.* 1990 Aug;12(4):357-63.
- 37) Fini C, Amoresano A, Andolfo A, D'auria S, Floridi A, Paolini S, Pucci P. *Eur J Biochem.* 2000 Aug;267(16):4978-87.
- 38) Hahner S, Ludemann HC, Kirpekar F, Nordhoff E, Roepstorff P, Galla HJ, Hillenkamp F. *Nucleic Acids Res.* 1997 May 15;25(10):1957-64.
- 39) Adachi J, Kumar C, Zhang Y, Olsen JV, Mann M. *Genome Biol.* 2006;7(9):R80.
- 40) Parker KC. *J Am Soc Mass Spectrom.* 2002 Jan;13(1):22-39.
- 41) Sutton CW, Pemberton KS, Cottrell JS, Corbett JM, Wheeler CH, Dunn MJ, Pappin DJ. *Electrophoresis.* 1995 Mar;16(3):308-16.
- 42) Waridel P, Frank A, Thomas H, Surendranath V, Sunyaev S, Pevzner P, Shevchenko A. *Proteomics.* 2007 Jul;7(14):2318-29.
- 43) Wielsch N, Thomas H, Surendranath V, Waridel P, Frank A, Pevzner P, Shevchenko A. *J Proteome Res.* 2006 Sep;5(9):2448-56.
- 44) Beck A, Moeschel K, Deeg M, Haring HU, Voelter W, Schleicher ED, Lehmann R. *J Am Soc Mass Spectrom.* 2003 Apr;14(4):401-5.
- 45) Oh H, Breuker K, Sze SK, Ge Y, Carpenter BK, McLafferty FW. *Proc Natl Acad Sci U S A.* 2002 Dec 10;99(25):15863-8. Epub 2002 Nov 20.
- 46) Hillenkamp F, Karas M, Beavis RC, Chait BT. *Anal Chem.* 1991 Dec 15;63(24):1193A-1203A.
- 47) Nordhoff E, Ingendoh A, Cramer R, Overberg A, Stahl B, Karas M, Hillenkamp F, Crain PF. *Rapid Commun Mass Spectrom.* 1992 Dec;6(12):771-6.
- 48) Nordhoff E, Cramer R, Karas M, Hillenkamp F, Kirpekar F, Kristiansen K, Roepstorff P. *Nucleic Acids Res.* 1993 Jul 25;21(15):3347-57.
- 49) Nakanishi T, Okamoto N, Tanaka K, Shimizu A. *Biol Mass Spectrom.* 1994 Apr;23(4):230-3.
- 50) Kirpekar F, Nordhoff E, Kristiansen K, Roepstorff P, Lezius A, Hahner S, Karas M, Hillenkamp F. *Nucleic Acids Res.* 1994 Sep 25;22(19):3866-70.

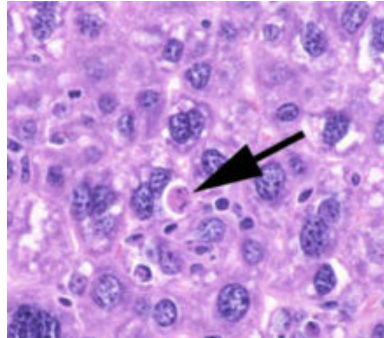
- 51) Ascenzi P, Ruoppolo M, Amoresano A, Pucci P, Consonni R, Zetta L, Pascarella S, Bortolotti F, Menegatti E. *Eur J Biochem.* 1999 Apr;261(1):275-84.
- 52) Bordini E, Hamdan M, Righetti PG. *Rapid Commun Mass Spectrom.* 1999;13(21):2209-15.
- 53) Pappin DJ, Hojrup P, Bleasby AJ. *Curr Biol.* 1993 Jun 1;3(6):327-32.
- 54) Kerr JF, Wyllie AH, Currie AR. *Br J Cancer.* 1972 Aug;26(4):239-57.
- 55) Abrams JM. *Cell.* 2002 Aug 23;110(4):403-6.
- 56) Ikegami T, Suzuki K. *Biosystems.* 2007 Jul 17
- 57) Lloyd D, Aon MA, Cortassa S. *Scientific World Journal.* 2001 Apr 4;1:133-45.
- 58) Kawasaki T, Kitao T, Nakagawa K, Fujisaki H, Takegawa Y, Koda K, Ago Y, Baba A, Matsuda T. *Glia.* 2007 Oct;55(13):1325-33.
- 59) Ueda H, Fujita R, Yoshida A, Matsunaga H, Ueda M. *J Cell Biol.* 2007 Mar 12;176(6):853-62.
- 60) Cao JJ, Kurimoto P, Boudignon B, Rosen C, Lima F, Halloran BP. *J Bone Miner Res.* 2007 Aug;22(8):1271-9.
- 61) Perl M, Chung CS, Perl U, Lomas-Neira J, de Paepe M, Cioffi WG, Ayala A. *Am J Respir Crit Care Med.* 2007 Sep 15;176(6):591-601
- 62) Hill MM, Adrain C, Martin SJ. *Mol Interv.* 2003 Feb;3(1):19-26.
- 63) Zhang JY, Wu HY, Xia XK, Liang YJ, Yan YY, She ZG, Lin YC, Fu LW. *Cancer Biol Ther.* 2007 Jun 5;6(9)
- 64) Rackham O, Nichols SJ, Leedman PJ, Berners-Price SJ, Filipovska A. *Biochem Pharmacol.* 2007 Oct 1;74(7):992-1002.
- 65) Luhrmann A, Roy CR. *Infect Immun.* 2007 Aug 20;
- 66) Heidari N, Goliaei B, Moghaddam PR, Rahbar-Roshandel N, Mahmoudian M. *Anticancer Drugs.* 2007 Nov;18(10):1139-47.
- 67) Goto HG, Nishizawa Y, Katayama H, Murashima T, Yamasaki M, Tanigaki Y, Kimura S, Fushiki S, Nishizawa Y. *Oncol Rep.* 2007 Jan;17(1):225-32.
- 68) Jabbour AM, Ho PK, Puryer MA, Ashley DM, Ekert PG, Hawkins CJ. *Cell Death Differ.* 2004 Dec;11(12):1309-16.
- 69) Costa C, Casinghino SR, Fodor WL. *Transplant Proc.* 2007 Sep;39(7):2443-2446.

- 70) Takashina T, Nakayama M. *FEBS Lett.* 2007 Sep 18;581(23):4479-84.
- 71) Ishizawa YH, Tamura K, Yamaguchi T, Matsumoto K, Komiyama M, Takamatsu N, Shiba T, Ito M. *Biol Cell.* 2006 Aug;98(8):465-78.
- 72) Dempsey PW, Doyle SE, He JQ, Cheng G. *Cytokine Growth Factor Rev.* 2003 Jun-Aug;14(3-4):193-209.
- 73) Petrovas C, Mueller YM, Yang G, Altork SR, Jacobson JM, Pitsakis PG, Mounzer KC, Altman JD, Katsikis PD. *Apoptosis.* 2007 Sep 21
- 74) Cheng EH, Sheiko TV, Fisher JK, Craigen WJ, Korsmeyer SJ. *Science.* 2003 Jul 25;301(5632):513-7.
- 75) Yamaki M, Umehara T, Chimura T, Horikoshi M. *Genes Cells.* 2001 Dec;6(12):1043-54.
- 76) Mirzayans R, Scott A, Andrais B, Pollock S, Murray D. *J Cell Physiol.* 2007 Sep 25
- 77) Pietraforte D, Matarrese P, Straface E, Gambardella L, Metere A, Scorza G, Leto TL, Malorni W, Minetti M. *Free Radic Biol Med.* 2007 Jan 15;42(2):202-14
- 78) Okinaga T, Kasai H, Tsujisawa T, Nishihara T. *J Med Microbiol.* 2007 Oct;56(Pt 10):1399-404.
- 79) Wang Q, Wang T, Wang Y, Wang W, Wang Y, Hu X, Shao S, Zhang J, Suo Z. *Anticancer Res.* 2007 Jul-Aug;27(4B):2359-64.
- 80) Longo VD, Gralla EB, Valentine JS. *J Biol Chem.* 1996 May 24;271(21):12275-80
- 81) Fabrizio P, Pozza F, Pletcher SD, Gendron CM, Longo VD. *Science.* 2001 Apr 13;292(5515):288-90. Epub 2001 Apr 5.
- 82) Maclean MJ, Aamodt R, Harris N, Alseth I, Seeberg E, Bjoras M, Piper PW. *Aging Cell.* 2003 Apr;2(2):93-104.
- 83) Chen C, Sytkowski AJ. *Biochem Biophys Res Commun.* 2005 Jul 22;333(1):51-7.
- 84) MacLean M, Harris N, Piper PW. *Yeast.* 2001 Apr;18(6):499-509.
- 85) Fleury C, Pampin M, Tarze A, Mignotte B. *Biosci Rep.* 2002 Feb;22(1):59-79.
- 86) Roepstorff P, Fohlman J. *Biomed Mass Spectrom.* 1984 Nov;11(11):601.

- 87) Antebi A. Dev Cell. 2004 Mar;6(3):315-6.
- 88) Farah ME, Amberg DC. Mol Biol Cell. 2007 Apr;18(4):1359-65.

Summary

Apoptosis is a process of deliberate life relinquishment by a cell in a multicellular organism. It is one of the main types of programmed cell death (PCD), and involves an orchestrated series of biochemical events leading to a characteristic cell morphology and death. The apoptotic process is executed in such a way as to safely dispose of cell corpses and fragments.



A section of mouse liver showing an apoptotic cell indicated by an arrow

In contrast to necrosis, which is a form of traumatic cell death that results from acute cellular injury, apoptosis is carried out in an orderly process that generally confers advantages during an organism's life cycle.

Apoptosis can occur when a cell is damaged beyond repair, infected with a virus, or undergoing stress conditions such as starvation or ageing. DNA damage from ionizing radiation or toxic chemicals can also induce apoptosis via the actions of the tumour-suppressing gene p53. The "decision" for apoptosis can come from the cell itself, from the surrounding tissue, or from a cell that is part of the immune system. In these cases apoptosis functions to remove the damaged cell, preventing it from sapping further nutrients from the organism, or to prevent the spread of viral infection.

Yeast provides a simple and powerful model for the study of cellular complex mechanisms such as apoptosis caused by ageing, due to the presence of simplified regulatory pathways, comparing to more complex organisms, such as *Homo sapiens*.

In yeast, two different forms of aging processes are studied: one is mother cell-specific aging in which only the mother cell ages, while the daughter cell resets the clock to zero.

Age in this case is measured by cell generations, not by calendar time. The daughter cells remain in the stem cell pool while the other cell has made the first step towards differentiation. Resetting the clock is also known as "rejuvenation", a process which is absolutely necessary for survival of the yeast strain.

The second process of aging that can be studied in yeast is chronological aging of postmitotic cells. This aging process simply is the process of deterioration and loss of viability of cells during stationary phase. Again, like in mother cell-specific replicative aging, chronological aging is a process of genetically controlled cell differentiation. To give an example, the cell wall of stationary cells undergoes genetically controlled structural changes and remodelling.

An increase in intracellular oxidative stress, in ROS and in “death factors” seems to be common to the two aging processes as reported by many authors. In both forms of ageing, the terminal yeast cells execute apoptosis.

Reactive oxygen species generated by aerobic metabolism cause oxidative damage to cell macromolecules such as proteins, DNA and lipids inducing structure alteration and in many cases loss of function. It is now widely accepted that accumulation of these dysfunctional molecules during lifespan of the cell plays a key role in ageing process and degenerative diseases. Harman’s “free radical theory of aging” is now fifty years old; today although ROS are believed as the major cause of ageing many questions remains opened. In particular is not clear the relationship between metabolism rate and ROS production. Furthermore, although many molecules are found in oxidized state during cell senescence, is not clear which are the relevant targets of oxidation and how their modification can affect lifespan.

The proteomic approach offers all the instruments to deeply understand the mechanisms of this phenomenon. The high capacity of the analytical technique used in proteomics to resolve complex mixture of proteins extracted from a cell and the very sensitive techniques used to identify them, led in the last few years to a better understanding of apoptosis.

A procedure for detecting proteins that contain oxidation-sensitive cysteine residues, as a means to

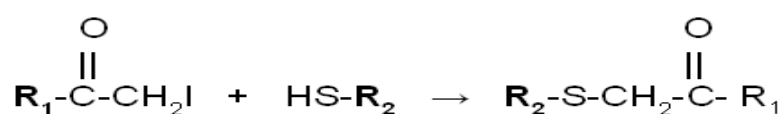
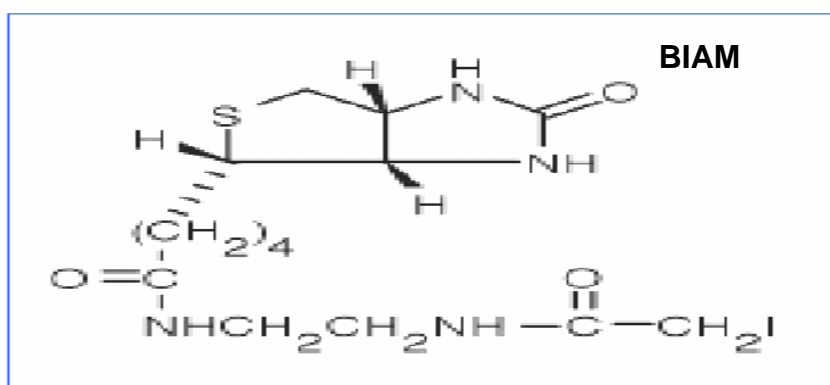


Fig 1. Reaction between BIAM and cysteine thiol group

study protein oxidation from different growth conditions in yeast cells, was the main goal of this project. The procedure is based on the fact that biotin-conjugated iodoacetamide (BIAM) selectively reacts with free thiols in cysteine residues (Fig 1), and that the decrease in the labelling of cell lysate proteins with BIAM can be monitored by western blot analysis.

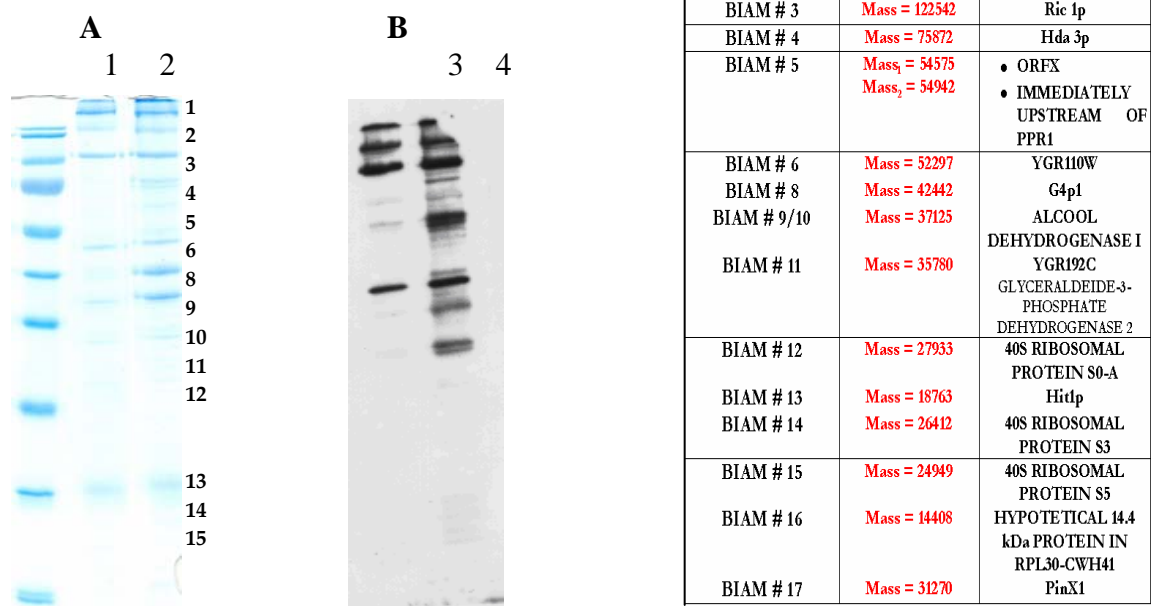
Thiol (SH) groups play a broad range of roles in the cell, since their redox state can affect the activity and the structure of enzymes, receptors and transcription factors.

In this study we evaluated the redox state of proteins combining a selective method for labelling proteins containing reduced cysteine residues and mono/two dimensional electrophoresis followed

by mass spectrometry. In fact cysteine residues can react with ROS and can function as detector of redox status of the cells. In particular we compared yeast cells exponentially growing with cells during chronological ageing.

During the first year I have focused my attention to set up a method to label, to isolate and to identify those proteins from a *S.cerevisiae* extract which in consequence of oxidative stress, endured irreversible oxidations of cystein thiol groups. The BIAM-labeled reaction mixtures and the control (cell lysate not incubated with BIAM) were subjected to affinity chromatography using streptavidin modified agarose beads. Eluted samples were separated by monodimensional SDS-PAGE, the separated proteins were transferred to a nitrocellulose membrane and detected with streptavidin HRP blot analysis (fig.2)

Fig.2 Mono dimensional SDS PAGE (A) and Western Blot analysis (B) of Cell lysate after BIAM labelling (lane 2 and 4) and not labelled with BIAM (lane 1 and 3)



Protein bands which gave positive signal to Western Blot analysis were submitted to an identification procedure by in situ hydrolysis, MALDI analysis of peptide mixtures and data bank interrogation, the results are summarized in table 1. However tab. 1 shows, in some cases, the identification of more than one protein in a single band; therefore we decided to increase the resolutive power of the separation technique, therefore after BIAM labelling protein extracts were separated by bi-dimensional electrophoresis avoiding affinity purification step. We therefore decided during the second year to focus our attention to set up an optimized method for this separation.

During this period we also set up a software image analysis of the two-dimensional maps and western blot, in order to identify the proteic spots corresponding to BIAM linked proteins and to identify spots which disappeared during ageing.

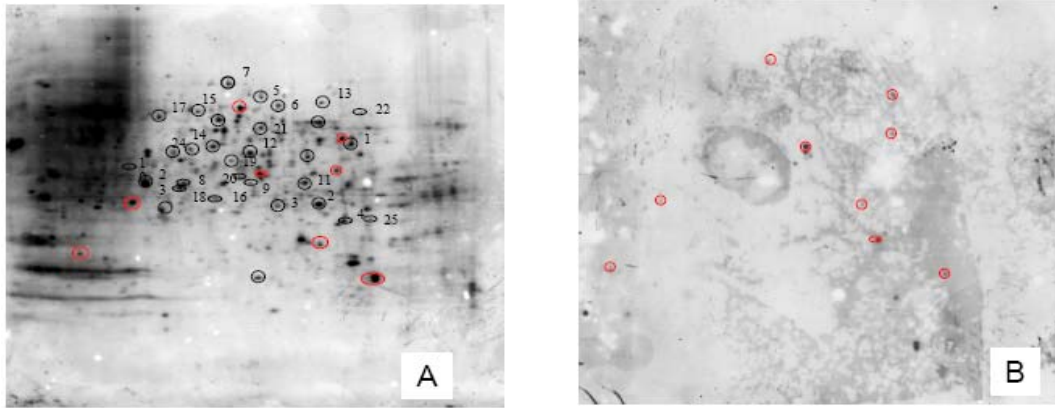
	Exponential phase Silver staining	Exponential phase Western-blot	72 hours Silver staining	72 hours Western-blot
Spot 1				
Spot 3				
Spot 2				

Example of image analysis

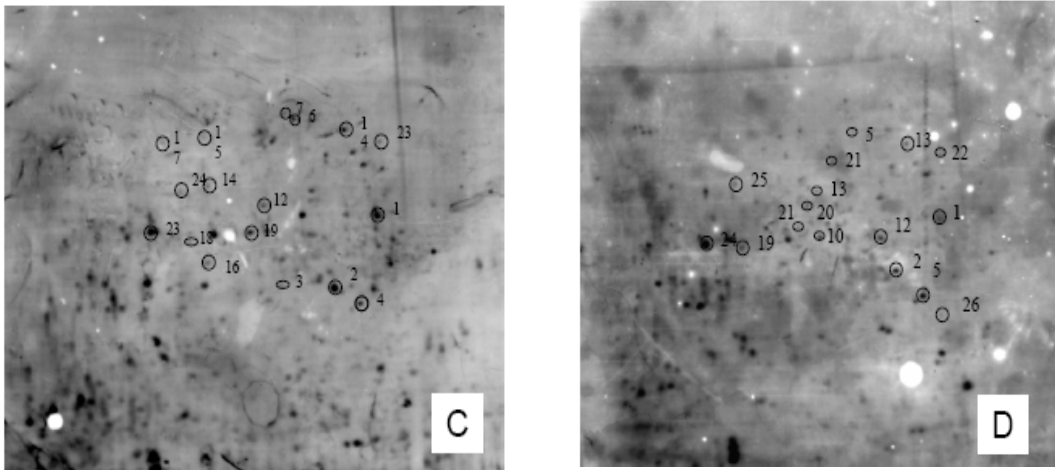
Optimized protocol was therefore used to investigate whether at pH 7, the BIAM-labeled proteins amount change on different carbon source and during chronological aging.

The experiments were performed in complete synthetic medium (SC) containing three different carbon source: glucose 2%, glucose 0,5% and 3% glycerol. SC plus 2% glucose is the standard medium used from many authors to study the chronological aging features. In this condition yeast cells initially obtain energy through fermentation pathway and approximately after 10 hours, when the glucose concentration reaches very low level, yeasts switch to respiration pathway. This switch is called “diauxic shift” and then yeast enter in the post-diauxic phase. In this phase cells grow slowly until about 48 hours and then stop dividing but the metabolic rate remain high until approximately one week. SD plus 0,5% glucose is the medium used to mimic caloric restriction; in this condition yeast cells show an increase of life span probably through a decrease in ROS production although the mechanism involved in this reduction is still debated. For the first time we also tested a role of a pour fermentable carbon source as glycerol on yeast chronological aging. In the last phase of the project, we first measured the vitality of the colonies grown on the different carbon sources. The results confirmed that both caloric restriction and non fermentable substrate prolonged vitality of yeasts. Furthermore we measured ROS production in yeast mitochondria (tanks to specific die) in the three colonies after 72 h. 2% glucose colonies showed a much bigger rate of ROS production, compared with the other two.

In order to identify the major target of oxidation in chronological aging in SCD extracts of young (exponentially growing) and old (72h of growth) cells, lysates were incubated with 40 μ M BIAM and the proteins submitted to 2D-GE followed by western blot anti-streptavidin. The results shown in figure 23 indicates that many proteins are in a reduced form (BIAM-linked) during exponential phase (Figure 2A) whereas at 72h a dramatically decrease of the BIAM labeled proteins is evident indicating a prevalence of oxidized cysteine residues (Figure 2B).



Western blot with HRP-conjugated streptavidin and ECL of 2D-gels from cells grown for 72 h in CR or SCG showed an increase in BIAM-labelling (Figure 2C and 2D respectively) in comparison to the same experiment from cells grown in SCD (Figure 2B).

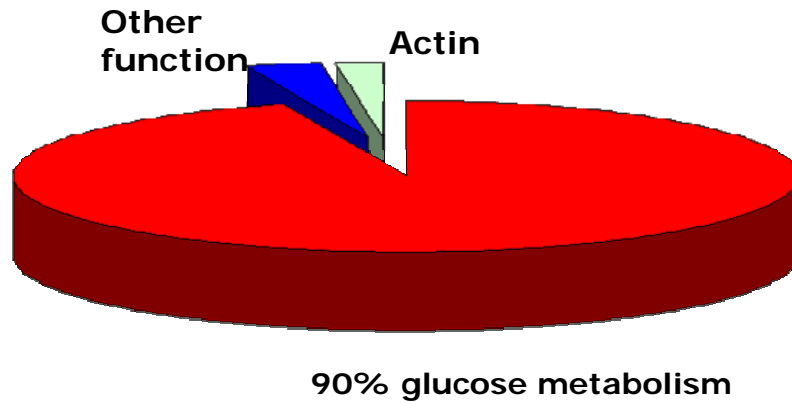


After an accurate image analysis using the MELANIE 4.0 software of the different repeated trials, we were able to localize on the 2D-GE spots corresponding to BIAM linked or non BIAM linked proteins. We were also able to compare different gels, in order to localize spots corresponding to proteins with an alteration in cysteine redox state during cell chronological ageing in different growth conditions.

During growth in exponential phase in SCD about 50 spots corresponding to BIAM-linked proteins were clearly detected in repeated trials (Figure 2A). Among these, 9 spots correspond to protein that are still reduced on cysteine residues after 72h in SCD (Figure 2A and 2B red circles) and 10 spots correspond to proteins that are not visible in silver stained 2D-gel of old cells. These spots were excluded by our analysis because they are undetectable on the 2-D gel. Among the remaining 31 spots (indicated by black circles) 25 (indicated by black circles and number in Figure 2A) were identified and the redox status of these spots were analysed, by BIAM-labelling, in chronological aged cells growth in CR (Figure 2C) and in SCG (Figure 2D) respectively.

The results reported showed that calorie restriction and respiration extend *S.cerevisiae* lifespan and that oxidative damage on cysteine residues in chronological-aged cells are different in cells grown on high glucose in comparison to cells grown in calorie restriction or in a respirable carbon source as glycerol. The viability of yeast strains varies dramatically in different media conditions.

In this study we also suggest the possibility that increased and better mitochondrial activity might promote longevity triggering mechanisms that protect cells against oxidative stress or reduced the damage to cellular components like proteins. These proteins targets include enzymes involved in glucose metabolism and actin, explaining why the replication rate decrease in the passage through the stationary phase.



Most of the enzymes of the glycolytic pathway such as GAPDHp, which we found to contain at least one Cys residue BIAM-labeled, Pdc1p, Eno1p and Eno2p, Pgc1p and Fba1p, were identified as targets for oxidation in old cells growth in high level of glucose. On the contrary the old cells growth in calorie restriction or in glycerol, showed marked differences in protein labelling patterns in comparison to the same cells on normal glucose. Respiration induced by caloric restriction or by a respirable carbon source reduces cystein oxidative damage to proteins increasing life span in *S.cerevisiae* because in these conditions there is an increase in the capacity of the mitochondrial electron transport chain. Using the yeast *S. cerevisiae* as a model organism we showed a decrease in intracellular oxidation in old cells growth in low glucose or glycerol which results in better vitality of yeast cells.